

FROM THE FACULTY OF MEDICINE  
OF THE UNIVERSITY OF REGENSBURG  
PROF. DR. MARKUS J. RIEMENSCHNEIDER  
DEPARTMENT OF NEUROPATHOLOGY

ANALYSIS OF THE SIGNIFICANCE OF miRNAs OF THE miRNA-200  
FAMILY IN THE MALIGNANT PHENOTYPE OF GLIOBLASTOMA

Inaugural-Dissertation  
to obtain the title of  
**Doctor of medicine (Dr. med.)**

from the Faculty of Medicine  
of the University of Regensburg

presented by  
Natalia Vélez Char, M.D., M.Sc.

2017



FROM THE FACULTY OF MEDICINE  
OF THE UNIVERSITY OF REGENSBURG  
PROF. DR. MARKUS J. RIEMENSCHNEIDER  
DEPARTMENT OF NEUROPATHOLOGY

ANALYSIS OF THE SIGNIFICANCE OF miRNAs OF THE miRNA-200  
FAMILY IN THE MALIGNANT PHENOTYPE OF GLIOBLASTOMA

Inaugural-Dissertation  
to obtain the title of  
**Doctor of medicine (Dr. med.)**

from the Faculty of Medicine  
of the University of Regensburg

presented by  
Natalia Vélez Char, M.D., M.Sc.

2017

Dean: Prof. Dr. Dr. Torsten E. Reichert

1. Rapporteur: Prof. Dr. Markus J. Riemenschneider

2. Rapporteur: Prof. Dr. Peter Hau

Oral examination date: Wednesday, August 2nd 2017

## Declaration

This doctoral thesis was designed, encouraged, supported and supervised by Prof. Dr. Markus J. Riemenschneider.

I hereby declare that I have done the present work independently and without any other tools or resources, except where otherwise stated, than the ones described in this thesis.

That where I have used data, concepts or resources taken directly or indirectly from other sources, this has always been clearly attributed and the corresponding source cited.

I have not directly nor indirectly received any remuneration of intermediary or advisory services (promotion consultants or other persons); and that no one has received directly or indirectly monetary benefits from this institution or me for work related to this content.

Furthermore, I certify that this research thesis or any part of it has not been previously submitted for a degree or any other qualification at the University of Regensburg or any other institution in Germany or abroad.

Regensburg, .....

.....

Natalia Vélez Char



## Zusammenfassung

Der miR200-Familie werden Tumorsuppressor-Eigenschaften in verschiedenen malignen epithelialen Tumoren zugeschrieben. Ihre Herunterregulation ist mit Tumoraggressivität, metastatischer Erkrankung, Tumorprogression, Chemoresistenz und schlechterer Prognose assoziiert. Im Glioblastom wurde gezeigt, dass einige Mitglieder der miR200-Familie auf sehr niedrigem Niveau exprimiert werden, und dieses Phänomen ist ebenfalls mit einer schlechten Prognose assoziiert. Auch wenn somit eine Rolle der miRNA 200-Familie bei Glioblastomen naheliegt, gibt es noch keine detaillierten Daten über die funktionalen Effekte einer Dysregulation ihrer beiden Strängen (3p vs. 5p) bzw. Daten darüber, welcher der beiden Stränge funktionell aktiv ist und ob eine Dysregulation einzelner miRNAs relevante funktionelle Effekte besitzt.

Zu diesem Zweck wurden U-87 MG- und U-251 MG-Zellen mit den jeweiligen 3p- und 5p-miRNA-Mimics der gesamten miR200-Familie transfiziert und funktionelle Assays sowie Next generation sequencing (NGS)-Analysen von RNA-Proben nach Transfektion durchgeführt, um die Effekte der miR200-Familie in Glioblastomzellen genauer zu charakterisieren. Die Ergebnisse dieser Arbeit zeigten, dass Glioblastom-Zelllinien ein niedrigeres Werte Expressionsniveau der 3p-Stränge der miR200-Familienmitglieder im Vergleich zu resezierten Tumoren und nicht-neoplastischem Hirngewebe aufzeigten und dass die induzierte Überexpression dieser Stränge zu einer Abnahme der Proliferation und einer Zunahme der Apoptose in U-87 MG- und U-251 MG-Zellen sowie zu einer Abnahme der Expression von ZEB1 und ZEB2 führte. Darüber hinaus zeigten sich in den NGS-Analysen eine funktionelle Gruppierung der Zellen mit einer Überexpression der 3p-Stränge nach ihren Seed-Sequenzen und eine klare Trennung von den Zellen mit Hochregulation der 5p Stränge. Die 3p-Überexpression induzierte eine Hochregulation von Targets des G2-M-DNA-Damage-Checkpoints, von E2F-Targets sowie von Targets der c-myc- und NFκβ-Signalwege. Weiterhin induzierte die 3p-Überexpression eine Herunterregulation von Targets des CDH1-Gens und der Hypoxie-Antwort (einschließlich HIF1α).

In Zusammenschau, all dieser Befunde deuten die Ergebnisse dieser Arbeit darauf hin, dass die 3p-Stränge der miR200-Familie in Gliomen tumorsuppressive Eigenschaften vermitteln, indem sie pathogenetisch relevante Signalwege beeinflussen und Mechanismen der DNA-Schädigung/-Reparatur, des Zellzyklus und der Zellvitalität, der Zellmotilität und Adhäsion sowie der Hypoxie regulieren.

## Abstract

The miR200 family has been described to exert tumor suppressing functions in different malignant epithelial tumors, and their down regulation has been associated with aggressiveness, metastatic disease, tumor progression, chemoresistance and worse prognosis. In glioblastoma, some members of the miR200 family have been shown to be expressed at very low levels, and this phenomenon has been associated to poor prognosis. Even though a role of the miRNA 200 family in glioblastomas has been suggested, no detailed data has been provided regarding differences in functional effects among their two strands. In other terms, it has not yet been established which of the two strands is functional active, and if dysregulation of isolated miRNAs of this family has relevant functional effects.

For this purpose, U-87 MG and U-251 MG cells were transfected with 3p and 5p miRNA mimics of the miR200 family, and functional assays as well as next generation sequencing of RNA samples after transfection were performed. Results showed that glioblastoma cell lines express lower levels of the 3p strands of the miR200 family members compared to glioma biopsy samples and non-neoplastic brain tissue, and that inducing overexpression of these strands leads to a decrease in proliferation and increase in apoptosis in U-87MG and U-251 MG cells, as well as a decrease in the expression of ZEB1 and ZEB2. Furthermore, NGS analyses showed a functional clustering of cells overexpressing the 3p strands in two groups according to their seed sequences, with clear separation of cells overexpressing the 5p strands. 3p overexpression caused upregulation of G2/ M DNA damage checkpoint and E2F target genes. Also, targets of the c-myc and NF $\kappa$ B signaling pathways were up- and targets of the CDH1 gene and of hypoxia response (including HIF1 $\alpha$ ) were downregulated.

In conclusion, the findings of this work suggest that the 3p strands of the miR200 family carry tumor suppressive functions in gliomas by interacting with major pathogenic pathways implicated in DNA damage/ repair, cell cycle, cell viability, cell motility/ adhesion and hypoxia response.



# Table of Contents

Zusammenfassung .....	i
Abstract.....	ii
1. Introduction .....	1
1.1. The miRNA 200 Family .....	1
1.1.1. Micro RNAs .....	1
1.1.2. The miRNA 200 family.....	2
1.2. Epithelial to mesenchymal transition (EMT) in cancer .....	3
1.2.1. Epithelial to mesenchymal transition .....	3
1.2.2. The role of the miRNA 200 Family in EMT .....	4
1.3. Glioblastoma .....	5
1.3.1. Glioblastoma .....	5
1.3.2. EMT and Glioblastoma .....	5
1.3.3. The role of the miRNA 200 Family in Glioblastoma.....	5
2. Aim of the study.....	7
3. Materials and Methods.....	8
3.1. Materials .....	8
3.1.1. Cell lines .....	8
3.1.2. Chemical substances.....	8
3.1.3. Expendable Supplies and Materials .....	9
3.1.4. Electrical Equipment .....	10
3.1.5. Kits.....	11
3.1.6. Medium and Supplements for Cell Culture and <i>in vitro</i> Assays.....	12
3.1.7. miRNA Primer Assays for qRT-PCR.....	12
3.1.8. miRNA Sequences for transient transfection .....	13
3.1.9. Non-expendable Supplies and Materials .....	14
3.1.10. Primer pairs for qRT-PCR.....	15
3.1.11. RNA samples .....	15
3.1.12. Solutions and other biochemical compounds/ materials.....	17

3.1.13. Software .....	17
3.2. Methods.....	18
3.2.1. Cell Biology Methods .....	18
3.2.2. Molecular Biology Procedures .....	21
3.2.3. Biochemical Methods .....	27
3.2.4. Bioinformatics .....	28
4. Results.....	32
4.1. Expression of the miR200 family.....	32
4.1.1. Expression of the miR200 family in glioblastoma samples extracted from The Cancer Genome Atlas (TCGA) .....	39
4.1.2. Expression of ZEB1 and ZEB2 in glioblastoma samples extracted from The Cancer Genome Atlas (TCGA) .....	42
4.2. Transfection .....	43
4.2.1. Expression of the other miR200 family members after transfection with one mimic .....	45
4.2.2. Effects of upregulation of the miR200 family members in glioma cell proliferation and apoptosis.....	47
4.2.3. Expression of ZEB1 and ZEB2 in cells transfected with mimics of the miR200 family.....	50
4.3. NGS.....	51
4.3.1. Multivariate Analysis.....	51
5. Discussion.....	58
6. Conclusion.....	63
Bibliography .....	64

# 1. Introduction

## 1.1. The miRNA 200 Family

### 1.1.1. Micro RNAs

Micro RNAs (miRNAs) are small (21-25 nt long), non-coding RNAs that regulate gene expression post-transcriptionally by binding to 3' untranslated regions or open reading frames of target mRNAs, leading to their degradation or repression of mRNA translation<sup>1, 2</sup>. They are transcribed either mono- or polycistronically in the cell nucleus by an RNA polymerase type II, resulting in hundred to thousand nucleotides long, polyadenylated and capped primary transcripts (primary miRNA, pri-miRNA)<sup>1, 2</sup>, which will later on be cleaved by Drosha, a type III RNase, to ~70 nucleotides long precursor miRNAs (pre-miRNA). These pre-miRs bind to exportin-5 to be transported to the cytosol, where they are cleaved again by a type III RNase called Dicer, to a final ~21–22 nucleotide long miRNA duplex. One of both strands (non-functional) will end up being degraded, while the remaining, functionally active strand will bind to Argonaute and enter the RNA induced silencing complex (RISC)<sup>1, 2</sup>. One of the two miRNA strands, usually miRNA 5p, was originally believed to have no functional effect and be the one to get degraded, but recent evidence suggests that any of the two strands (3p or 5p) could be functionally active and therefore of biological significance (Yang et al., *Nucleic Acids Res.* 2013). Once bound to RISC, miRNAs bind, according to their seed sequences, to complementary sequences in the 3' UTRs of target mRNAs, leading to mRNA degradation or translation inhibition<sup>3</sup>.

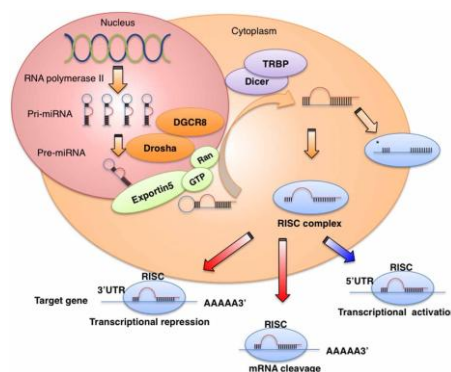


Figure 1. miRNA synthesis and function. Pri-miRNAs are transcribed and cleaved in the nucleus (pre-miRNAs). Pre-miRNAs are transported to the cytosol where they are cleaved again into a final 22 nucleotide long mature miRNA. After binding to RISC, miRNAs bind according to their seed sequence to mRNA to either silence or degrade it (Source: Takahashi et al. *Frontiers in Genetics* 2014).<sup>4</sup>

### 1.1.2. The miRNA 200 family

The miRNA 200 family is composed of 5 members coded in two different genomic clusters: miRNA-200a, -200b and -429 in chromosome 12, and miRNA-200c and -141 clustered in chromosome 1. They possess a seed sequence located at position 2 to 5 from the 5' end of their functional, mature miRNA strand, which is responsible for the specificity of the miRNA-mRNA targeting. The seed sequences among all 5 members differ in only one nucleotide in position 3, clustering the miRNAs members further, in two functional groups, which each share the same seed sequence: miRNA-200a together with -141, and miRNAs-200b, -200c and -429.<sup>1,2</sup>

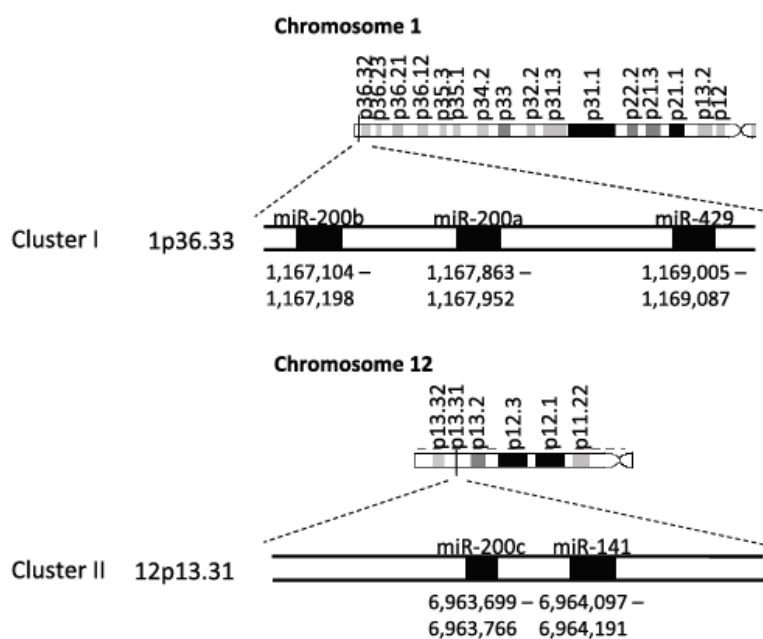


Figure 1: The miR-200 family two clusters are located on two different chromosomes. The miR-200 family consists of two clusters: Cluster I (miR-200b, -200a, and -429 is located on chromosome 1) and Cluster II (miR-200c and -141 is located on chromosome 12).

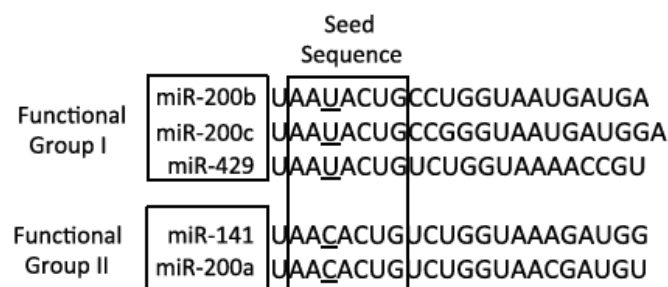


Figure 2. Genomic and functional clustering of the miRNA 200 family members. While miRNAs 200a, 200b and 429 cluster in chromosome 1 and miRNAs 200c and 141 in chromosome 12, they also cluster functionally according to their seed sequence in two different groups, where miRNAs 200b, 200c and 429 and miRNA 200a and 141 cluster together in (Source: Humphries et al. Oncotarget 2015).<sup>2</sup>

## 1.2. Epithelial to mesenchymal transition (EMT) in cancer

### 1.2.1. Epithelial to mesenchymal transition

In several types of cancer, the embryonic process known as epithelial mesenchymal transition (EMT) has been described and associated with increased migration, invasive capacities and metastasis<sup>5-7</sup>, as well as with the acquisition of molecular and functional properties of cancer cells<sup>8, 9</sup>. EMT is an embryonic process that triggers the transformation of epithelial cells into a mesenchymal, motile phenotype that allows the migration of cells required during embryogenesis<sup>6, 8</sup>. In adults, this process comes active during wound repair and tissue regeneration<sup>10</sup>. It is characterized by a gain of spindle-shaped morphology in cells, the loss of E-cadherin and the *de novo* expression of mesenchymal associated genes like N-cadherin, fibronectin,  $\alpha$ -smooth muscle actin and vimentin<sup>10</sup>.

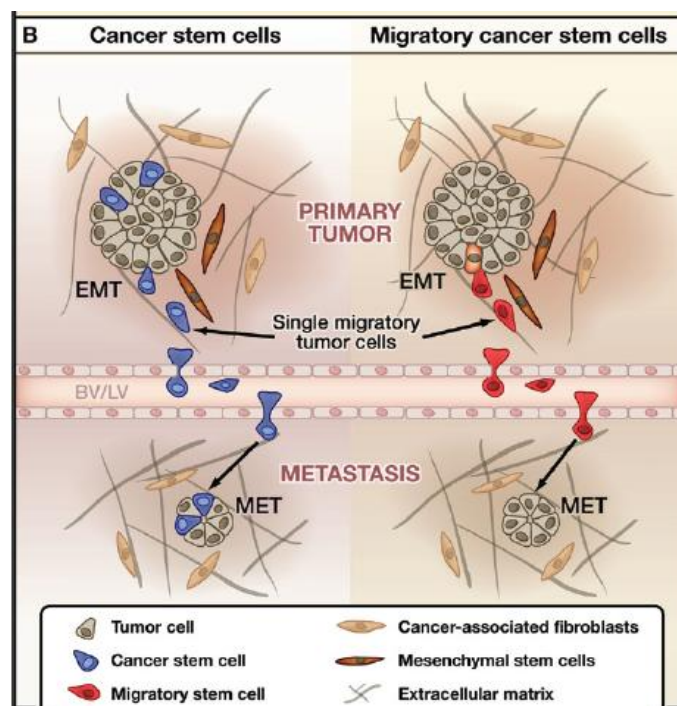


Figure 3. Epithelial to mesenchymal transition (EMT) in cancer cells. Cells in primary tumor undergo EMT, acquiring motility and the capacity to invade new organs, where a reverse mesenchymal to epithelial transformation (MET) occurs leading to tumor cell colonization, proliferation and metastasis (Source: Thiery et al. Cell 2009).<sup>5</sup>

Various transcription factors and extracellular stimuli have been described as *de novo* inducers of EMT.

### 1.2.2. The role of the miRNA 200 Family in EMT

In different types of epithelial tumors, the miRNA 200 family has been shown to be deregulated, and this phenomenon was associated with either oncogenic or tumor suppressive functions<sup>2, 10-12</sup>. Most studies have shown a decreased expression of the miRNA 200 family in different types of cancers, which correlates to the activity of the key master regulators of the epithelial to mesenchymal transformation (EMT), ZEB1 and ZEB2<sup>10, 11</sup>, and consequently to the inhibition of EMT signature proteins like E-cadherin and Vimentin<sup>12, 13</sup>. Target sites for the miR200 Family in the 3'UTR of both ZEB1 and ZEB2 have been identified<sup>14, 15</sup>. Furthermore, silencing of ZEB1 has been shown to induce miR200 expression in a negative feedback loop by direct binding to Ebox sites present upstream of both miR200 clusters<sup>16, 17</sup>. Via these same mechanisms, expression of the miR200 family has been shown to play a regulatory role in tumor aggressiveness and metastasis, in cancer stem cell self-renewal and differentiation as well as in chemoresistance, and has even shown to have an impact in overall prognosis of patients with high grade gliomas<sup>2, 18</sup>.

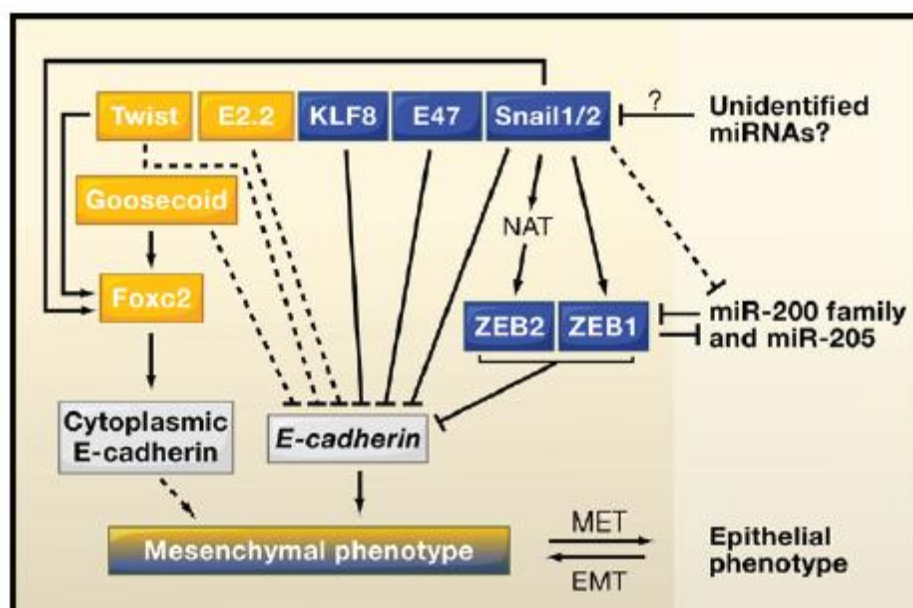


Figure 4. Role of the miRNA200 family in EMT. The miRNA200 family have been associated with the activity of ZEB1/ ZEB2 and the expression of e-cadherin, as well as with the preservation of an epithelial phenotype in tumor cells. (Source: Thiery et al. Cell 2009).<sup>5</sup>

## 1.3. Glioblastoma

### 1.3.1. Glioblastoma

WHO Grade IV astrocytoma, also known as glioblastoma, is a malignant tumor characterized by hypercellularity, nuclear atypia, mitotic figures and evidence of angiogenesis and/or necrosis upon histological examination. Their typical diffuse tissue-distribution pattern, with extensive dissemination of cancer cells in the brain's parenchyma makes a microscopically total surgical resection an almost impossible task<sup>19</sup>. They can arise de novo (primary GBM) or from the malignant progression of a low-grade astrocytoma (secondary GBM)<sup>20</sup>. These tumors harbor major genetic alterations. Primary GBM frequently bear amplification and/or mutations of the gene encoding the epidermal growth factor receptor (EGFR), occurring in up to 60% of all tumors<sup>21-23</sup>. The most common mutation is a gain of function of EGFR, which might be associated to proliferation and invasion; other major genetic alterations include deletion of the lipid phosphatase gene, PTEN, which results in increased AKT/mTOR activity, and may be responsible of promoting cancer cell survival, proliferation and invasion<sup>22, 24-26</sup>. Hypermethylation of the promoter gene encoding the DNA-repair enzyme, MGMT, is also a frequent occurrence, being present in 36% of primary GBM and in 75% of secondary GBM, and is associated with a better response to chemotherapy<sup>27-29</sup>. The prognosis of glioblastoma is poor, and the median survival for these patients is in average 12-18 months<sup>29, 30</sup>, with a median survival when radiotherapy and chemotherapy are combined of 14.6 months<sup>31</sup>.

### 1.3.2. EMT and Glioblastoma

In 2010, Carro et al. published a reverse-engineering and unbiased interrogation study of a glioma-specific regulatory network, which revealed that similar processes to EMT in epithelial cancers also play a role in gliomas, and that a complex transcriptional regulatory network produces a more aggressive mesenchymal glioma cell phenotype<sup>32</sup>. Moreover, glioblastomas can be subclassified according to different patterns of gene expression into various categories (classical, mesenchymal, neural and proneural) in which the mesenchymal subtype has been associated with a higher grade of aggressiveness (Veshaak et al., *Cancer Cell* 2010).

### 1.3.3. The role of the miRNA 200 Family in Glioblastoma

The microRNA 200 family has been shown to have an effect on cell proliferation, cell cycle, and tumor growth in gliomas and in brain tumor initiating cells<sup>33</sup>. One of its members, miR-200a, has

been proven to downregulate single-minded homolog 2-short form (SIM2-s), a protein which has been found to be overexpressed in many human cancers including gliomas<sup>35</sup>. Another of its members, miR200b, has been shown to be downregulated in high grade gliomas<sup>34, 35</sup>, and to suppress tumor cell growth when it is overexpressed<sup>33</sup>. Furthermore, Men et al. could confirm that lower miR-200b expression correlates with worse progression-free survival and overall survival in patients with WHO grade III and IV gliomas<sup>36</sup>. In U-87 MG glioma cells an epigenetic silencing of the miRNA 200a/200b/429 cluster could be shown, a phenomenon mainly mediated in a synergistic co-work between DNA methyltransferase 1 (DNMT1) and the PcG protein Enhancer of Zeste homolog 2 (EZH2), a histone methyltransferase<sup>37</sup>. In an experimental study with the chemotherapeutical molecule NPV-LDE-225 an inhibition of EMT by upregulating E-cadherin and inhibiting N-cadherin, Snail, Slug, and Zeb1 through modulating the miR-200 family was observed in brain tumor initiating cells<sup>38</sup>. Furthermore, the ZEB1-miR-200 feedback loop has been shown to play a key role in tumorigenesis, invasion and chemoresistance in glioblastoma through activation of downstream effectors like ROBO1 and c- MYB, as well of MGMT<sup>39</sup>. Siebzehnrübl et al. concomitantly showed that ZEB1 expression in glioblastoma patients is predictive of shorter survival and poor Temozolomide response<sup>39</sup>.



## 2. Aim of the study

In light of the findings listed in 1.3.3. there seems to be a relevance of miRNA 200 family signaling in glioblastomas, however, the functionalities have not yet been systematically assessed.

Based on the findings from Carro et al.<sup>32</sup>, which revealed that similar processes to EMT in epithelial cancers also play a role in gliomas, and that a complex transcriptional regulatory network produces a more aggressive mesenchymal glioma cell phenotype, the aim of this study was to more specifically define the role of the miRNA 200 family in the formation of the malignant phenotype of glioblastoma.

### 3. Materials and Methods

#### 3.1. Materials

##### 3.1.1. Cell lines

For all experiments carried out in this work, human adherent glioblastoma cell lines were used. These were obtained from *CLS Cell Lines Service GmbH* (Eppelheim)<sup>40</sup>.

Table 1. List of cell lines used. N/A = not available.

<b>U-87 MG</b>	Glioblastoma (WHO-Grade IV)	44 years	Male
<b>U-118 MG</b>	Glioblastoma (WHO-Grade IV)	50 years	Male
<b>U-251 MG</b>	Glioblastoma (WHO-Grade IV)	N/A	Male

RNA from seven human glioblastoma stem cell lines cultured and expanded in our laboratory (NCH421k, NCH465, NCH601, NCH636, NCH644, NCH660h, NCH1425)<sup>41</sup> was also used in a series of experiments (gene expression analysis by qRT-PCR). These cell lines were kindly provided by Professor Christel Herold-Mende, Department of Neurosurgery at the University Clinic Heidelberg.

STR (*Short Tandem Repeat*)-Analyses were performed in all glioblastoma cell lines (CLS Cell Lines Service GmbH (Eppelheim)) in order to confirm their origin<sup>42</sup>.

##### 3.1.2. Chemical substances

Table 2. List of all chemical substances used in the experiments described in this work, including their manufacturing company.

<b>Acetic acid</b>	Carl Roth GmbH & Co. KG, Karlsruhe, Germany
<b>Agarose (universal)</b>	peqGOLD Universal Agarose, pequLab, VWR International, Ismaning, Germany

<b>beta-Mercaptoethanol</b>	Carl Roth GmbH & Co. KG, Karlsruhe, Germany
<b>Chloroform (Trichlormethane)</b>	Carl Roth GmbH & Co. KG, Karlsruhe, Germany
<b>DMSO</b>	Carl Roth GmbH & Co. KG, Karlsruhe, Germany
<b>EDTA</b>	Carl Roth GmbH & Co. KG, Karlsruhe, Germany
<b>Ethanol (70%, denaturated)</b>	Otto Fischar & Co. KG, Saarbrücken, Germany
<b>Ethanol (ROTIPURAN® ≥ 99,8%)</b>	Carl Roth GmbH & Co. KG, Karlsruhe, Germany
<b>Orange G (C.I.16230)</b>	Carl Roth GmbH & Co. KG, Karlsruhe, Germany
<b>RedSafe™ nucleic acid staining solution</b>	iNtRON Biotechnology, Seongnam, Korea
<b>Trizma base</b>	Sigma Aldrich, St. Louis (MO), USA

### 3.1.3. Expendable Supplies and Materials

Table 3. List of all expendable supplies and materials used in experiments carried out in this work. The manufacturing company is listed on the right column.

<b>BD Discardit™ II syringes (2 ml)</b>	BD GmbH, Heidelberg, Germany
<b>BD Microbalance™ 3 Needles 20G</b> 20 G x 1 <sup>1/2</sup> " Nr.1, 0,9 mm x 40 mm	BD GmbH, Heidelberg, Germany
<b>Combitips</b> (1, 2 and 5 ml)	Eppendorf, Hamburg, Germany
<b>Cellstar® Cell Culture Flasks</b>	Greiner Bio-One GmbH, Frickenhausen, Germany

(T-25cm <sup>2</sup> , T-75cm <sup>2</sup> )	
<b>Disposable gloves</b>	Peha-soft, nitrile (Fino), HARTMANN Gruppe, Heidenheim an der Brenz, Germany; NeoTouch, Neoprene (powder free), Ansell, Iselin (NJ), USA
<b>Disposable glass Pasteur pipettes</b>	VWR International GmbH, Ismaning, Germany
<b>Filter tips</b> (10, 20, 200 and 1.000 µl)	Bioposphere® filtered, Sarstedt, Nümbrecht, Germany
<b>96-Well PCR Plates</b>	4titude, Dorking, UK
<b>qPCR seal sheets</b>	4titude, Dorking, UK
<b>Sterile serological Pipettes</b> (2, 5, 10 and 25 ml)	Sarstedt, Nümbrecht, Germany
<b>Test plates</b> (6-well, 24-well, 96-well)	Sarstedt, Nümbrecht, Germany (Clear 6-well plates); Greiner Bio-One, Frickenhausen, Germany (96-wells plates with black walls, clear floor); Thermo Fisher Scientific, Waltham (MA), USA (96-well plates with black walls and floor)
<b>Test tubes</b> (8-Lid Chain PCR tubes (flat), SafeSeal 1,5 and 2 µl, 15 and 30 ml Tubes)	Sarstedt, Nümbrecht, Germany

### 3.1.4. Electrical Equipment

Table 4. List of all electrical equipment used, including the name of the manufacturing/ developing company.

<b>CO<sub>2</sub>-Incubator</b>	HERAcell <sup>240i</sup>	Thermo Fisher Scientific, Waltham (MA) USA
<b>Safety cabinet</b> (cell culture laminar flow Hood)	HERAsafe KS/KSP	Thermo Fisher Scientific, Waltham (MA) USA
<b>Centrifuge</b>	Rotina 420R	HettichLab, Tuttlingen, Germany
<b>Centrifuge</b>	Mini Star	VWR International GmbH, Ismaning, Germany
<b>Centrifuge</b>	Mikro 200R	HettichLab, Tuttlingen, Germany

<b>Elektrophoresis chamber</b>	Wide Mini-Sub Cell GT	Bio-Rad, Hercules (CA), USA
<b>Elektrophoresis Power Supply</b>	POWER PAC 3000	Bio-Rad, Hercules (CA), USA
<b>Lab Scale</b>	PBS/PBJ	Kern & Sohn GmbH, Balingen, Germany
<b>Lab tubes rotator</b>	Revolver™ Adjustable Lab Rotator H5600	VWR International GmbH, Ismaning, Germany
<b>Microplate Reader</b>	FLUOStar Omega	BMG Labtech, Ortenberg, Germany
<b>Microscope</b>	Leitz DM IL	Leica Microsystems, Wetzlar, Germany
<b>Multipipette</b>	plus	Eppendorf, Hamburg, Germany
<b>PCR-System (real-time)</b>	StepOnePlus™	Applied Biosystems, Foster City (CA), USA
<b>pH-Meter</b>	FiveEasy™	Mettler Toledo, Columbus (OH), USA
<b>Pipette controller</b>	accu-jet® pro	Brand GmbH & Co. KG, Wertheim, Germany
<b>Test tube shaker</b>	100-2500 1/min	VWR International GmbH, Ismaning, Germany
<b>Sequencer (NGS)</b>	HiSeq 1000	Illumina, San Diego (CA), USA
<b>Spectrophotometer</b>	NanoDrop 2000	Thermo Fisher Scientific, Waltham (MA), USA
<b>Thermocycler</b>	T3000	Biometra, Göttingen, Germany
<b>Thermo-Mixer</b>	compact	Eppendorf, Hamburg, Germany
<b>Water bath</b>	AL 25	Lauda, Lauda-Königshofen, Germany

### 3.1.5. Kits

Table 5. Overview of the Kits used in this work, including the name of the company they were acquired from and the assays they were used for. N/A = not available.

<b>Apo-ONE® Homogeneous Caspase-3/7 Assay</b>	Promega, Madison (WI), USA (Cat. No. G7790)	Apoptosis
<b>Cell proliferation ELISA, BrdU (chemiluminescent)</b>	Roche/ Sigma Aldrich, St. Louis (MI), USA (Cat. No. 11669915001)	Proliferation
<b>miRNeasy Mini Kit</b>	Qiagen, Hilden, Germany	miRNA isolation

	(Cat. No. 217004)	
<b>miScript II RT Kit (50)</b>	Qiagen, Hilden, Germany (Cat. No. 218161)	cDNA transcription
<b>miScript SYBR® Green PCR Kit</b>	Qiagen, Hilden, Germany (Cat. No. 218075)	qRT-PCR
<b>SensiFAST™ SYBR® Hi-ROX Mix</b>	Bioline, London, UK (Cat. No. BIO-92005)	qRT-PCR
<b>TruSeq® RNA Sample Preparation Kit v2</b>	Illumina, San Diego (CA), USA (Cat. No. RS-122-2002)	miRNASeq

### 3.1.6. Medium and Supplements for Cell Culture and *in vitro* Assays

Table 6. List of all media and reagents used for cell culture, including their producing company.

<b>Dulbecco's modified Eagle's Medium (DMEM)</b> With high Glucose (4500mg/dl, L-Glutamine and sodium bicarbonate, without sodium pyruvate, liquid, sterile-filtered, suitable for cell culture.	Sigma Aldrich, St. Louis, MO, USA
<b>Fetal Bovine Serum Premium (10% v/v)</b>	PAN Biotech GmbH, Aidenbach, Germany
<b>Opti-MEM® I Reduced Serum Medium</b>	GIBCO™ (Life Technologies), Thermo Fisher Scientific, Waltham (MA), USA
<b>Dulbecco's Phosphate Buffered Saline (PBS)</b>	Sigma Aldrich, St. Louis (MO), USA
<b>Penicillin (100U/ml)/Streptomycin (100 µg/ml)</b>	Life Technologies, Thermo Fisher Scientific, Waltham (MA), USA
<b>Trypsin-EDTA Solution</b>	Sigma-Aldrich, St. Louis (MO), USA

### 3.1.7. miRNA Primer Assays for qRT-PCR

Table 7. List of micro RNAs PCR primer assays used to assess expression of the miRNA200 family through qRT-PCR.

<b>Hs_miR-200a_1 miScript Primer</b>	5'-UAACACUGUCUGGUAACGAUGU-3'	Cat. No. MS00003738
--------------------------------------	------------------------------	---------------------

<b>Assay (miR200a 3p)</b>		Qiagen, Hilden, Germany
<b>Hs_miR-200a*_2 miScript Primer Assay (miR200a 5p)</b>	5'-CAUCUUACCGGACAGUGCUGGA-3'	Cat. No. MS00009009 Qiagen
<b>Hs_miR-200b_3 miScript Primer Assay (miR200b 3p)</b>	5'-UAAUACUGCCUGGUAAUGAUGA-3'	Cat. No. MS00009016 Qiagen
<b>Hs_miR-200b*_1 miScript Primer Assay (miR200b 5p)</b>	5'-CAUCUUACUGGGCAGCAUUGGA-3'	Cat. No. MS00009023 Qiagen
<b>Hs_miR-200c_1 miScript Primer Assay (miR200c 3p)</b>	5'-UAAUACUGCCGGGUAAUGAUGGA-3'	Cat. No. MS00003752 Qiagen
<b>Hs_miR-200c*_1 miScript Primer Assay (miR200c 5p)</b>	5'-CGUCUUACCCAGCAGUGUUUGG-3'	Cat. No. MS00009030 Qiagen
<b>Hs_miR-141_1 miScript Primer Assay (miR141 3p)</b>	5'-UAACACUGUCUGGUAAAGAUGG-3'	Cat. No. MS00003507 Qiagen
<b>Hs_miR-141*_1 miScript Primer Assay (miR141 5p)</b>	5'-CAUCUUCAGUACAGUGUUGGA-3'	Cat. No. MS00008680 Qiagen
<b>Hs_miR-429_1 miScript Primer Assay (miR429)</b>	5'-UAAUACUGUCUGGUAAAACCGU-3'	Cat. No. MS00004193 Qiagen

### 3.1.8. miRNA Sequences for transient transfection

Table 8. List of micro-RNA mimics, including their sequence and manufacturing company, used in transient transfection assays.

<b>hsa-miR-200a-3p mirVana® mimics</b>	5'-UAACACUGUCUGGUAAACGAUGU-3'	Assay Id. MC10991 Thermo Fischer Scientific, USA
<b>hsa-miR-200a-5p mirVana® mimics</b>	5'-CAUCUUACCGGACAGUGCUGGA-3'	Assay Id. MC10250 Thermo Fischer Scientific
<b>hsa-miR-200b-3p mirVana® mimics</b>	5'-UAAUACUGCCUGGUAAUGAUGA-3'	Assay Id. MC10492 Thermo Fischer Scientific
<b>hsa-miR-200b-5p mirVana® mimics</b>	5'-CAUCUUACUGGGCAGCAUUGGA-3'	Assay Id. MC12857

<b>mimics</b>		Thermo Fischer Scientific
<b>hsa-miR-200c-3p mirVana® mimics</b>	5'-UAAUACUGCCGGGUAUGAUGGA-3'	Assay Id. MC11714 Thermo Fischer Scientific
<b>hsa-miR-200c-5p mirVana® mimics</b>	5'-CGUCUACCCAGCAGUGUUUGG-3'	Assay Id. MC12741 Thermo Fischer Scientific
<b>hsa-miR-141-3p mirVana® mimics</b>	5'-UAACACUGUCUGGUAAGAUGG-3'	Assay Id. MC10860 Thermo Fischer Scientific
<b>hsa-miR-141-5p mirVana® mimics</b>	5'-CAUCUCCAGUACAGUGUUGGA-3'	Assay Id. MC13054 Thermo Fischer Scientific
<b>Has-miR-429 mirVana® mimics</b>	5'-UAAUACUGUCUGGUAACCGU-3'	Assay Id. MC10221 Thermo Fischer Scientific

### 3.1.9. Non-expendable Supplies and Materials

Table 9. List of all non-expendable supplies and materials used in this work, including the name of the company they were purchased from.

<b>Precision cover slips 18 x 18 mm</b>	Carl Roth GmbH & Co. KG, Karlsruhe, Germany
<b>Magnetic Stand-96</b>	Life Technologies, Thermo Fisher Scientific, Waltham (MA), USA
<b>Neubauer cell counting chamber (0,1 mm)</b>	Assistent, Glaswarenfabrik Karl Hecht GmbH & Co KG, Sondheim/Rhön, Germany; Marienfeld-Superior, Lauda-Königshofen, Germany
<b>Pipettes, Research plus</b> (0,5-10 µl; 2-20 µl; 20-200 µl; 100-1.000 µl)	Eppendorf, Hamburg, Germany



### 3.1.10. Primer pairs for qRT-PCR

Table 10. List of PCR primers including their sequences, used in qRT-PCR assays.

<b>ZEB1</b>	GATGATGAATGCGAGTCAGATGC	ACAGCAGTGTCTTGTGTTGT	86 bp	MWG (eurofins), Ebersberg, Germany
<b>ZEB2</b>	GCGATGGTCATGCAGTCAG	CAGGTGGCAGGTCATTTTCTT	138 bp	MWG (eurofins)
<b><math>\beta</math>2MG</b>	ACCCCACTGAAAAGATGA	ATCTTCAAACCTCCATGATG	114 bp	MWG (eurofins)

### 3.1.11. RNA samples

Table 11. Purchased RNA samples from human, non-neoplastic brain tissue. Sample concentration, patient data and manufacturing company are listed on the right columns.

<b>Temporal lobe</b>	2,25	26	M	BioChain®, Newark (CA), USA
<b>Frontal lobe</b>	2,53	27	M	BioChain®, Newark (CA), USA
<b>Occipital lobe</b>	1,90	41	M	BioChain®, Newark (CA), USA
<b>Corpus callosum</b>	1,69	26	M	BioChain®, Newark (CA), USA
<b>Total human brain</b>	1	18	M	BioChain®, Newark (CA), USA
<b>Total adult brain</b>	1	66	F	Agilent Technologies, Santa Clara (CA), USA
<b>Human Universal Reference</b>	1	N/A	N/A	Agilent Technologies, Santa Clara (CA), USA

In Table 12 is a list of RNA samples from glioma tumors obtained from patients that underwent surgery at the Department of Neurosurgery (Prof. Dr. A. Brawanski and Prof. Dr. M. Proescholdt) at Regensburg University Hospital, after informed and written consent had been given. Tissue samples were initially snap frozen and stored at -80°C. RNA was extracted only from tissue samples that had a tumor content of more than 80%. Experiments were approved by the ethics committee of the University of Regensburg (#13-101-0005).

Table 12. List of RNA extracted from glioma tumors obtained from the department of neurosurgery of the University of Regensburg Hospital. Patient information as well as RNA concentration are also listed above.

<b>A2</b>	303	Diffuse Astrozytoma (WHO grade II)	40	M
<b>AA7</b>	367	Anaplastic Astrozytoma (WHO grade III)	37	M

<b>GB42</b>	1213	Glioblastoma (WHO grade IV)	68	F
<b>GB44</b>	1434	Glioblastoma (WHO grade IV)	45	M
<b>GB45</b>	323	Glioblastoma (WHO grade IV)	69	M
<b>GB46</b>	130	Glioblastoma (WHO grade IV)	61	F
<b>GB47</b>	222	Glioblastoma (WHO grade IV)	51	F
<b>GB49</b>	283	Glioblastoma (WHO grade IV)	65	M
<b>GB50</b>	230	Glioblastoma (WHO grade IV)	71	F
<b>GB52</b>	61	Glioblastoma (WHO grade IV)	43	M
<b>GB53</b>	118	Glioblastoma (WHO grade IV)	48	M

Moreover, RNA from other commercially available immortalized glioblastoma cell lines was retrieved and included in gene expression assays. RNA from MeJuSo cells, corresponding to a melanoma cell line with epithelial morphology<sup>43, 44</sup>, was kindly provided by the research group of Prof. Anja Bosserhoff (Chair of biochemistry and molecular medicine at the University of Erlangen).

Table 13. List of cell lines with their corresponding tumor of origin, patient data.

<b>A-172</b>	Glioblastoma (WHO-Grade IV)	53	M
<b>T98G</b>	Glioblastoma (WHO-Grade IV)	61	M
<b>TP365</b>	Glioblastoma (WHO-Grade IV)	N/A	F
<b>MeJuSo</b>	Melanoma	58	F

Also, RNA from seven human glioblastoma stem cell lines was included in this work.

Table 14. RNA concentration extracted from glioblastoma initiating stem cell lines.

<b>NCH644</b>
<b>NCH421K</b>
<b>NCH601</b>
<b>NCH465</b>
<b>NCH660K</b>
<b>NCH711</b>
<b>NCH636</b>
<b>NCH14225</b>

### 3.1.12. Solutions and other biochemical compounds/ materials

Table 15. List of solutions and other biochemical compounds/ materials used in this work.

<b>100 bp-DNA-Ladder</b>	Fermentas, Waltham (MA), USA
<b>DEPC-Water (DNase/RNase-free)</b>	Bioline, London, UK
<b>RNase-free Water</b>	Qiagen, Hilden, Germany
<b>Tris-EDTA buffer (JETquick Plasmid Miniprep Spin Kit)</b>	Genomed GmbH, Löhne, Germany

### 3.1.13. Software

In the following table all software used throughout the course of this work are listed.

Table 16. List of softwares and their developing companies which were used during this work.

<b>CASAVA1.8.2</b>	Illumina, San Diego (CA), USA
<b>cutadapt v1.11</b>	Department of Computer Science, TU Dortmund, Germany
<b>DAVID (Database for Annotation, Visualization and Integrated Discovery)</b>	Leidos Biomedical Research, Inc., National Cancer Institute at Frederick, Frederick (MD), USA
<b>EndNote (Version X7.5)</b>	Thomson Reuters, New York City (NY), USA
<b>FASTQC v 0.11.5</b>	Babraham Bioinformatics, Cambridge, UK.
<b>Genome Reference Consortium Human Build 38 (GRCh38.p7)</b>	ENSEMBLE gene annotation system, <a href="#">European Bioinformatics Institute</a>

<b>GraphPad Prism (Version 6.1)</b>	GraphPad Software, La Jolla (CA), USA
<b>GenePattern GSEA module v16</b>	Broad Institute, Cambridge (MA), USA
<b>hisat2-2.0.4</b>	Center for Computational Biology, Johns Hopkins University, Baltimore (MD), USA
<b>MARS Data Analysis Software (Version 2.41)</b>	BMG Labtech, Ortenberg, Germany
<b>Microsoft Office (Version 2007)</b>	Microsoft, Redmond (WA), USA
<b>NanoDrop 2000-Software (Version 1.4.2)</b>	Thermo Fisher Scientific, Waltham (MA), USA
<b>Omega Control-Software (Version 3.00)</b>	BMG Labtech, Ortenberg, Germany
<b>R (Version 3.1.2)</b>	<a href="https://www.r-project.org/">https://www.r-project.org/</a>
<b>StepOne™ Software (Version 2.1)</b>	Applied Biosystems, Foster City (CA), USA
<b>Venny 2.1.0.</b>	BioinfoGP, Spanish National Biotechnology Center, Madrid, Spain

## 3.2. Methods

### 3.2.1. Cell Biology Methods

#### 3.2.1.1. Cell thawing and culture

All cells were purchased from CLS cell lines service (see section 3.1.). These were frozen in FBS containing 10 % DMSO, and stored in liquid Nitrogen. For subculturing purposes, frozen-stored cells were quickly thawed in a water bath adjusted to 37°C. The cell-containing solution was then

pipetted under the laminar flow hood, into a culture Flask containing 10 ml DMEM cell culture medium with 10% FBS (v/v), 100 U/ml Penicillin and 100 ug/ml Streptomycin (cDMEM)<sup>45</sup>. A medium change was done 24 hours after.

#### 3.2.1.2. Culture of glioblastoma cell lines

For the experiments carried out in this work, cells were cultured under normoxic conditions (21% O<sub>2</sub> and 5% CO<sub>2</sub>, with 95% atmospheric humidity, at 37°C), in cDMEM medium, as explained before. When cultured cells achieved a confluency between 70 to 80%, they were splitted with the use of Trypsin 1X (Sigma-Aldrich). Trypsin is a catalytic enzyme, which cleaves proteins on cell surfaces allowing cells to detach from one another as well as from the culture flask<sup>46</sup>. For this purpose, old medium was first removed by aspiration, and cells were washed with prewarmed 10 ml DPBS. After complete removal of DPBS by aspiration, 1.5 ml (for T75 m2 Flasks) of trypsin was given directly to the cells. Incubation was performed at 37°C in the cell culture incubator under normoxic conditions, for a maximum of 2 minutes. In order to stop the lytic actions of trypsin in the cells, 8.5 ml fresh cDMEM medium was added, and remaining attached cells were mechanically detached from the flasks bottom (by pipetting). The complete solution (medium containing detached cells) was recollected in a 15 ml Tube and centrifuged for 4 minutes at room temperature at a maximum of 1,000 x *g*. After removing the supernatant, 10 ml fresh Medium (containing FCS and antibiotics) was added to dissolve the cell pellet. For culture, 1 ml of the cell suspension was added to a new flask containing 9 ml fresh Medium (1:10 splitting).

#### 3.2.1.3. Cell Harvesting

Single cell suspensions were obtained either for gene expression analyses (qRT-PCR, transfection) or functional assays (transfection, proliferation). For harvesting single cell suspensions, medium was aspirated and the cells were washed with DPBS. Afterwards, 1.5 ml trypsin-EDTA were added and incubated for a maximum of 2 minutes at 37°C. After all cells were detached and passed on to a 15 ml tube, they were centrifuged at 1,000 x *g* for 4 minutes at room temperature. Supernatant was discarded; 10 ml medium was added to dissolve the cell pellet. Once the cell pellet was dissolved in cDMEM, approximately 1 ml was transferred onto a 1.5 ml tube and counted with a Neubauer Chamber. The cell counting chamber should be prepared by fixing a glass cover on its central area. Afterwards, around 10 µl of cell suspension were carefully pipetted onto the chamber. Under the microscope, cells lying inside the four external counting grids were counted (see Figure 1), using the following formula: concentration of cells/ml = No. of cells/ Volumen (ml)) x 10,000, where Volume is

the total amount of grids counted (4) and 10,000 accounts for the total volume of Medium in which cells were diluted in. In this way a total amount of cells per ml was obtained.<sup>47</sup>

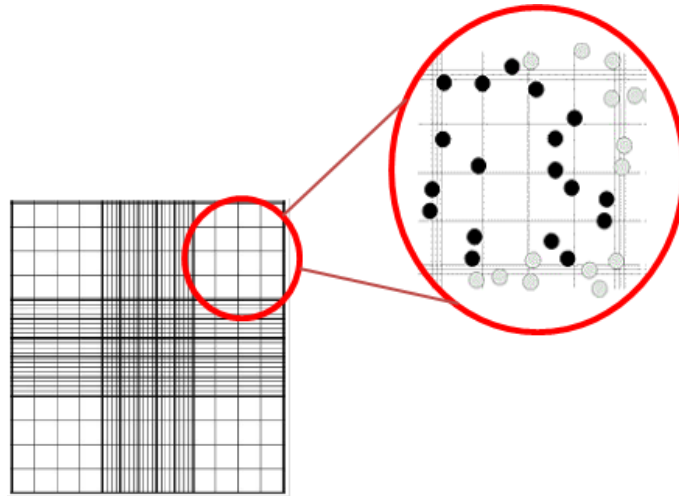


Figure 1. Neubauer cell counting chamber. The four external counting grids are used during this process. Viable cells inside the squares (black dots) are counted and used in the formula described above to determine the number of cells per ml. (Images adapted from Celeromics.com).<sup>48</sup>

#### 3.2.1.4. Transfection of GBM cell lines with miRNA mimics

Transfection is the process of introducing foreign nucleic acids into cells<sup>48</sup>. For this procedure, Lipofectamine™ 2000 transfection reagent was used. Lipofectamine™ 2000 is a cationic liposome reagent that allows the passage of nucleic acids across the cell membrane by wrapping them in liposomes, a process known as lipofection<sup>49</sup>.

*RNAi*. RNA interference (RNAi) is the process of regulating the expression of protein-coding genes, using double-stranded RNA<sup>20</sup>, by loading on to Argonaute 2 (Ago2), the core catalytic component of the RNA-induced-silencing-complex (RISC)<sup>51, 52</sup>. In the cytoplasm, small interfering RNAs are cleaved, the so called “passenger” strand is degraded, and the remaining strand, called “guide” strand, will bind to RISC, and guide it into recognizing and binding to the target mRNA<sup>53</sup>.

*miRNA mimics*. For transient miRNA transfections, miRNA *mirVana* mimics (Thermo Fischer Scientific, Waltham (MA), USA) were purchased. Micro-RNA (miRNA) mimics are chemically synthesized, 20-23 nucleotide-long, double-stranded, RNA molecules that mimic endogenous miRNAs and enable functional analysis of miRNAs<sup>54</sup>. The negative control miRNA *mirVana* mimic Negative Control #1 was used. All mimics came lyophilized and were dissolved in sterile conditions

under a laminar flow hood using RNase-free water to obtain a concentration of 5  $\mu$ M. Aliquots were prepared and stored at -20°C.

*Transfection.* For transfection, depending on the plate's size, a determined amount of cells (see table 18) were seeded in DMEM medium with 10% FBS without antibiotics. After 24 hours, when a confluency between 70-80% was reached, cells were transfected with miRNA mimics. Two separate tubes were prepared, containing 50 to 250  $\mu$ l of prewarmed OPTI-MEM® I medium. In the Lipofectamine™ 2000 mix 0.75 - 5  $\mu$ l/well Lipofectamine™ 2000 was added, mixed by gentle tapping, and incubated at room temperature for 5 minutes. In the miRNA-containing mix, 30nM/well miRNA mimic was added and mixed by gentle tapping. Afterwards, Lipofectamine™ 2000- and miRNA-containing solutions were mixed into a same tube and incubated at room temperature for 20 minutes. During this time, medium was exchanged (DMEM with 10% FBS without antibiotics). Afterwards, Lipofectamine™ 2000 plus miRNA solution was added in a dropwise fashion into each well. Cells were then incubated at 37 °C and 5% CO<sub>2</sub> conditions. After 48 hours post-transfection cells were either harvested and lysed for RNA isolation, or used in functional assays.<sup>55, 56</sup>

Table 17. Components for miRNA Transfection with Lipofectamine™ 2000. Table adapted from Invitrogen.com.

Culture Vessel	Number of cells	Shared Reagents		RNAi Transfection	
		Vol. of plating medium	Vol. of dilution Medium	miRNA mimic	Lipofectamine™ 2000
96-well plate	7.500/ well	100 $\mu$ l	2 x 25 $\mu$ l	30 nM	0.75 $\mu$ l
6-well plate	250.000/ well	2.5 ml	2 x 250 ml	30 nM	5 $\mu$ l

### 3.2.2. Molecular Biology Procedures

#### 3.2.2.1. miRNA Extraction

Total RNA containing miRNAs was extracted from transfected and untransfected cells using the Qiagen miRNeasy mini kit (Qiagen, Hilden, Germany). Its principle relies on a silica membrane with selective binding properties, and a specialized high-salt buffer system that allows the binding of miRNA molecules to the silica membrane<sup>57</sup>.

Cells in culture plates or cell pellets containing ~500,000 cells were used for this procedure. For RNA isolation, cells and/or pellets were washed with DPBS and lysed using 750 µl of QIAzol lysis reagent (included in the miRNeasy Mini Kit). This solution is a highly denaturing monophasic solution of phenol and guanidine thiocyanate, which inactivates RNases to ensure RNA integrity. The solution was homogenized by pipetting the lysate at least 5 times up and down. In order to separate nucleic acids from other organic cellular components, chloroform (140 µl) was added and mixed with the lysate, which was afterwards centrifuged 15 minutes at 4°C at a speed of 12,000 x *g*. The aqueous upper phase was then transferred into a new collection tube, and the lower phase was discarded. To allow appropriate RNA binding conditions, one volume (~550µl) of RNase-free 70% EtOH was added, and the solution was well mixed by pipetting. The whole solution was then transferred to an RNeasy spin column placed in a 2ml collection tube. It was centrifuged for 15 seconds at 8,000 x *g* at RT and the flow through was discarded. The membrane was washed with 700 µl of buffer RWT. Afterwards, samples were washed adding 500µl RPE buffer to the RNeasy spin column and centrifuging it for 15 seconds at 8,000 x *g*. The flow-through was discarded, and this step was repeated prolonging the centrifuging time to 2 minutes. The spin column was then placed in a new 2ml collection tube, and centrifuged once more at 12,000 x *g* for 1 minute. After this step, the miRNeasy spin column was placed in a new 1.5 ml tube, and 30 µl RNase-free water was added directly to the spin column membrane. RNA was eluted by centrifugation at 8,000 x *g*. Samples were placed on ice immediately. To determine the final RNA concentration, absorbance at 260 nm was measured.

#### 3.2.2.2. Reverse Transcription of cDNA

Reverse transcription is the process by which a reverse transcriptase (RNA-dependent polymerase) transcribes from a single strand RNA a complementary DNA strand (cDNA). For this procedure, the miScript RT II Kit from Qiagen (Qiagen, Hilden, Germany) was used. 1 µg total RNA was used for reverse transcription. Afterwards a 2 µl reverse transcriptase-containing Master Mix was added, to achieve a final volume of 20 µl (see tables 20 and 21). For the RT-containing master mix miScript HiFlex Buffer was used. This kit allows to specifically detect miRNAs, by polyadenylation of mature miRNAs. During cDNA reverse transcription, oligo-dT primers which possess a 3' degenerate anchor are used, and a universal tag sequence on the 5' end is added, which allows amplification of mature miRNA during qRT-PCR<sup>58</sup>. The reverse transcription reaction was at last placed on the Thermocycler using the program described in table 19. cDNA samples were stored at -20°C.



Table 18. RT Master Mix Components (1x). \*The use of HiFlex Buffer allows real-time PCR quantification of mature miRNA, precursor miRNA, ncRNA, and/or mRNA using individual miRNA primer assays.

Reagent	Volume of 20 $\mu$ l/ sample
HiFlex Buffer*	4 $\mu$ l
10x nucleic mix	2 $\mu$ l
RNase-free Water	Variable
miScript reverse transcriptase mix	2 $\mu$ l
Template RNA	variable

Table 19. cDNA Transcription Program in Thermo Cycler.

Time	Temperature
60 minutes	37°C
5 minutes	95°C
Indefinitely	4°C

### 3.2.2.3. Quantitative Real Time PCR

Real-time quantitative reverse-transcription PCR, also known as qRT-PCR, is the measurement of the increase in double stranded DNA (dsDNA) in the course of the reaction (in real time)<sup>59</sup> and is therefore used for quantification of gene expression. It follows usually 3 steps: denaturation, annealing and elongation. During denaturation, the cDNA samples are exposed to high temperatures in order to break apart their hydrogen bonds to separate the DNA strands. In the annealing phase primers will attach to the cDNA strand. During elongation the DNA-polymerase will add complementary nucleotides on to the single-stranded cDNA forming new double-stranded DNA fragments.

SensiFAST™ SYBR® Hi-ROX Mix (Bioline, Luckenwalde, Germany) and miScript SYBR Green PCR Kit (Qiagen, Hilden, Germany) were used for this purpose. SYBR Green is an asymmetrical cyanine dye that binds to the DNA double strand. The resulting DNA-dye complex absorbs blue light ( $\lambda_{\max}$  = 488 nm) and emits green light ( $\lambda_{\max}$  = 522 nm). During the exponential phase of the PCR reaction, the fluorescence is proportional to the amount of PCR products obtained.

SensiFAST™ SYBR® Hi-ROX Mix was used to evaluate the expression of ZEB1 and ZEB2 in control and transfected cells, using  $\beta$ 2-MG as reference (housekeeping) gene. miScript SYBR Green PCR Kit was used to confirm the overexpression of miRNAs 200a/b/c, 141 and 429 in transfected cells compared to cells transfected with a negative control as well as to untransfected cells. Samples were prepared in triplicates, including a negative, water only-containing control (*RNase-free* water from Qiagen). Samples were all previously diluted 1:10 with RNase-free water. The qRT-PCR reaction was performed as described below.<sup>60</sup>

Table 20. Components of the master mixes prepared for qRT-PCR reactions using both Hi-ROX and miScript SYBR Green mixes.

SensiFAST™ SYBR® Hi-ROX mix		miScript SYBR Green mix	
Components	Volume of 20 $\mu$ l /probe	Components	Volume of 25 $\mu$ l /probe
SensiFAST™ SYBR® Hi-ROX Mix	12.5 $\mu$ l	miScript SYBR Green	12.5 $\mu$ l
Primer Reverse	0.75 $\mu$ l	10x miScript Universal Primer	2.5 $\mu$ l
Primer Forward	0.75 $\mu$ l	10x miScript Primer Assay	2.5 $\mu$ l
RNase-free H <sub>2</sub> O	6 $\mu$ l	RNase-free H <sub>2</sub> O	6.5 $\mu$ l
cDNA	1 $\mu$ l	cDNA	1 $\mu$ l

Primer assays to evaluate the expression of the miRNA 200 Family (200a, 200b, 200c, 141 and 429) in glioblastoma cell lines, glioblastoma tumors (RNA), glioblastoma stem cells (RNA) and normal brain tissue (RNA) were purchased from Qiagen (miScript primer assays (Qiagen, Hilden, Germany)). These are synthesized mature miRNA forward primer sequences (see Table 8, section 3.1.8) that, together with the use of a universal reverse primer (supplied in the miScript SYBR Green Kit (Qiagen, Hilden, Germany)), specifically target each one of the miRNAs mentioned above. As housekeeping RNA Hs\_SNORD68\_11, an extra miScript primer assay coding small nucleolar RNA, C/D box 68<sup>61</sup>, was used. The primers came lyophilized and were dissolved in sterile conditions under a laminar flow hood, using 550  $\mu$ L TE Buffer (TE contained in the JETKit from Genomed GmbH, Löhne, Germany) as suggested by the manufacturer. They were aliquoted and stored at -20°C.

All other primers for qRT-PCR were custom-synthesized (Eurofins, Jena, DE). The ZEB1/ ZEB2 primer pair sequences were obtained from the Harvard primer bank<sup>62</sup>.  $\beta$ 2-Microtubulin ( $\beta$ 2MG) was used as housekeeping gene. Primers came lyophilized, and were later dissolved in sterile conditions under a cell culture hood, using RNase-free water (from Qiagen, Hilden, Germany) to obtain a concentration of 100  $\mu$ M. They were stored at -20°C, and thawed shortly before being used in a reaction.

PCR-plates were used for this procedure. All reagents were kept on ice at all times.

Table 21. Parameter settings for the qRT-PCR using Eurofins primers.

1	95	02:00
40	95	00:50
	60	00:15
1	95	00:15
	60	01:00
	95	00:15

Table 22. Parameter Setting for the qRT-PCR using miScript primer assays primers.

1	95	15:00
40	95	00:15
	55	00:30
	70	00:30
1	95	00:15
	60	01:00
	95	00:15

Analyses were performed using the comparative Ct( $2^{-\Delta\Delta C_t}$ ) method module within the StepOne™ Software (Version 2.1) (Applied Biosystems (Foster city (CA), USA)).

#### 3.2.2.4. Agarose-Gel electrophoresis

PCR products can be analyzed by agarose-gel electrophoresis, in order to confirm specificity of the replicated DNA fragment by assessing its length (nucleotides). For this purpose, PCR samples were mixed with loading buffer (Orange G (Carl Roth GmbH & Co. KG, Karlsruhe, Germany)) and loaded onto a 2% agarose gel. Electrophoresis was done at 120 V. Smaller molecules are able to advance further on the gel compared to bigger ones. The size of the molecules is assessed with the help of a DNA-ladder loaded parallel with the PCR products, which displays bands along the gel with a determined size based on amount of base pairs.

Table 23. Composition of agarose gel and TAE-Buffers used for Agarose-Gel Electrophoresis of PCR products. \*(1x TAE buffer is made out of 200 ml 50x TAE and 800 ml H<sub>2</sub>O).

Agarose Gel and TAE-Buffers	
<b>Agarose Gel (2%)</b>	<ul style="list-style-type: none"> <li>- 2 g Agarose (universal, peqGOLD Universal Agarose, pequLab, VWR International, Ismaning, Deutschland) dissolved in 100 ml 1x TAE-Puffer*</li> <li>- 5 µl Red Safe (iNtRON Biotechnology, Seongnam, Korea)</li> </ul>
<b>TAE-Buffer (50x)</b>	<ul style="list-style-type: none"> <li>- 242 g Tris base (Sigma Aldrich, St. Louis (MO), USA)</li> <li>- 57,1 ml Acetic acid (Carl Roth GmbH &amp; Co. KG, Karlsruhe, Germany)</li> <li>- 100 ml 0,5 M EDTA (Carl Roth GmbH &amp; Co. KG, Karlsruhe, Germany)</li> <li>- Adjust pH to 8,0</li> <li>- Add 1L H<sub>2</sub>O</li> </ul>

The DNA was visualized using UV light (Gel iX manager, Intas, Göttingen, DE).

### 3.2.2.5. Next Generation Sequencing (NGS)

*mRNA libraries.* Libraries for Next Generation Sequencing (NGS) were prepared using 500 ng mRNA previously isolated from transfected and untransfected cells (miRNease mini Kit (Qiagen, Hilden, Germany)) and the TruSeq<sup>®</sup> RNA Sample Preparation Kit v2 (Illumina, San Diego, CA, USA). Instructions from the manufacturer were adapted to a 60% protocol.

The first step was to purify and denature the RNA molecules. For this purpose, RNA purification beads (RPB) were added to the samples, incubated (Thermocycler) at 65°C for five minutes - to allow RNA to bind to the beads - and later on washed on a 96-well plate (Bead Washing Buffer, BWB), eluted (Elution Buffer, EB) and allowed to rebind (Bead Binding Buffer). The manufacturer provided all buffers and reagents. After a second wash, RPBs were re-suspended in Elution, Prime, Fragment mix (EPF) and incubated (Thermocycler) at 94°C for eight minutes.

The next step was to transcribe RNA into cDNA. This starts with the synthesis of a first strand cDNA using a SuperScript II reverse-transcriptase-containing first strand master mix (supplied by Illumina). The incubation (Thermocycler) times were as follows: 10 minutes at 25°C, 50 minutes at 42°C and 15 minutes at 70°C. Afterwards, a second strand cDNA was synthesized incubating the RBDs with a second strand mix at 16°C for one hour. The resulting double stranded cDNA was purified using AMPure XP beads (Beckman Coulter, Brea, CA, USA).

After creating a double stranded cDNA an end repair had to be performed. For this step, the RPBs were incubated (Thermocycler) in End Repair Mix (ERM) for 30 minutes at 30°C, and afterwards cleaned up again with AMPure XP beads. Up to this point, the following step was to add A-nucleotides to the 3' end of the cDNA by adding an A-tailing mix (incubation details: 37°C for 30 minutes followed by 70°C for five minutes). Indexed adapters were ligated to the end-repaired A-tailed cDNA at 30°C for ten minutes, a Ligation Control mix was added and the libraries were cleaned up again with AMPure XP beads.

Finally an enrichment of DNA fragments was done through PCR amplification. This was performed with PCR reagents provided in the kit. The following cycling conditions were applied: denaturation at 98°C for 30 seconds, 15 cycles of 10 seconds at 98°C, 30 seconds at 60°C, 30 seconds at 72°C and a final extension at 72°C for five minutes. The amplified libraries were one last time purified with AMPure XP beads. Quality control was assessed with the use of a Bioanalyzer® (Agilent, Santa Clara (CA), USA) and Next Generation Sequencing (NGS) was finally performed using a HiSeq 1000 sequencer (Illumina, San Diego (CA), USA).

*Next Generation Sequencing.* Sequencing of the miRNA libraries was performed in a Core Facility on Campus of the University of Regensburg, in the competence Center for fluorescence bioanalytics (Kompetenzzentrum für Bioanalytik (KFB)) using a HiSeq 1000 sequencer from Illumina (Illumina, San Diego (CA), USA). Libraries were quantified using the KAPA SYBR FAST ABI Prism Library Quantification Kit (Kapa Biosystems, Woburn (MA), USA). Equimolar amounts of each library were used for cluster generation on the cBot with the TruSeq SR Cluster Kit v3 (Illumina, San Diego (CA), USA). The sequencing run was performed using the indexed, 50 cycles single read (SR) protocol and the TruSeq SBS v3 Kit (Illumina, San Diego, CA, USA).

### 3.2.3. Biochemical Methods

#### 3.2.3.1. Proliferation Assay

Bromodeoxyuridine (5-bromo-2'-deoxyuridine, BrdU) is a synthetic nucleoside, analogous to thymidine, which is commonly used in the detection of proliferating cells in living tissues. BrdU substitutes thymidine during DNA replication, being able to be incorporated itself into the DNA of the cell. The amount of incorporated BrdU can be measured by detection with a specific antibody.<sup>63</sup>

For this assay, cells were seeded in black 96-well plates with clear bottom (Greiner Bio-One GmbH, Frickenhausen, Deutschland) and transfected as previously described (see transfection section

above). After 48 hours, old medium was replaced with 100 µl fresh DMEM containing 10% FBS and antibiotics. Afterwards, 10 µl of BrdU labelling reagent diluted 1:100 in DMEM was added, and cells were incubated for 3 hours at 37°C and 5% CO<sub>2</sub>. After the incubation period, the solution (medium and BrdU reagent) was removed, and cells were fixed and partially denaturated with Fix Denat solution (200 µl for 30 minutes) provided in the kit. The next step involved the antibody-containing solution (100 µl, 1:100), which was incubated for a total time of 1.5 hours at room temperature. Cells were washed three times with 200 µl (1:10) washing solution (washing buffer plus dH<sub>2</sub>O). Finally, the 1:100 diluted substrate solution (100 µl) was added to each well. The 96-well plate was taken to a luminometer (Fluostar), where the chemoluminescence was measured.

### 3.2.3.2. Apoptosis Assay

Programmed cell death (apoptosis) occurs either as part of a normal developmental process, or as a mechanism of defense to avoid replication of damaged cells. It is first initiated by either intrinsic or extrinsic signals that activate the caspase cascade (mainly caspases 3, 6 and 7)<sup>64, 65</sup>. Here, the activity of caspase 3/7 was measured in cells overexpressing miRNAs of the 200 family compared to negative controls. This assay consists of a buffer solution which permeabilizes cell membranes allowing the caspase-3/7 profluorescent substrate rhodamine 110 (bis-(N-CBZL-aspartyl-L-glutamyl-L-valyl-L-aspartic acid amide; Z-DEVD-R110)) to enter the cell. Caspase 3/7 later cleaves DEVD peptides the rhodamine-containing caspase substrate, which at an excitation of 499nm emits a fluorescent signal, proportional to the amount of caspase 3/7 activity, which has a maximum emission of 521nm.<sup>65</sup>

For this purpose, cells previously seeded in black 96-well plates without clear bottoms (Thermo Fisher Scientific) were transfected with miRNAs as described in section 3.2.1.4. of this chapter. 48 hours after transfection medium was replaced with DMEM containing 10% FBS and antibiotics (50 µl) and 50 µl of Apo-ONE<sup>®</sup> were added to each well, including one blank (no cells with Apo-ONE<sup>®</sup>) and a negative control (cells without Apo-ONE<sup>®</sup>). Cells were incubated at room temperature in the dark for approximately 4 hours. The fluorescence intensity was measured with a spectrophotometer (Fluostar), using an excitation wavelength of 475 nm and an emission wavelength of 500-550 nm<sup>66</sup>.

### 3.2.4. Bioinformatics

#### 3.2.4.1. The Cancer Genome Atlas

The **Cancer Genome Atlas** (TCGA) database<sup>67</sup> (<https://tcga-data.nci.nih.gov>) was accessed and data extracted on 21.10.2013. For analysis of miRNAs, raw (level 1) data for the one-color miRNA platform h-mirna\_8x15k was downloaded for 10 normal brain and 537 glioblastoma samples.

Analysis was performed with R v3.1.1 and the package limma<sup>68</sup>. Background correction was performed with the normexp method<sup>69</sup> and normalization in between arrays with the quantile method<sup>70</sup>. Differential expression was calculated with limma and p-values were adjusted according to Benjamini-Hochberg<sup>71</sup>. For analysis of survival or comparison of glioblastoma subgroups, clinical or subgroup data from Brennan et al.<sup>67</sup> and the normalized expression values for the miRNAs of interest were matched. For survival analysis, the dataset was divided into a low-expression and a high-expression subgroup by the median of miRNA expression. Survival analysis was performed with GraphPad Prism v5.0. A log-rank test (Mantel-Cox) was applied to compare the survival of the low- and high expression subgroup.

For gene expression data, prenormalized data (level 3) for 10 non-neoplastic brain tissue samples and 563 glioblastoma samples were downloaded for the gene expression platform Agilent G4502A and survival analysis was performed as described above.

#### 3.2.4.2. NGS Analysis

Image analysis and base calling resulted in .bcl files which were then converted into .fastq files by the CASAVA1.8.2 software (Illumina, San Diego (CA), USA). Analysis of NGS data was performed with freely (online-) available software. Reads were trimmed with cutadapt v1.11 (Department of Computer Science, TU Dortmund, Germany, <http://code.google.com/p/cutadapt/>), quality control was performed with FASTQC v 0.11.5 (see Table 16)<sup>72</sup> and trimmed reads were aligned with hisat2-2.0.4 (Center for Computational Biology, Johns Hopkins University, Baltimore (MD), US, <https://ccb.jhu.edu/software/hisat2/>) with standard settings against the human genome assembly GRCh38 (ENSEMBLE gene annotation system, European Bioinformatics Institute) allowing no mismatch. Read counting for each ENSEMBLE gene was performed with the function "feature counts" from the subread package v1.5.1 using the gene set version GRCh38.87.

All further analyzes were performed with the free software R v3.1.1, Bioconductor v3.0<sup>73</sup>.

#### 3.2.4.3. Principal component analysis (PCA)

Principal Component Analysis (PCA) is a mathematical algorithm used to reduce the dimensionality of a dataset while preserving "the most variability possible"<sup>74</sup>. PCA analysis was used in this work to analyze the results obtained from mRNA libraries, to search for differentially expressed genes in cells either transfected with miRNA mimics or an inactive miRNA negative control. For the generation of a PCA plot, rlog normalized values were used. These were plotted onto a so-called biplot, in which an x

(PCA1) and y (PCA2) axis are drawn, which carry adjusted values depending on the characteristics of the dataset used. This serves to simplify variability and cluster similarities<sup>75</sup>. Differential expression was calculated with DESeq2 v. Based on the PCA results, samples were divided into 3 groups for each cell line, corresponding to cluster A (miR200a3p and miR1413p), cluster B (miR200b3p, miR200c3p and miR429) and cluster C (miR200a 5p,miR200c 5p and negative control miRNA).

#### 3.2.4.4. Venn Analysis

Venny 2.1.0. (<http://bioinfogp.cnb.csic.es/tools/venny/>) is an interactive tool used to compare data lists using Venn Diagrams<sup>76</sup>. The objective is to find overlapping components between different datasets. For this purpose, based on the results from the PCA analysis, an excel table was created dividing the dataset into six groups: A (miR200a 3p and miR141 3p) and B (miR200b 3p, miR200c 3p and miR429) as well as negative controls (miR negative control, miR200a 5p and miR200c 5p) for each cell line (U87 and U251). From this table, the significant downregulated and upregulated genes were copied into a new table (adjusted p-value < 0.05 and fold logarithmic change of  $\leq -0.6$  and  $\geq 0.6$  respectively). The list of genes that applied to these criteria was then used to map a Venn diagram. The results showed overlapping deregulated genes among the datasets.

#### 3.2.4.4. GO term enrichment analysis

The identification of enriched biological terms, so-called gene ontology (GO) terms, was carried out using the Database for Annotation, Visualization and Integrated Discovery (DAVID) (<https://david.ncifcrf.gov/>)<sup>77,78</sup>. The list of significantly deregulated genes (Ensembl genes) in each group was imported for the analysis (<http://www.ensembl.org/index.html>). After the appropriate background species (Homo sapiens) was chosen, the software searched for the enriched GO terms (biological process, cellular component and/or molecular function) in the imported list. After selecting the functional annotation chart, GO terms identified in the imported list were displayed and sorted according to their Benjamini-corrected p-value of <0.05.

#### 3.2.4.5. Gene Set Enrichment Analysis (GSEA)

Gene set enrichment analysis is a tool used for analysis of gene expression data, aiming to find enrichment of groups of genes that share a common biological function, chromosomal location, or regulation (gene sets) in a determined sample group<sup>79</sup>. For this work, RPKM values were analysed using GenePattern and the GSEA module v16 (<http://software.broadinstitute.org/cancer/software/genepattern>)<sup>80</sup>. The cut off values were a false discovery rate (FDR) <0.25 and a normalized p-value of <0.05.



#### 3.2.4.6. Other statistical methods

Further statistical analyzes and evaluations were carried out using the programs Microsoft Office Excel (version 2007) or GraphPad Prism (v6.1). p-values  $<0.05$  were respectively considered to be statistically significant.

## 4. Results

### 4.1. Expression of the miR200 family

The first step was to see how the different members (and different strands) of the miR200 family were expressed in glioblastoma cell lines and glioblastoma tumors. Gene expression of glioblastoma cell lines including the malignant melanoma cell line MelJuSo were analyzed through quantitative, real time polymerase chain reaction (qRT-PCR) using miRNA primer assays specific for mature members of the miR200 family, strands 3p and 5p. Human universal reference RNA (HUR) was used as the calibrator between genes. Normalization was done using the  $2^{-\Delta\Delta Ct}$  method according to the Livak and Schmittgen model<sup>81</sup>. As seen in figure 1, the overall expression of the 3p strand of miR200 family members is lower (min. expression fold change of 0.019 (miR200c 3p in TP365 cells) and max. expression fold change of 0.59 (miR141 3p in TP365) compared to 5p strands (min. expression fold change of 0.16 (miR141 5p in U118) and max. expression fold change of 5.64 (miR200b 5p in U118)). There was no relevant difference in expression levels of the miR200 family strands 3p and 5p in glioblastoma cell lines compared to malignant melanoma cells.

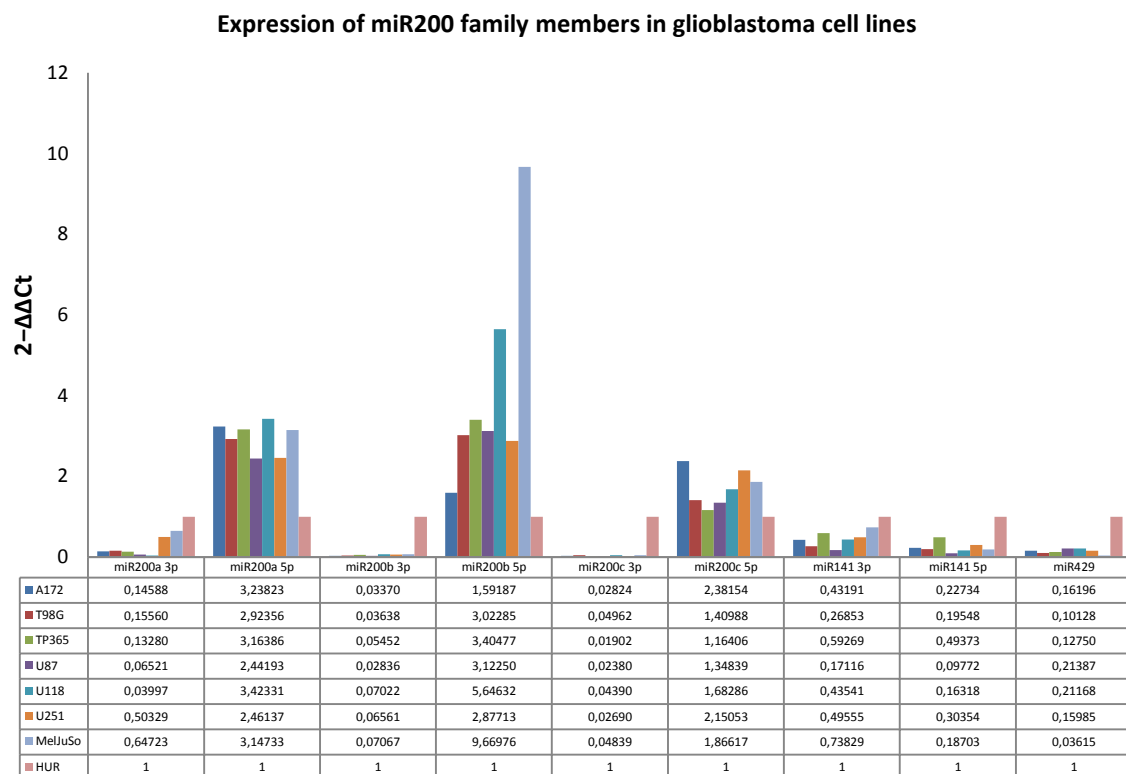


Figure 1. Relative miRNA expression in glioblastoma cell lines. Cell lines show higher levels of the 5p strand of the miR200 family members compared to 3p. No significant expression difference is seen between glioblastoma cell lines and the malignant melanoma cell line MelJuSo.

In glioblastoma tumors, the expression levels of miRNAs 200a 3p and 141c 3p showed higher values in all samples compared to their counterparts (miR200a 5p and miR141c 5p; max. expression fold change of 45 (miR200a 3p) and 35 (miR141 3p) respectively), as well as to all other members of the miR200 family strands 3p and 5p. miRNA expression levels in glioblastoma tumors were also compared to diffuse astrocytoma and anaplastic astrocytoma (WHO-grades II and III respectively). The miR200 family members were expressed at lower values in diffuse astrocytoma (WHO grade II) and anaplastic astrocytoma (WHO grade III) compared to glioblastoma (WHO grade IV).

**Expression of miR200 in glioblastoma tumors**

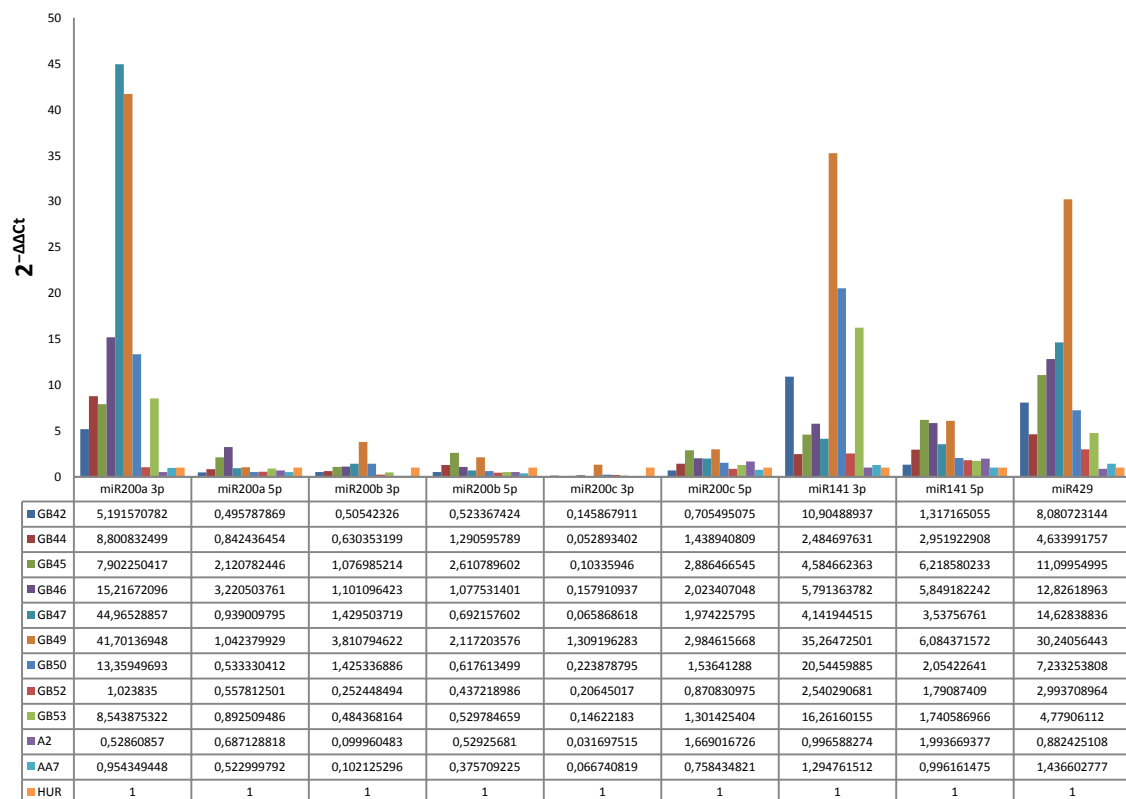


Figure 2. Relative miRNA expression in tumors. Expression of the 3p and 5p strands of the miRNA 200 family in Glioblastoma (WHO grade IV) compared to diffuse astrocytoma (WHO grade II) and anaplastic astrocytoma (WHO grade III).

An overall expression graph including glioblastoma samples compared to glioblastoma cell lines and non-neoplastic brain tissue showed a difference in expression pattern between tumors and cell lines. Whereas in glioblastoma tumors the 3p strands of miR200a and miR200c are expressed at significantly higher levels as the rest of the miR200 family members, the expression patterns observed in glioblastoma cell lines suggests a higher expression of the 5p strand in all miR200 family members and a lower expression of the 3p strand.

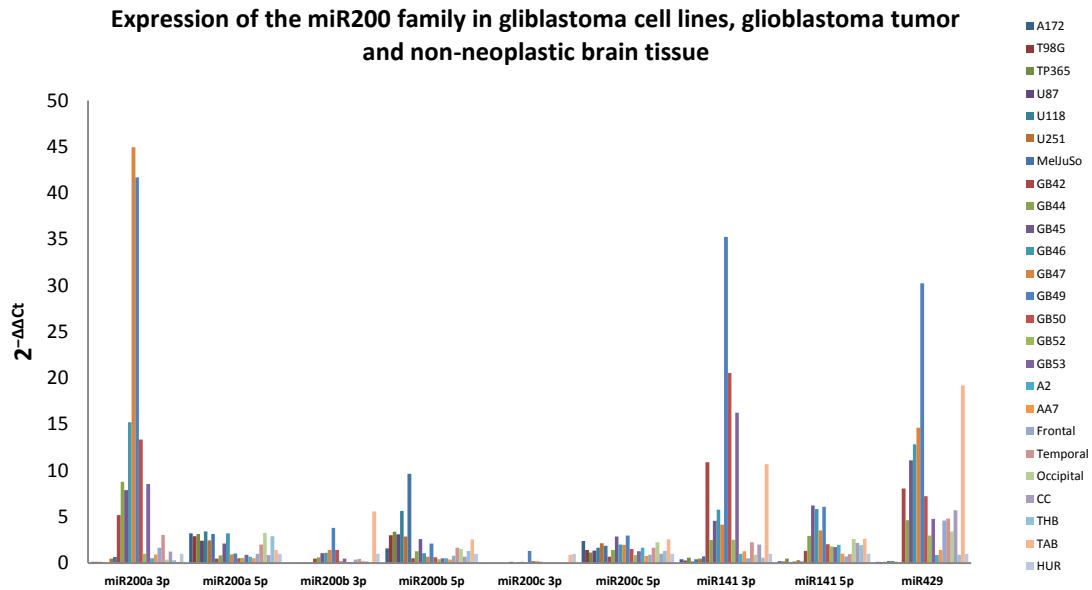


Figure 3. Relative miRNA expression. Expression of the 3p and 5p strands of the miRNA 200 family in glioblastoma cell lines, astrocytic gliomas (WHO grades II to IV) and non-neoplastic brain tissue.

Furthermore, the expression of the miR200 family members was analyzed in glioblastoma stem cells. Other than a low expression of miR200c 3p, no relevant overall expression differences were found among the samples other than high fold-change differences between stem cell lines.

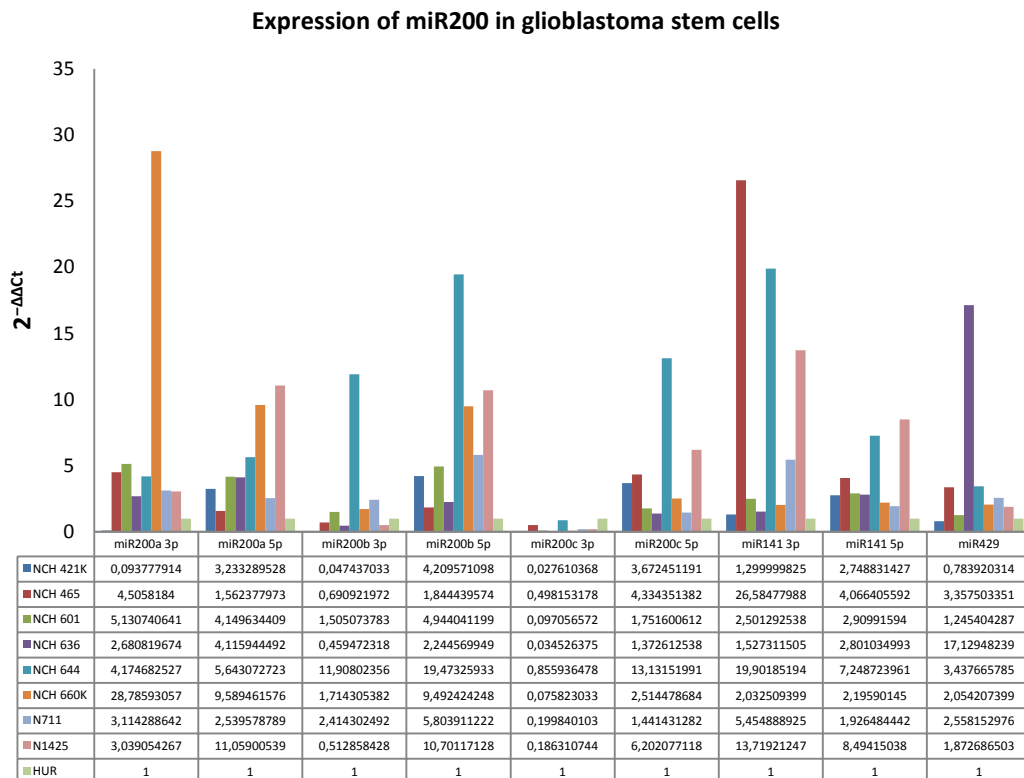


Figure 3. Relative miRNA expression in glioblastoma stem cells. Expression levels of the 3p and 5p strands of the miRNA 200 family in glioblastoma stem cell lines.

To better assess the statistical significance of the expression differences observed among the different sample types, one-way Anova analyses were performed. In cell lines, the 3p strands of miR200a, miR200b and miR200c were expressed at significantly lower levels compared to their 5p counterparts (95% CI -3.702 to -1.834, p-value <0.0001; 95% CI -4.163 to -2.296, p-value <0.0001; 95% CI -2.592 to -0.7237, p-value <0.0001, respectively); no differences were observed for miR141. Moreover, the expression of miR429 was found to be significantly lower compared to the 5p strands of miR200a, miR200b and miR200c (95% CI 1.845 to 3.713, p-value <0.0001; 95% CI 2.181 to 4.049, p-value <0.0001; 95% CI 0.593 to 2.461, p-value 0.0001).

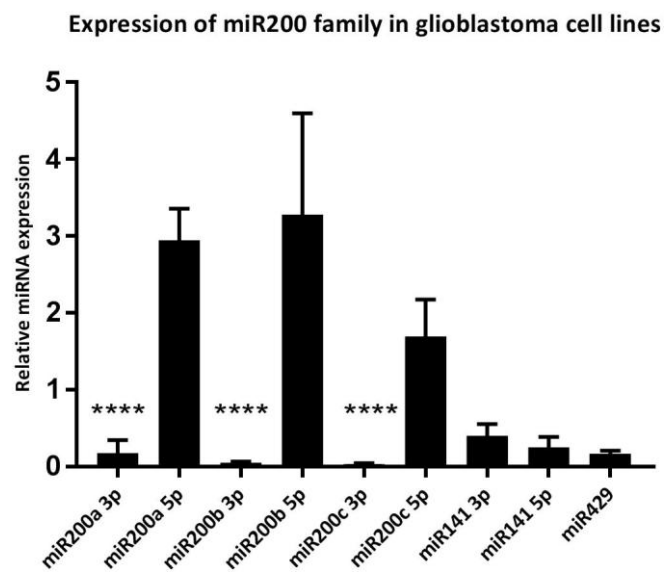


Figure 4. Statistical analysis of the relative miRNA expression of the miR200 family in glioblastoma (WHO grade IV) cell lines shows a significant lower expression of the 3p strands. \*p < 0.05, \*\*p < 0.005, \*\*\*p < 0.001, \*\*\*\*p ≤ 0.0001

Table 1. Statistical analysis of the relative miRNA expression of the miR200 family in glioblastoma (WHO grade IV) cell lines.

Tukey's multiple comparisons test	Mean Diff.	95% CI of diff.	Adj. p-value
miR200a 3p vs. miR200a 5p	-2.768	-3.702 to -1.834	<0.0001
miR200b 3p vs. miR200b 5p	-3.229	-4.163 to -2.296	<0.0001
miR200c 3p vs. miR200c 5p	-1.658	-2.592 to -0.7237	<0.0001
miR141 3p vs. miR141 5p	0.1524	-0.7815 to 1.086	0.9998
miR200a 3p vs. miR429	0.0111	-0.9228 to 0.945	>0.9999
miR200a 5p vs. miR429	2.779	1.845 to 3.713	<0.0001
miR200b 3p vs. miR429	-0.1146	-1.048 to 0.8193	>0.9999
miR200b 5p vs. miR429	3.115	2.181 to 4.049	<0.0001
miR200c 3p vs. miR429	-0.1308	-1.065 to 0.8031	>0.9999
miR200c 5p vs. miR429	1.527	0.593 to 2.461	0.0001
miR141 3p vs. miR429	0.2365	-0.6974 to 1.17	0.9955
miR141 5p vs. miR429	0.08414	-0.8497 to 1.018	>0.9999

In glioblastoma tumors, only a significant difference was observed in the expression difference in miR200a, where the 3p strand was overexpressed compared to the 5p strand (95% CI 5.618 to 24.62, p-value <0.0001). The expression of miR429 was significantly higher compared miR200a 3p, miR200b 3p, miR200 5p and miR200c 3p (95% CI -19.04 to -0.04165, p-value 0.0481; 95% CI -19.03 to -0.03368, p-value 0.0485; 95% CI -19.12 to -0.1248, p-value 0.0446; 95% CI -19.96 to -0.9564, p-value 0.0201, respectively).

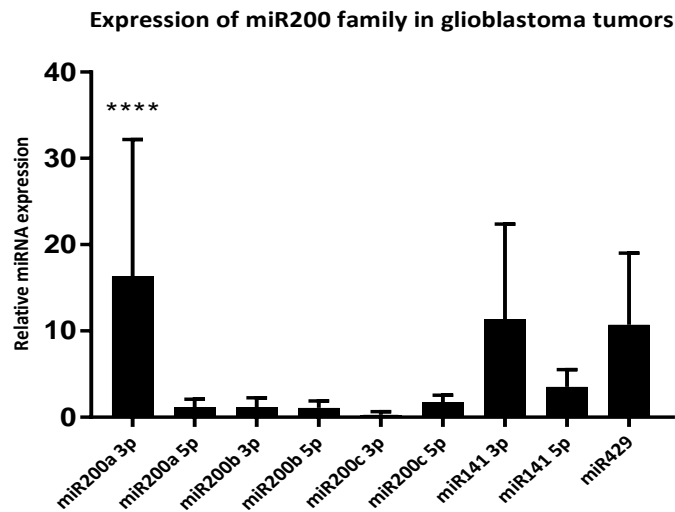


Figure 5. Statistical analysis of the relative miRNA expression of the miR200 family in glioblastoma (WHO grade IV) tumors. Here, in comparison to expression levels in cell lines, the 3p strands of miR200a and miR141 (functional cluster A) are expressed at significantly higher levels as their counterparts and to the other miR200 family members. \*p < 0.05, \*\*p < 0.005, \*\*\*p < 0.001, \*\*\*\*p ≤ 0.0001

Table 2. Statistical analysis of the relative miRNA expression of the miR200 family in glioblastoma (WHO grade IV) tumors.

Tukey's multiple comparisons test	Mean Diff.	95,00% CI of diff.	Adjusted p-value
miR200a 3p vs. miR200a 5p	15.12	5.618 to 24.62	<0.0001
miR200b 3p vs. miR200b 5p	0.09112	-9.408 to 9.591	>0.9999
miR200c 3p vs. miR200c 5p	-1.479	-10.98 to 8.021	0.9999
miR141 3p vs. miR141 5p	7.886	-1.614 to 17.39	0.1845
miR200a 3p vs. miR429	5,577	-3.923 to 15.08	0.6352
miR200a 5p vs. miR429	-9.541	-19.04 to -0.04165	0.0481
miR200b 3p vs. miR429	-9,533	-19.03 to -0.03368	0.0485
miR200b 5p vs. miR429	-9.624	-19.12 to -0.1248	0.0446
miR200c 3p vs. miR429	-10.46	-19.96 to -0.9564	0.0201
miR200c 5p vs. miR429	-8.977	-18.48 to 0.5225	0.079
miR141 3p vs. miR429	0.667	-8.833 to 10.17	>0.9999
miR141 5p vs. miR429	-7.219	-16.72 to 2.281	0.2865

There was no significant difference in expression of the miR200 family in non-neoplastic brain tissue samples, except for miR429, which was significantly overexpressed compared to miR200a 3p, miR200b 3p and miR200c 3p (95% CI -10.41 to -0.2368, p-value 0.034; 95% CI -10.39 to -0.2141, p-value 0.0353; 95% CI -11.35 to -1.172, p-value 0.0064, respectively).

Expression of miR200 family in non-neoplastic brain tissue

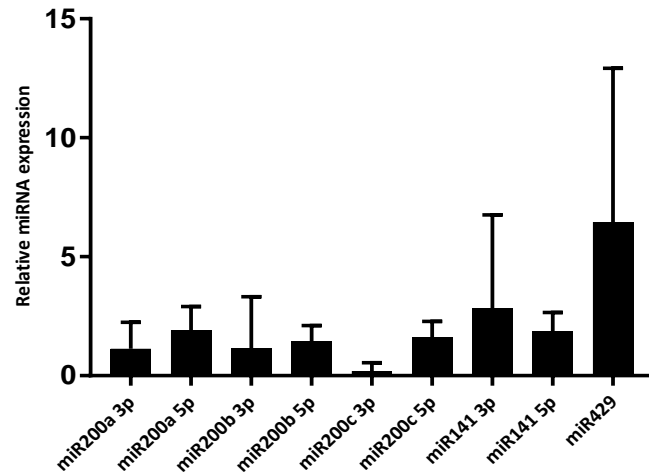


Figure 6. Statistical analysis of the relative miRNA expression of the miR200 family in non-neoplastic brain tissue shows no statistical significant difference among the miR200 family members or among their 3p and 5p strands. \*p < 0.05, \*\*p < 0.005, \*\*\*p < 0.001, \*\*\*\*p ≤ 0.0001

Table 3. Statistical analysis of the relative miRNA expression of the miR200 family in non-neoplastic brain tissue.

Tukey's multiple comparisons test	Mean Diff.	95,00% CI of diff.	Adjusted p-value
miR200a 3p vs. miR200a 5p	-0.7917	-5.878 to 4.295	0.9999
miR200b 3p vs. miR200b 5p	-0.2771	-5.364 to 4.81	>0.9999
miR200c 3p vs. miR200c 5p	-1.426	-6.513 to 3.661	0.9911
miR141 3p vs. miR141 5p	0.9847	-4.102 to 6.071	0.9993
miR200a 3p vs. miR429	-5.324	-10.41 to -0.2368	0.034
miR200a 5p vs. miR429	-4.532	-9.619 to 0.5549	0.1155
miR200b 3p vs. miR429	-5.301	-10.39 to -0.2141	0.0353
miR200b 5p vs. miR429	-5.024	-10.11 to 0.06302	0.0553
miR200c 3p vs. miR429	-6.259	-11.35 to -1.172	0.0064
miR200c 5p vs. miR429	-4.833	-9.919 to 0.2541	0.0743
miR141 3p vs. miR429	-3.619	-8.706 to 1.468	0.3538
miR141 5p vs. miR429	-4.604	-9.691 to 0.483	0.1042

An overall Anova analysis was performed to compare the mean expression values of the different strands of all miR200 family members in tumor cell lines, glioblastoma tumors and non-neoplastic brain tissue. Glioblastoma tumors showed significantly higher expression values of miR200a 3p and miR141 3p than tumor cell lines and non-neoplastic brain samples (functional cluster A; miR200a 3p: 95% CI -8.593 to -3.634, p-value <0.0001; 95% CI 2.484 to 7.443, p-value <0.0001, respectively; miR141 3p: 95% CI -9.442 to -4.483, p-value <0.0001; 95% CI 3.617 to 8.576, p-value <0.0001). On the other hand, glioblastoma cell lines expressed significantly higher values of miR200b 5p than glioblastoma tumors and non-neoplastic brain samples (95% CI 0.05682 to 5.016, p-value 0.0437; 95% CI -0.06771 to 4.891, p-value 0.0584, respectively). In comparison to cell lines, glioblastoma tumors also showed a significant higher expression of miR141 5p (95% CI -5.033 to -0.07355, p-value

0.042). Furthermore, miR429 showed significantly lower expression values in cell lines compared to tumor samples (95% CI -8.634 to -3,675, p-value <0.0001).

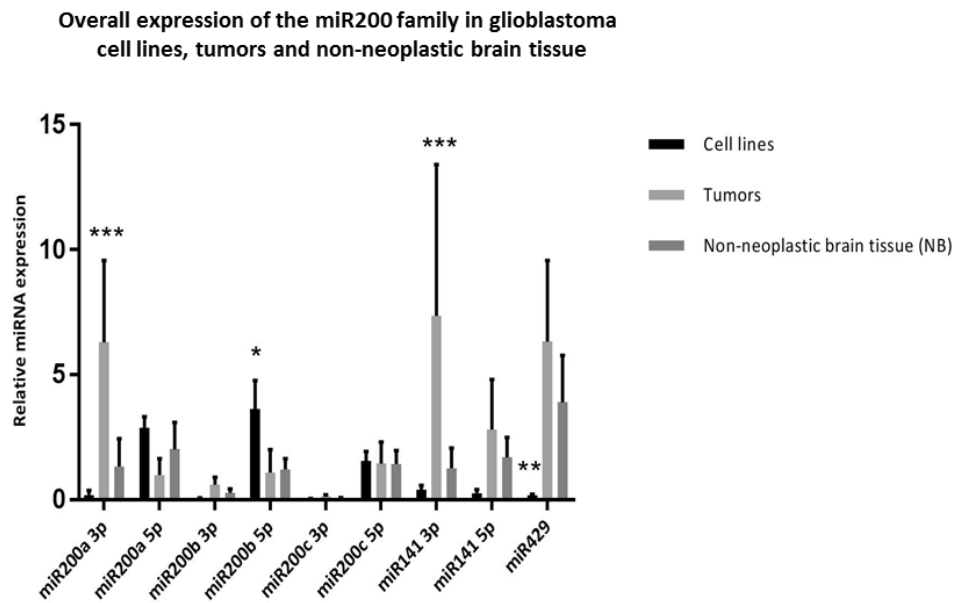


Figure 7. Overall analysis of the relative miRNA expression of the miR200 family in glioblastoma (WHO grade IV) cell lines, tumors and non-neoplastic brain tissue. \*p < 0.05, \*\*p < 0.005, \*\*\*p < 0.001, \*\*\*\*p ≤ 0.0001

Table 4. Statistical analysis of the relative miRNA expression of the miR200 family in glioblastoma (WHO grade IV) cell lines, tumors and non-neoplastic brain tissue.

Tukey's multiple comparisons test	Mean Diff	95,00% CI of diff,	Adjusted p-value
<b>miR200a 3p</b>			
Cell lines vs. Tumors	-6.113	-8.593 to -3.634	<0.0001
Cell lines vs. Brain	-1.15	-3.63 to 1.33	0.5148
Tumors vs. Brain	4.963	2.484 to 7.443	<0.0001
<b>miR200a 5p</b>			
Cell lines vs. Tumors	1.901	-0.5786 to 4.38	0.1673
Cell lines vs. Brain	0.8655	-1.614 to 3.345	0.6856
Tumors vs. Brain	-1.035	-3.515 to 1.444	0.5832
<b>miR200b 3p</b>			
Cell lines vs. Tumors	-0.5389	-3.018 to 1.941	0.8635
Cell lines vs. Brain	-0.2156	-2.695 to 2.264	0.9767
Tumors vs. Brain	0.3232	-2.156 to 2.803	0.9485
<b>miR200b 5p</b>			
Cell lines vs. Tumors	2.536	0.05682 to 5.016	0.0437
Cell lines vs. Brain	2.412	-0.06771 to 4.891	0.0584



Tumors vs. Brain	-0.1245	-2.604 to 2.355	0.9922
<b>miR200c 3p</b>			
Cell lines vs. Tumors	-0.09831	-2.578 to 2.381	0.9951
Cell lines vs. Brain	-0.01698	-2.497 to 2.463	0.9999
Tumors vs. Brain	0.08133	-2.398 to 2.561	0.9967
<b>miR200c 5p</b>			
Cell lines vs. Tumors	0.1105	-2.369 to 2.59	0.9938
Cell lines vs. Brain	0.1186	-2.361 to 2.598	0.9929
Tumors vs. Brain	0.008126	-2.471 to 2.488	>0.9999
<b>miR141 3p</b>			
Cell lines vs. Tumors	-6.963	-9.442 to -4.483	<0.0001
Cell lines vs. Brain	-0.8665	-3.346 to 1.613	0.685
Tumors vs. Brain	6.096	3.617 to 8.576	<0.0001
<b>miR141 5p</b>			
Cell lines vs. Tumors	-2.553	-5.033 to -0.07355	0.042
Cell lines vs. Brain	-1.442	-3.921 to 1.038	0.354
Tumors vs. Brain	1.111	-1.368 to 3.591	0.5377
<b>miR429</b>			
Cell lines vs. Tumors	-6.155	-8.634 to -3.675	<0.0001
Cell lines vs. Brain	-3.736	-6.216 to -1.256	0.0015
Tumors vs. Brain	2.419	-0.06099 to 4.898	0.0575

#### 4.1.1. Expression of the miR200 family in glioblastoma samples extracted from The Cancer Genome Atlas (TCGA)

Overall expression analysis of miR200 family in glioblastoma compared to matched normal brain samples didn't show any significant difference for most of the miR200 family members, except for miR200b 3p (average expression of 6.47, p-value 0.04) (See figure 8 and table 5).

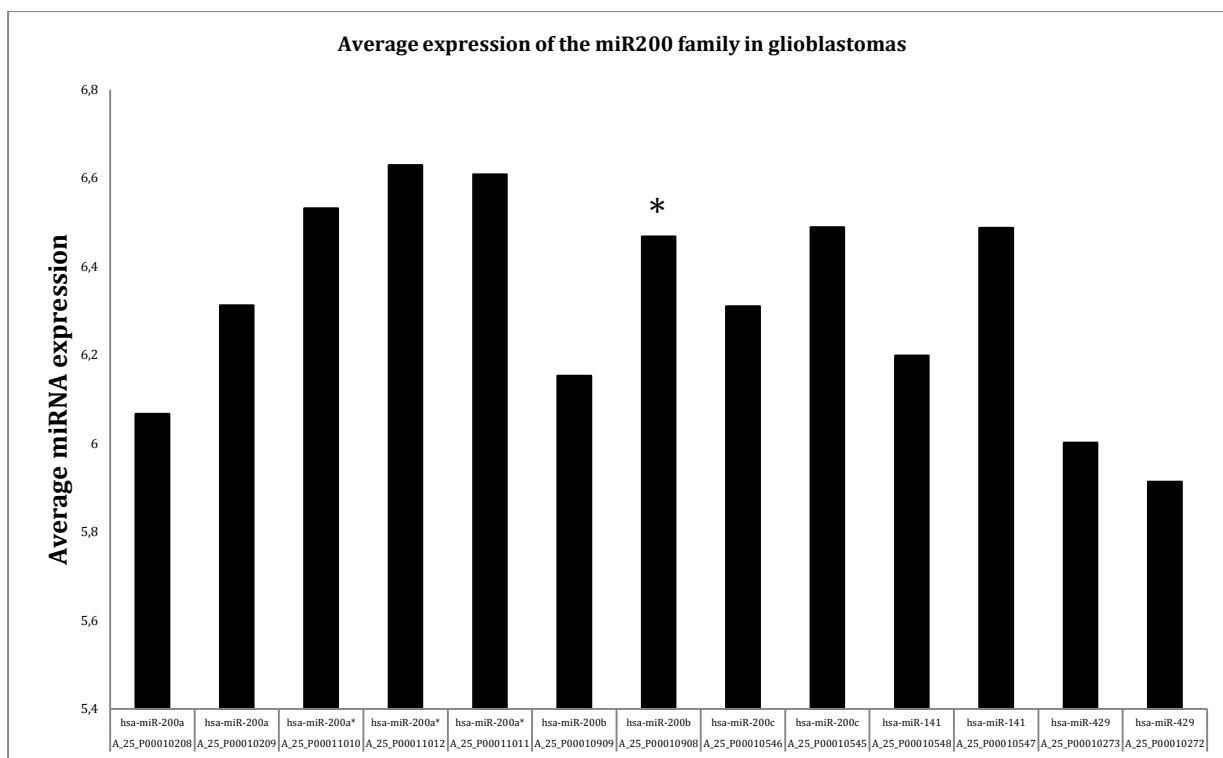


Figure 8. The average expression values of the miR200 family members were plotted in the following graph. \*p-value < 0.05

Table 5. Average expression of the miR200 family in glioblastoma samples.

Probe_ID	GeneName	logFC	AveExpr	P.Value
A_25_P00010909	hsa-miR-200b	-0.136148722	6.152913123	0.11191403
A_25_P00011011	hsa-miR-200a*	-0.218227584	6.608096991	0.18679189
A_25_P00010546	hsa-miR-200c	-0.193166591	6.310053665	0.1122011
A_25_P00010208	hsa-miR-200a	-0.069014147	6.067062773	0.36288045
A_25_P00010545	hsa-miR-200c	-0.308190022	6.488402675	0.06301133
A_25_P00011012	hsa-miR-200a*	-0.234191902	6.629320729	0.18525172
A_25_P00010209	hsa-miR-200a	-0.176497515	6.311986377	0.1736565
A_25_P00010908	hsa-miR-200b	-0.341239593	6.467553226	0.04015078
A_25_P00011010	hsa-miR-200a*	-0.216122396	6.531510002	0.14425325
A_25_P00010273	hsa-miR-429	-0.056435052	6.001904536	0.3676655
A_25_P00010272	hsa-miR-429	-0.040486782	5.913695298	0.30127172
A_25_P00010548	hsa-miR-141	-0.103196963	6.198265671	0.27537335
A_25_P00010547	hsa-miR-141	-0.269717479	6.487582571	0.08029085

The overall expression of the miR200 family in glioblastomas compared to non-neoplastic brain tissue wasn't significantly deregulated in most members, with the only exception of miR200b 3p, in which a significant (p-value 0.04, log. fold change -0.341) downregulation could be seen.

A further analysis to characterize tumors significantly overexpressing miR200b 3p showed a higher (statistically non-significant) expression in IDH-wildtype, MGMT-promoter unmethylated and in primary glioblastomas.

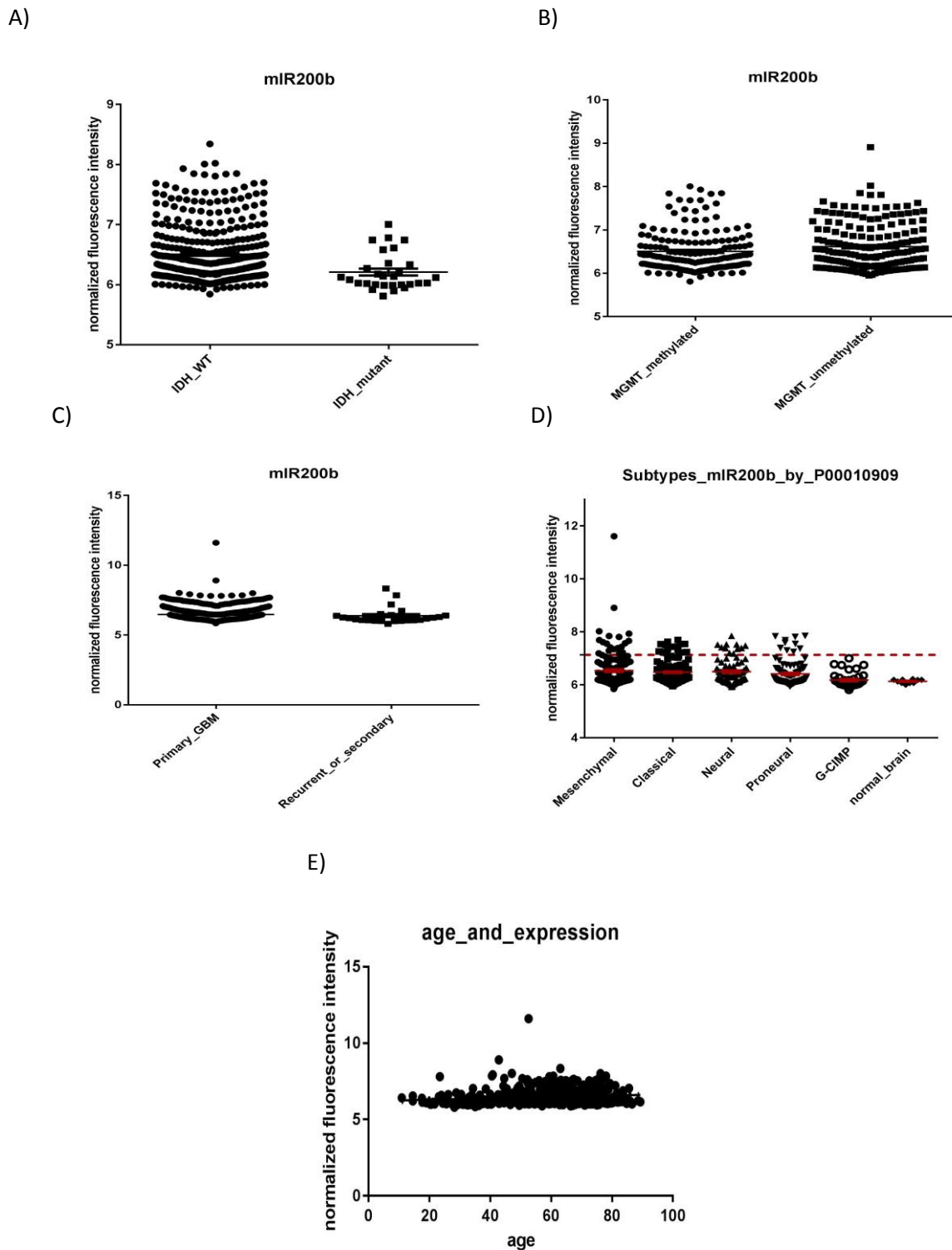


Figure 9. Expression patterns of miR200b 3p in different glioblastoma cohort subtypes. IDH wildtype tumors express lower levels of miR200b 3p (A). Similar findings are seen for glioblastomas lacking MGMT promoter methylation (B) as well as in primary (de novo) tumors (C). Even though relative expression seems to differ only slightly among molecular subtypes (D), a tendency towards a higher frequency of lower expression can be seen in mesenchymal tumors. No difference is seen among different age groups (E).

Kaplan-Meier survival curves were performed, to assess the impact of expression of the miR200 family in overall survival. In patients with glioblastoma harboring high expression of miR200a 3p and miR200b 3p lower overall survival was observed ( $p$ -value  $< 0.05$ ). For the other members of the miR200 family there was no significant differences observed.

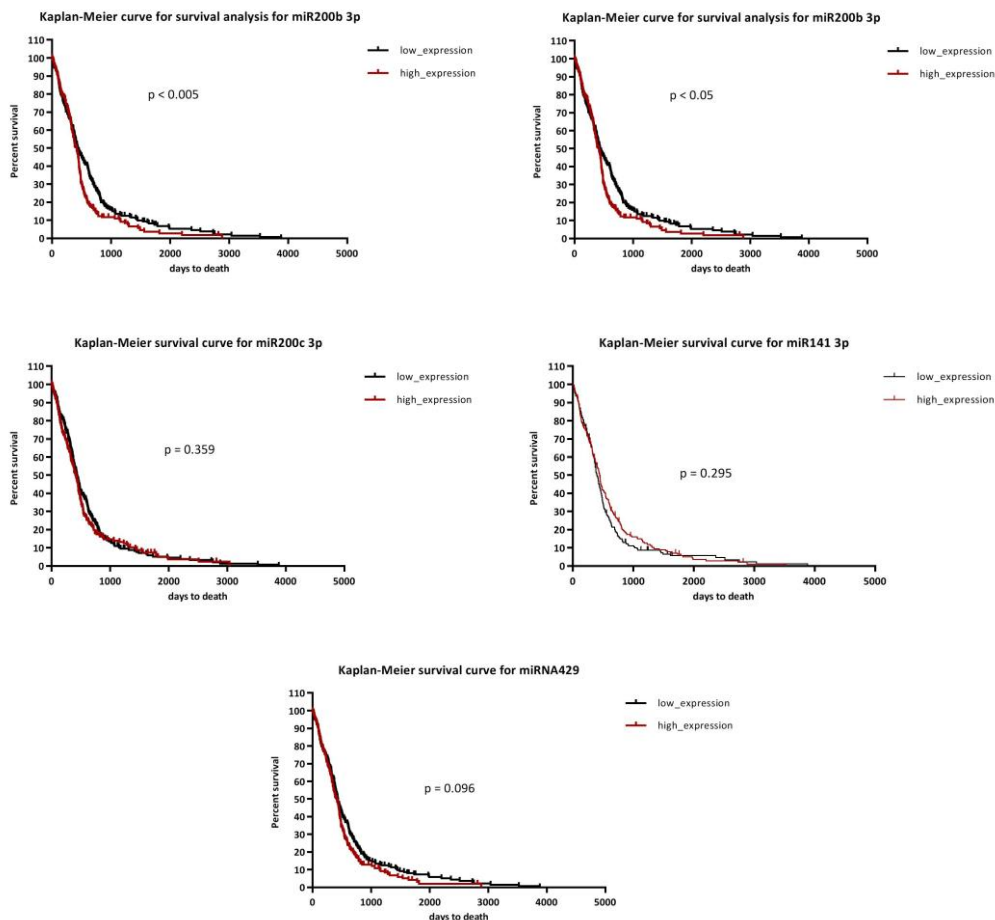


Figure 10. Kaplan-Meier survival curves comparing high vs. low expression of the miR200 family. There is only a significant poorer survival rate in patients expressing lower levels of miR200a 3p and miR200b 3p compared to the 3p strands of the remaining miR200 family members. No data regarding 5p strands were found among the TCGA database for glioblastomas.

#### 4.1.2. Expression of ZEB1 and ZEB2 in glioblastoma samples extracted from The Cancer Genome Atlas (TCGA)

Since ZEB1/ ZEB2 have been described as direct targets of the miR200 family, being controlled through a double-negative feedback loop, it was of interest to see how ZEB1 and ZEB2 expression behaved according to molecular subtypes in the glioblastoma cohort of the cancer genome atlas database, and how their expression associated to prognosis.

Analysis of the expression of ZEB1 and ZEB2 in glioblastomas according to molecular subtype showed no statistical differences in expression among all groups. Kaplan-Meier survival curves didn't show an impact on overall survival between high and low expression of ZEB1 or ZEB2 in glioblastoma.

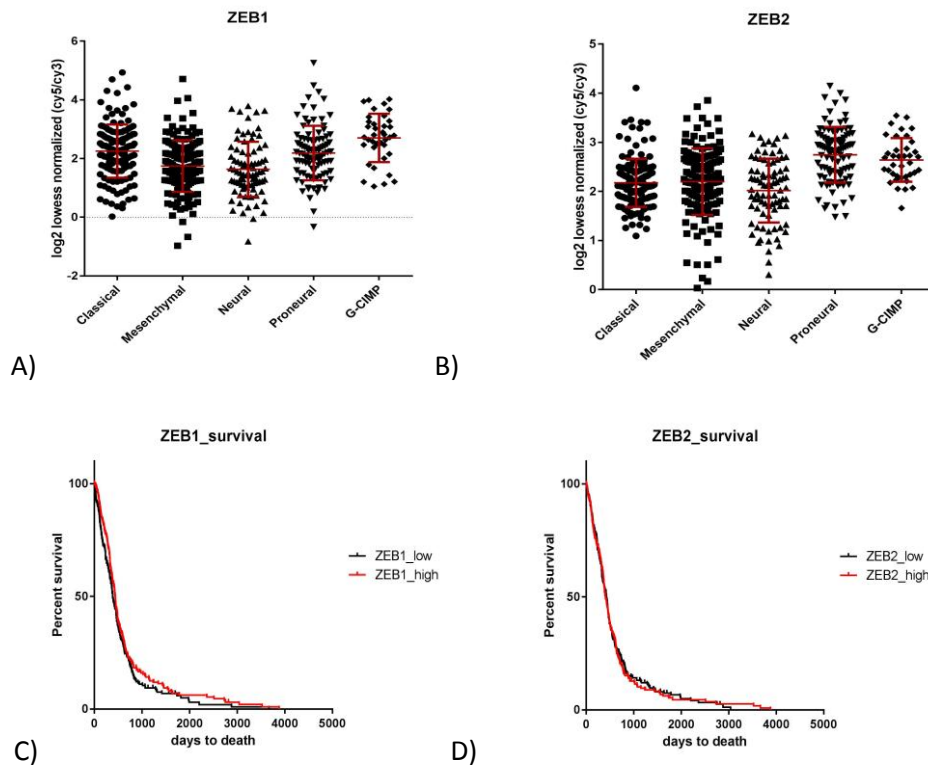
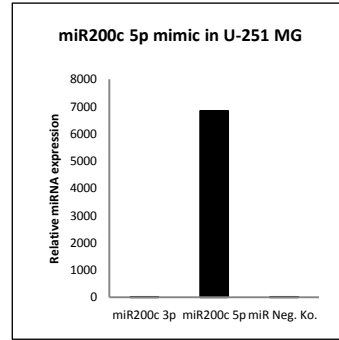
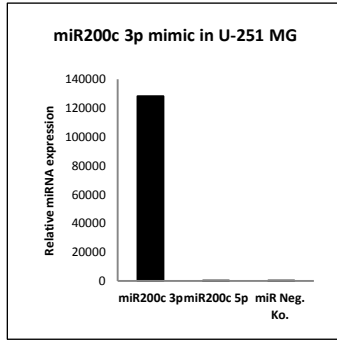
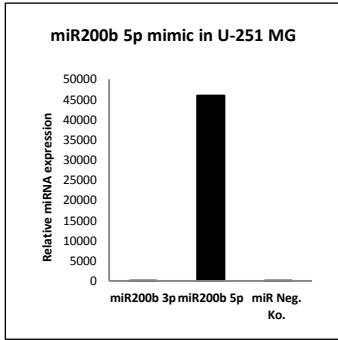
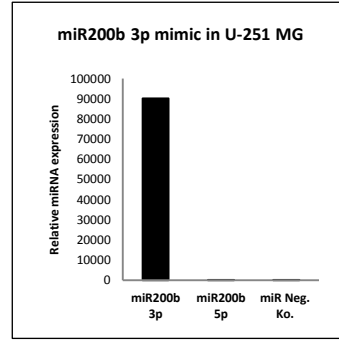
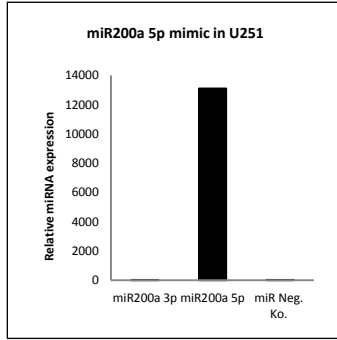
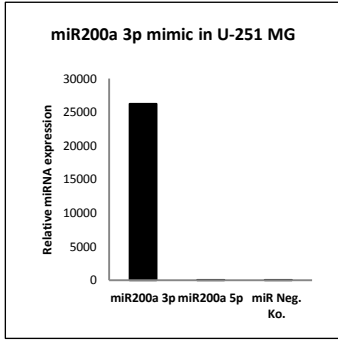
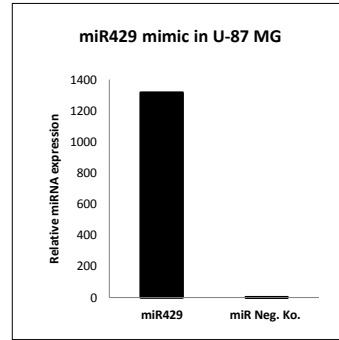
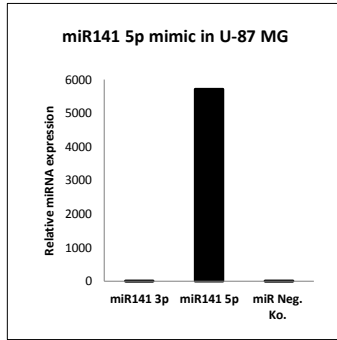
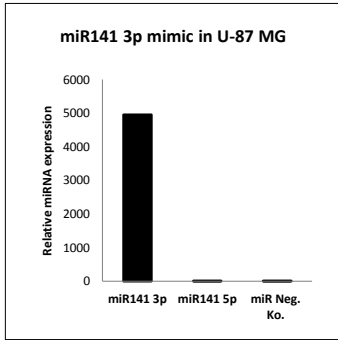
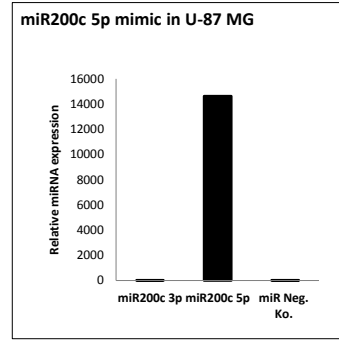
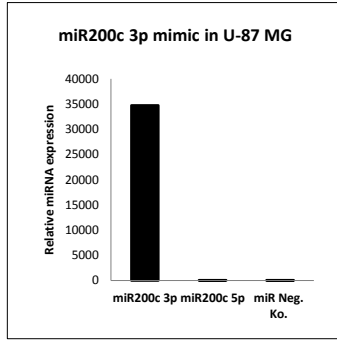
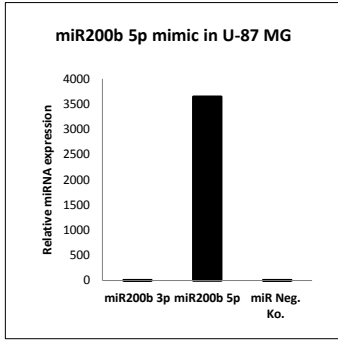
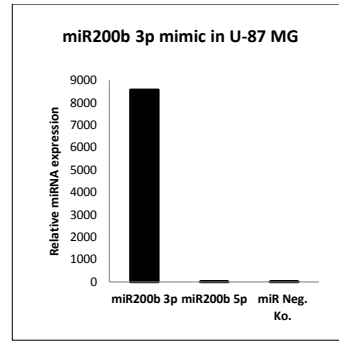
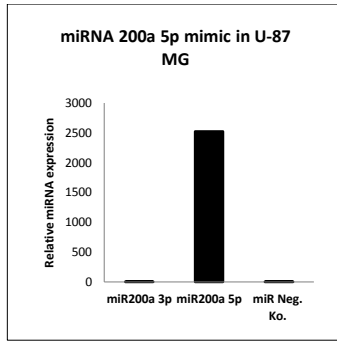
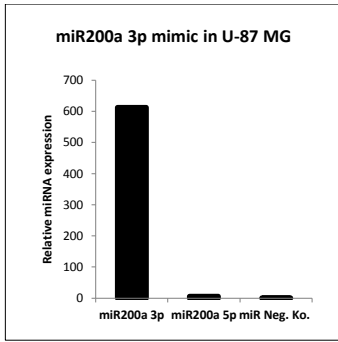


Figure 11. Figures A and B show no major differences in ZEB1 and ZEB2 expression among the different molecular subtypes. In figures C and D are depicted Kaplan-Meier survival curves in which no difference on survival was observed among high and low expressions of ZEB1 and ZEB2.

## 4.2. Transfection

Since the expression of the miR200 family in glioblastoma cell lines was diminished, miRNA mimics for both strands were introduced to three cell lines (U-87 MG, U-118 MG and U-251 MG) to induce an overexpression of the miR200 family. As seen on figure 12, transfecting 30 nM of miRNA mirvana mimics (Ambion) into the cells produced higher expression levels even 48 hours after transfection, for both strands (3p and 5p) of the miR200 family members.



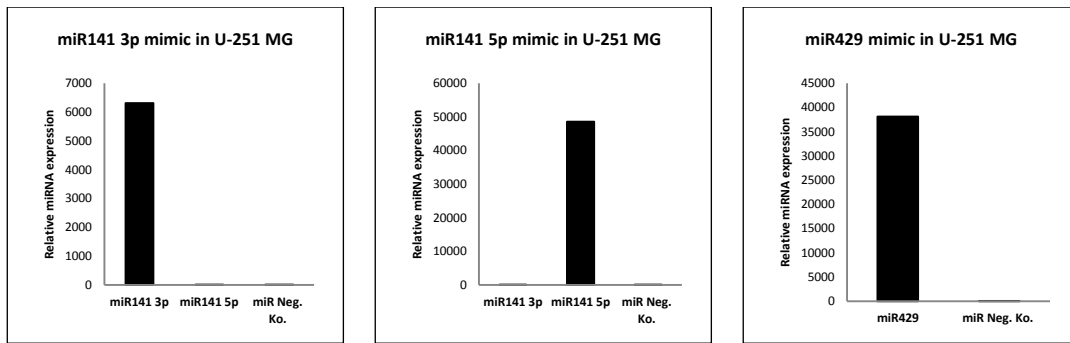
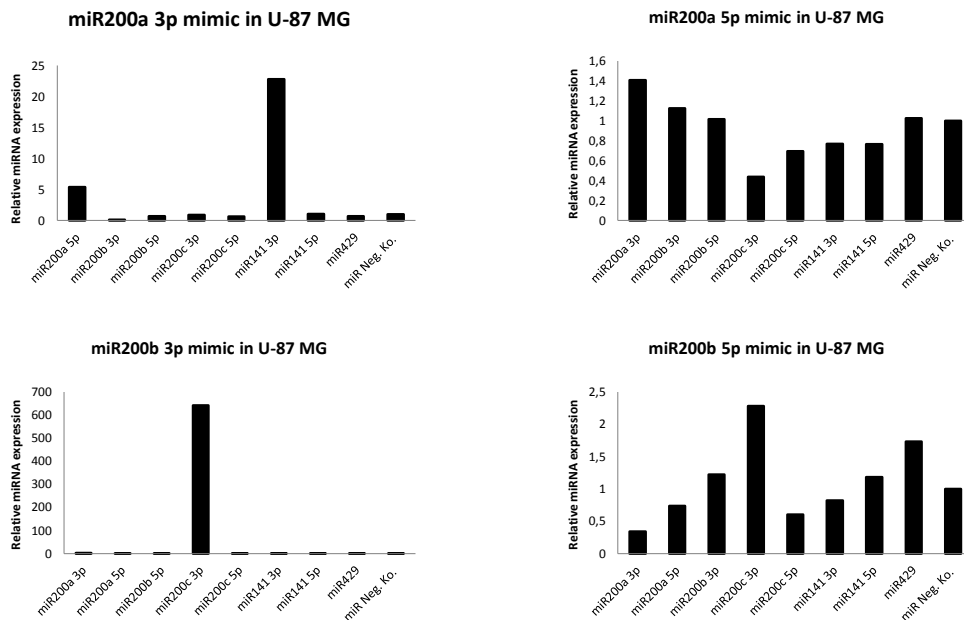
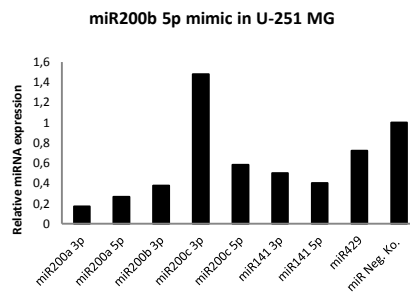
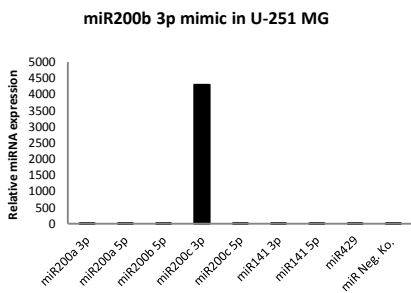
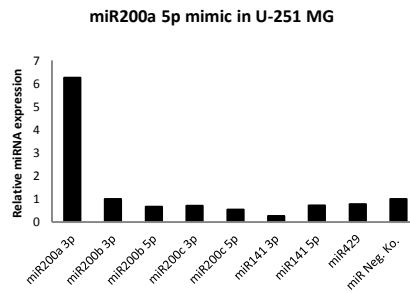
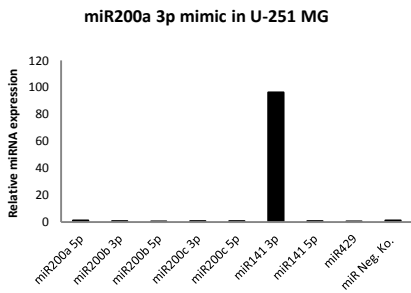
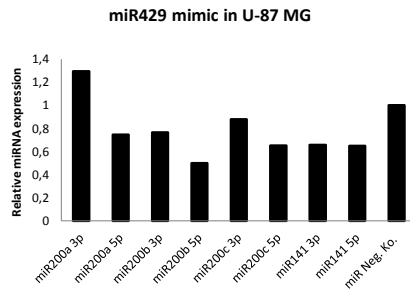
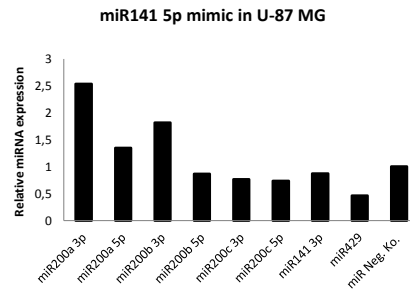
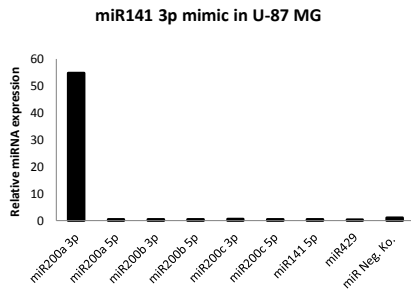
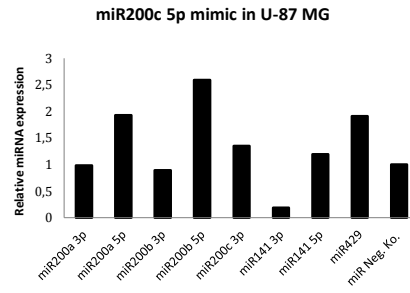
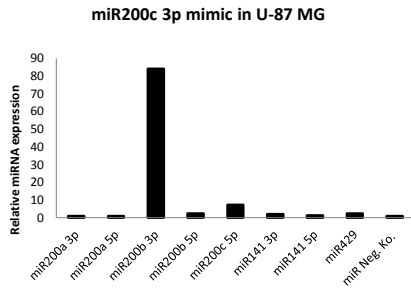


Figure 12. Expression of strands 3p and 5p 48 hours post-transfection with miRNA mimics of the miR200 family, compared to cells transfected with a negative control miRNA.

#### 4.2.1. Expression of the other miR200 family members after transfection with one mimic

Further analysis of the expression of the miR200 family members after transfection of the 3p strand showed a concomitant upregulation of miRNAs of the same functional cluster (see Figure). After transfection with miR200a 3p, a concomitant overexpression of miR141 3p was observed and vice versa. The same observations were noted for miR200b 3p, which produced an overexpression of miR200c 3p, as well as overexpression of miR200c 3p produced an overexpression of miR200b 3p. No differences were noticed when transfecting with miRNAs of the 5p strand. Neither was a difference observed after mimicking the expression of miR429.







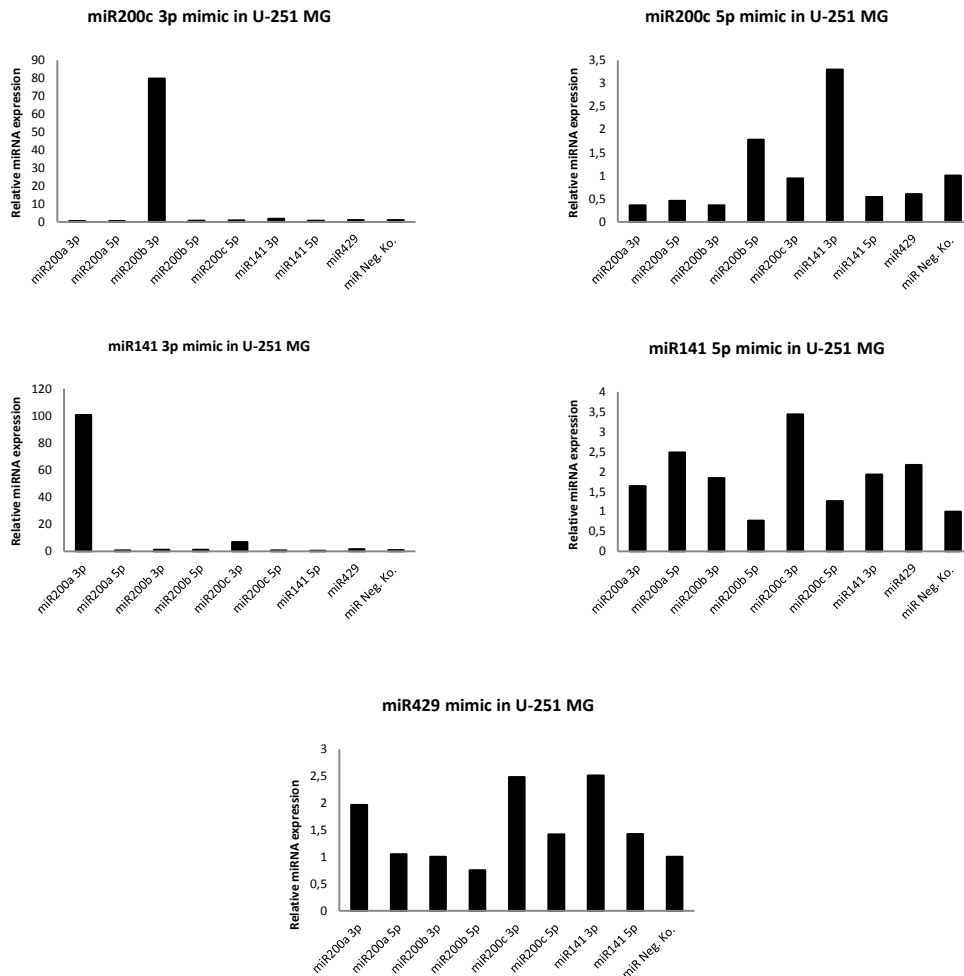


Figure 13. Expression levels of the remaining members of the miR200 family 48 hours post-transfection with a specific miRNA mimic (not depicted in the graph).

Even though in U-251 MG cells transfected with miR200a 5p mimics the expression levels of miR200a 3p also went up, these values were still very low compared to the over expression achieved for the 5p strand.

#### 4.2.2. Effects of upregulation of the miR200 family members in glioma cell proliferation and apoptosis

After achieving successful transient transfections of miRNA mimics, the next step was to evaluate the effect of overexpressing miRNAs of the miR200 family, and if there was any difference between 3p and 5p strands. For this purpose, transfections were carried out in 96-well plates, and 24 hours after transfection functional assays to measure proliferation and apoptosis rates were performed (Figures 14 and 15).

There was a significant reduction in proliferation in U-87 MG and U-251 MG cells overexpressing the miR200 family 3p strand compared to negative control, as well a tendency in the 5p strand, only significant for miR200a 5p in U-87 MG, to an increase in proliferation.

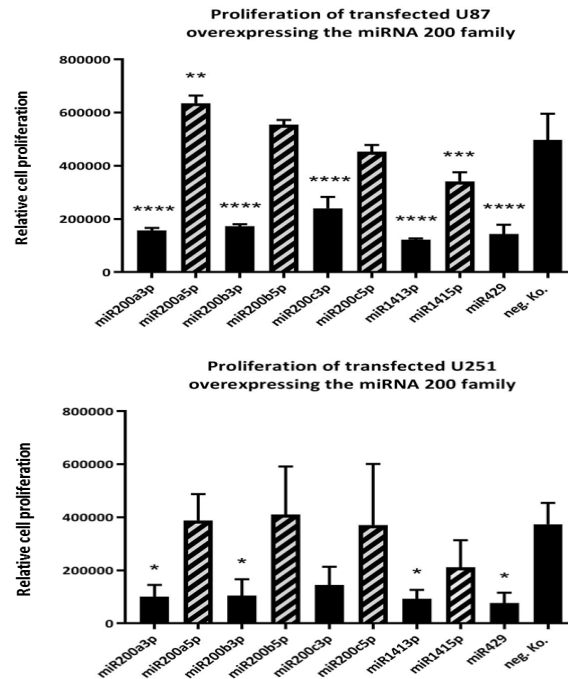


Figure 14. Incorporation of BrdU in cells overexpressing the miR200 family. As seen on the graphs, cells expressing higher levels of the 3p strands show lower incorporation of BrdU, which translates into lower rates of proliferation among these cells. \*p < 0.05, \*\*p < 0.005, \*\*\*p < 0.001, \*\*\*\*p ≤ 0.0001

Table 6. Statistical analysis of BrdU incorporation among cells overexpressing the miR200 family.

Dunnett's multiple comparisons test							
U87 MG				U251 MG			
	Mean Diff.	95% CI of diff.	Adj. p-value		Mean Diff.	95% CI of diff.	Adj. p-value
neg. Ko. vs. miR200a3p	339890	244269 to 435512	0.0001	neg. Ko. vs. miR200a3p	273066	3886 to 542247	0.0458
neg. Ko. vs. miR200a5p	-138617	-234238 to -42995	0.0027	neg. Ko. vs. miR200a5p	-14555	-283736 to 254625	0.9998
neg. Ko. vs. miR200b3p	324551	228930 to 420173	0.0001	neg. Ko. vs. miR200b3p	269742	561,2 to 538923	0.0493
neg. Ko. vs. miR200b5p	-57520	-153142 to 38102	0.4116	neg. Ko. vs. miR200b5p	-37083	-306263 to 232098	0.9994
neg. Ko. vs. miR200c3p	256849	161227 to 352470	0.0001	neg. Ko. vs. miR200c3p	229018	-40163 to 498198	0.1196
neg. Ko. vs. miR200c5p	44072	-51550 to 139693	0.685	neg. Ko. vs. miR200c5p	3040	-266140 to 272221	0.9999
neg. Ko. vs. miR1413p	375040	279418 to 470662	0.0001	neg. Ko. vs. miR1413p	281481	12300 to 550662	0.0378
neg. Ko. vs. miR1415p	155367	59745 to 250988	0.0008	neg. Ko. vs. miR1415p	162543	-106638 to 431723	0.4076
neg. Ko. vs. miR429	353877	258256 to 449499	0.0001	neg. Ko. vs. miR429	296797	27616 to 565977	0.0265

In apoptosis, there was a tendency to increase in apoptosis in cells overexpressing the miR200 family 3p strands compared to cells transfected with the negative control. Only in U-251 MG was there a significant increase in apoptosis in cells overexpressing miR200b 3p and miR429. Likewise, there was a tendency in decreased apoptosis in cells carrying mimics for the miR200 family 5p strands.

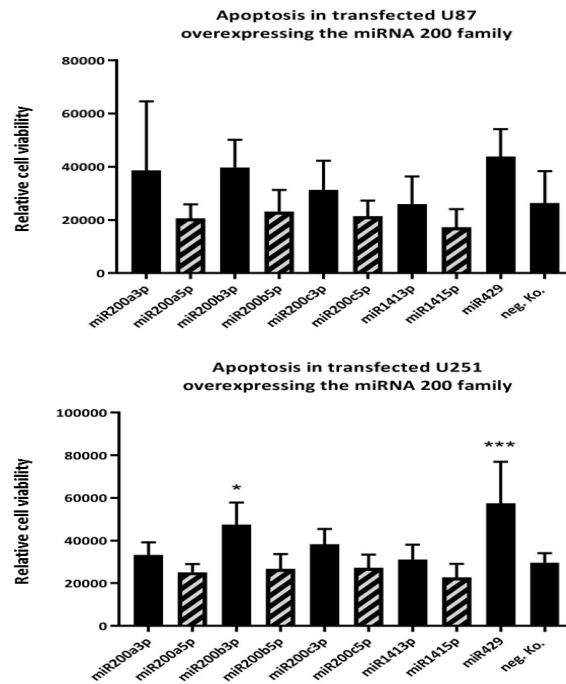


Figure 15. Incorporation of Caspase 3/4 in cells overexpressing the miR200 family. Cells overexpressing 3p strands of the miR200 family show higher incorporation of Caspase 3/4. \*p < 0.05, \*\*p < 0.005, \*\*\*p < 0.001, \*\*\*\*p ≤ 0.0001

Table 7. Statistical analysis of Caspase 3/4 incorporation among cells overexpressing the miR200 family.

Dunnett's multiple comparisons test							
U87 MG				U251 MG			
	Mean Diff.	95% CI of diff.	Adj. p-value		Mean Diff.	95% CI of diff.	Adj. p-value
neg. Ko. vs. miR200a3p	-12233	-36440 to 11975	0.6225	neg. Ko. vs. miR200a3p	-3730	-21542 to 14083	0.9936
neg. Ko. vs. miR200a5p	5734	-18474 to 29941	0.9896	neg. Ko. vs. miR200a5p	4438	-13375 to 22250	0.9854
neg. Ko. vs. miR200b3p	-13402	-37609 to 10806	0.5251	neg. Ko. vs. miR200b3p	-17883	-35695 to -70,11	0.0487
neg. Ko. vs. miR200b5p	3147	-21061 to 27354	0.9994	neg. Ko. vs. miR200b5p	2871	-14941 to 20684	0.9977
neg. Ko. vs. miR200c3p	-4997	-29204 to 19210	0.994	neg. Ko. vs. miR200c3p	-8626	-26438 to 9186	0.6655
neg. Ko. vs. miR200c5p	4977	-19230 to 29185	0.994	neg. Ko. vs. miR200c5p	2345	-15468 to 20157	0.9994
neg. Ko. vs. miR1413p	368,3	-23839 to 24576	0.9999	neg. Ko. vs. miR1413p	-1535	-19348 to 16277	0.9997
neg. Ko. vs. miR1415p	9066	-15142 to 33273	0.8681	neg. Ko. vs. miR1415p	6975	-10837 to 24788	0.8411
neg. Ko. vs. miR429	-17474	-41681 to 6734	0.25	neg. Ko. vs. miR429	-27891	-45703 to -10078	0.0008

#### 4.2.3. Expression of ZEB1 and ZEB2 in cells transfected with mimics of the miR200 family

To assess if overexpression of the miR200 family had an effect on the expression of ZEB1 and/or ZEB2, qRT-PCRs were performed to evaluate gene expression levels of ZEB1/ ZEB2 in transfected cells.

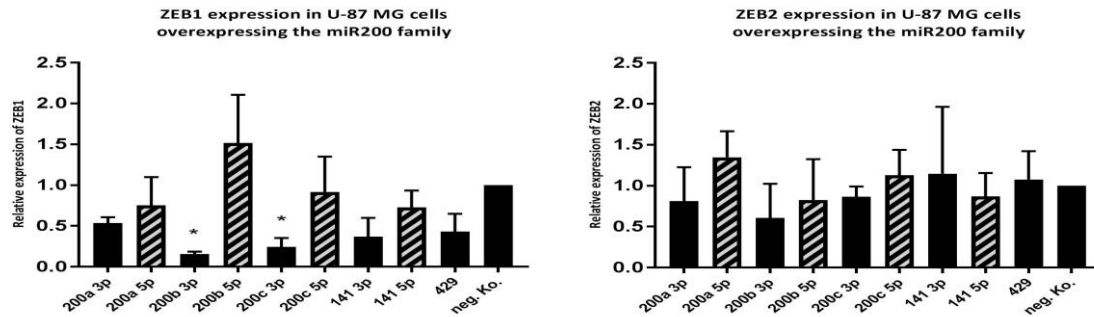


Figure 16. Relative expression of ZEB1 in cells overexpressing the miR200 family showed in U-87 MG a statistically significant decreased in the expression of ZEB1 in cells with higher levels of miR200b 3p and miR200c 3p (functional cluster B). \* $p < 0.05$ , \*\* $p < 0.005$ , \*\*\* $p < 0.001$ , \*\*\*\* $p \leq 0.0001$

Table 8. Statistical analysis of the relative expression of ZEB1 in U-87 MG and U-251 MG cells overexpressing the miR200 family.

Dunnnett's multiple comparisons test							
U87 MG				U251 MG			
	Mean Diff.	95% CI of diff.	Adj. p-value		Mean Diff.	95% CI of diff.	Adj. p-value
neg. Ko. vs. 200a 3p	0.4653	-0.222 to 1.153	0.2937	neg Ko vs. 200a 3p	0.4218	-0.255 to 1.099	0.375
neg. Ko. vs. 200a 5p	0.2476	-0.4397 to 0.9349	0.8697	neg Ko vs. 200a 5p	0.3618	-0.3151 to 1.039	0.5362
neg. Ko. vs. 200b 3p	0.8435	0.1563 to 1.531	0.0119	neg Ko vs. 200b 3p	0.6504	-0.02647 to 1.327	0.0633
neg. Ko. vs. 200b 5p	-0.5164	-1.204 to 0.1709	0.2037	neg Ko vs. 200b 5p	0.06696	-0.6099 to 0.7438	0.9996
neg. Ko. vs. 200c 3p	0.7545	0.06724 to 1.442	0.0273	neg Ko vs. 200c 3p	0.437	-0.2398 to 1.114	0.3395
neg. Ko. vs. 200c 5p	0.08234	-0.6049 to 0.7696	0.9995	neg Ko vs. 200c 5p	0.02564	-0.6512 to 0.7025	0.9999
neg. Ko. vs. 141 3p	0.6308	-0.05643 to 1.318	0.0815	neg Ko vs. 141 3p	0.08108	-0.5957 to 0.7579	0.9995
neg. Ko. vs. 141 5p	0.2709	-0.4163 to 0.9582	0.8135	neg Ko vs. 141 5p	-0.1618	-0.8386 to 0.515	0.9851
neg. Ko. vs. 429	0.5696	-0.1177 to 1.257	0.135	neg Ko vs. 429	0.4861	-0.1907 to 1.163	0.2408

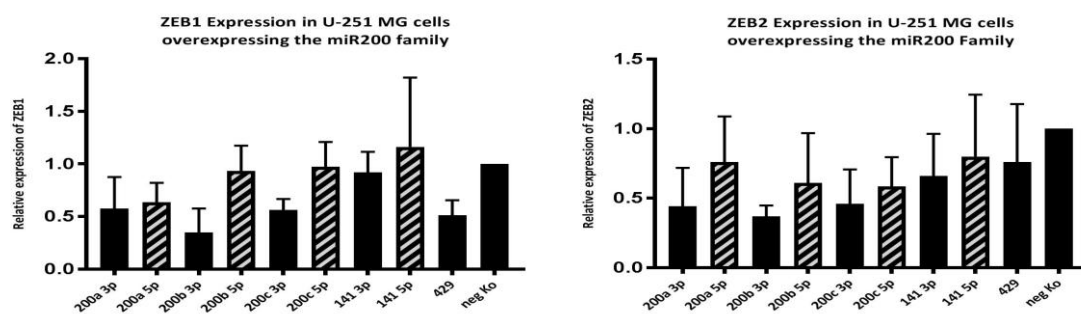


Figure 17. Analyses of the relative expression of ZEB2 in cells overexpressing the miR200 family showed no statistically significant differences.

Table 9. Statistical analysis of the relative expression of ZEB2 in U-87 MG and U-251 MG cells overexpressing the miR200 family.

Dunnett's multiple comparisons test							
U87 MG				U251 MG			
	Mean Diff.	95% CI of diff.	Adj. p-value		Mean Diff.	95% CI of diff.	Adj. p-value
neg. Ko. vs. 200a 3p	0.1872	-0.7993 to 1.174	0.9965	neg Ko vs. 200a 3p	0.5587	-0.1574 to 1.275	0.1754
neg. Ko. vs. 200a 5p	-0.3465	-1.333 to 0.6401	0.883	neg Ko vs. 200a 5p	0.2397	-0.4764 to 0.9558	0.9056
neg. Ko. vs. 200b 3p	0.3948	-0.5918 to 1.381	0.8029	neg Ko vs. 200b 3p	0.6295	-0.08657 to 1.346	0.1019
neg. Ko. vs. 200b 5p	0.1748	-0.8118 to 1.161	0.9969	neg Ko vs. 200b 5p	0.3902	-0.3259 to 1.106	0.5159
neg. Ko. vs. 200c 3p	0.1345	-0.852 to 1.121	0.9994	neg Ko vs. 200c 3p	0.5392	-0.1769 to 1.255	0.202
neg. Ko. vs. 200c 5p	-0.1281	-1.115 to 0.8584	0.9994	neg Ko vs. 200c 5p	0.4155	-0.3006 to 1.132	0.4495
neg. Ko. vs. 141 3p	-0.1459	-1.132 to 0.8407	0.9993	neg Ko vs. 141 3p	0.3406	-0.3755 to 1.057	0.655
neg. Ko. vs. 141 5p	0.13	-0.8565 to 1.117	0.9994	neg Ko vs. 141 5p	0.2008	-0.5153 to 0.9169	0.9612
neg. Ko. vs. 429	-0.07551	-1.062 to 0.9111	0.9997	neg Ko vs. 429	0.2391	-0.477 to 0.9552	0.9067

48 hours post transfection with miRNA 200 family mimics showed a statistically significant downregulation in expression levels of ZEB1 in U-87 MG cells overexpressing miR200b 3p and miR200c 3p. A tendency was as well observed to a decreased expression of ZEB1 in remaining 3p members in U-87 MG as well as in U-251 cells. A tendency (no statistical significance) to a downregulation of ZEB2 in cells overexpressing 3p strands was also observed.

### 4.3. NGS

#### 4.3.1. Multivariate Analysis

Principal Component Analysis (PCA) based on the top 1000 RLog normalized expression values (centered and scaled) was performed for each cell line as seen on the figures below.

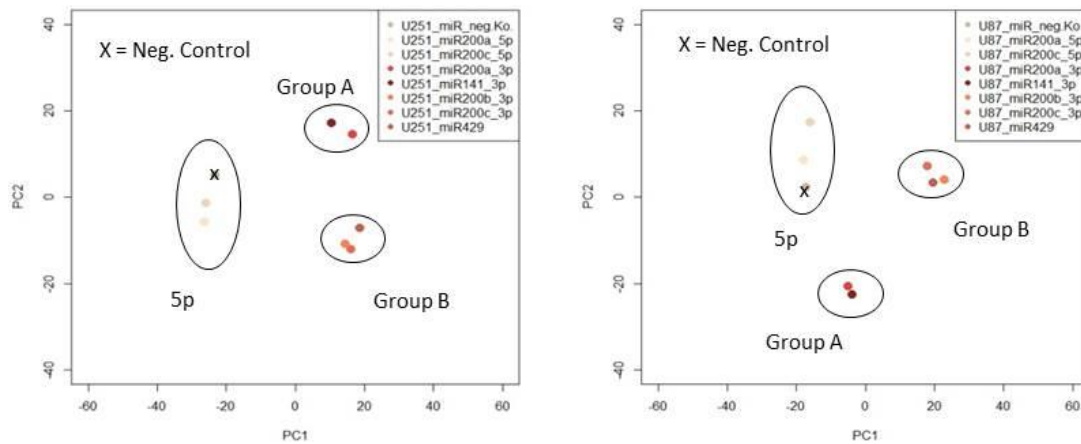


Figure 18. Principal component analysis (PCA) showed a clustering into three different groups that separate 3p strands from 5p strands. While 3p strands cluster in 2 groups that match their functional clusters (A: miR200a 3p and miR141 3p; B: miR200b 3p, miR200c 3p and miR429), 5p strands cluster together with the negative control.

200a 3p and 141 3p (Group A), 200b 3p, 200c 3p and 429 (group B) are nicely separated from the controls (200a 5p, 200c 5p and neg. Ko). Using the PCA data, applying as cut off an adjusted p-value of < 0.05 and a logarithmic 2 fold change of either  $\leq -0.6$  (for upregulated genes) or  $\geq 0.6$  (for downregulated genes), a list of deregulated genes in each cell line, according to their cluster group, was established (see table xx). Applying Venn diagrams, the overlapping genes in both cell lines according to their clustering group were listed on the following table.

Table 10. Average expression of the miR200 family in glioblastoma samples.

	Diff reg genes padj <0.05 log2FC $\geq$ 0.6		Diff reg genes padj <0.05 log2FC $\leq$ -0.6	
	Gruppe A down	Gruppe B down	Gruppe A up	Gruppe B up
<b>U87</b>	<b>145</b>	<b>476</b>	<b>235</b>	<b>497</b>
<b>U251</b>	<b>490</b>	<b>484</b>	<b>640</b>	<b>970</b>
<b>overlap</b>	<b>42</b>	<b>59</b>	<b>61</b>	<b>87</b>

A total of 101 genes appeared to be downregulated (adjusted p-value <0.05 and logarithmic 2 fold change  $\geq 0.6$ ) in both cell lines overexpressing the 3p strand of the miR200 family, of which 42 were only downregulated in group A (miR200a 3p and miR141 3p) and 59 in group B (miR200b 3p, miR200c 3p and miR429). A total of 148 genes were upregulated in cells overexpressing the 3p strand of the miR200 family. While group A showed a total of 61 common deregulated genes, in group B 87 common genes appeared to be upregulated in both cell lines. The detailed list of common deregulated genes in both cell lines according to group clustering is shown below.

Table 11. Significantly down- and upregulated genes (p-adj < 0.05) in groups A and B common in both cell lines. \*\*Discrepancies in the number of deregulated genes in each column correspond to (missing) data not identified by the DAVID Bioinformatics software.

Downregulated genes in Group A	Downregulated genes in Group B	Upregulated genes in Group A	Upregulated genes in Group B
1. 6-phosphofructo-2-kinase/fructose-2,6-biphosphatase 4(PFKFB4)	1. activating transcription factor 3(ATF3)	1. ABL proto-oncogene 2, non-receptor tyrosine kinase(ABL2)	1. adaptor related protein complex 1 sigma 2 subunit(AP152)
2. 53nkyrin53 3(ADD3)	2. ADP ribosylation factor like GTPase 14 effector protein like(ARL14EPL)	2. acyl-CoA thioesterase 7 pseudogene(LOC344967)	2. ADP ribosylation factor like GTPase 2 binding protein(ARL2BP)
3. adrenomedullin(ADM)	3. aldo-keto reductase family 1 member C1(AKR1C1)	3. acyl-CoA thioesterase 7(ACOT7)	3. anaphase promoting complex subunit 13(ANAPC13)
4. 53nkyrin repeat and zinc finger domain containing 1(ANKZF1)	4. aldo-keto reductase family 1 member C2(AKR1C2)	4. BICD cargo adaptor 2(BICD2)	4. angiominin like 2(AMOTL2)
5. ARFGEF family member 3(ARFGEF3)	5. aldo-keto reductase family 1 member C3(AKR1C3)	5. cannabinoid receptor interacting protein 1(CNRIP1)	5. 53nkyrin repeat and SOCS box containing 13(ASB13)
6. arrestin domain containing 3(ARRDC3)	6. anoctamin 7(ANO7)	6. cyclin dependent kinase 8(CDK8)	6. ATPase phospholipid transporting 11(ATP11C)
7. carbonic anhydrase 12(CA12)	7. ATPase phospholipid transporting 8B3(ATP8B3)	7. cysteine rich angiogenic inducer 61(CYR61)	7. beta-1,4-glucuronyltransferase 1(B4GAT1)
8. CDP-diacylglycerol synthase 1(CDS1)	8. BICD family like cargo adaptor 1(BICDL1)	8. dedicator of cytokinesis 10(DOCK10)	8. cadherin like and PC-esterase domain containing 1(CPED1)
9. cellular retinoic acid binding protein 2(CRABP2)	9. cadherin 3(CDH3)	9. dickkopf WNT signaling pathway inhibitor 1(DKK1)	9. cartilage associated protein(CRTAP)
10. chitinase 3 like 1(CH13L1)	10. CD24 molecule(CD24)	10. ELK3, ETS transcription factor(ELK3)	10. cofilin 2(CFL2)
11. c-Maf inducing protein(CMIP)	11. CDC42 binding protein kinase gamma(CDC42BPG)	11. EPH receptor A2(EPHA2)	11. cyclin dependent kinase 17(CDK17)
12. collagen type IV alpha 4 chain(COL4A4)	12. CDP-diacylglycerol synthase 1(CDS1)	12. family with sequence similarity 160 member B1(FAM160B1)	12. DAZ interacting zinc finger protein 1(DZIP1)
13. complement C1r subcomponent like(C1RL)	13. ChaC glutathione specific gamma-glutamylcydotransferase 1(CHAC1)	13. gem nuclear organelle associated protein 5(GEMIN5)	13. DENN domain containing 5B(DENND5B)
14. complement C3(C3)	14. CKLF like MARVEL transmembrane domain containing 4(CMTM4)	14. glutaredoxin 2(GLRX2)	14. EH domain containing 1(EHD1)
15. cyclin dependent kinase 18(CDK18)	15. claudin 4(CLDN4)	15. GTP binding protein overexpressed in skeletal muscle(GEM)	15. fasciculation and elongation protein zeta 2(FE22)
16. DARS antisense RNA 1(DARS-AS1)	16. collagen type IV alpha 3 chain(COL4A3)	16. importin 5(IPO5)	16. fermitin family member 2(FERMT2)
17. dehydrogenase/reductase 9(DHRS9)	17. collagen type IV alpha 4 chain(COL4A4)	17. Kruppel like factor 2(KLF2)	17. fibroblast growth factor 1(FGF1)
18. dihydropyrimidinase like 4(DPYSL4)	18. complement C3(C3)	18. mitogen-activated protein kinase kinase 3(MAP3K3)	18. formin homology 2 domain containing 1(FHOD1)
19. ELOVL fatty acid elongase 7(ELOVL7)	19. coxsackie virus and adenovirus receptor(CXADR)	19. neuron navigator 3(NAV3)	19. GLI family zinc finger 3(GLI3)
20. ephrin A3(EFNA3)	20. cyclin dependent kinase 6(CDK6)	20. nexilin F-actin binding protein(NEXN)	20. GTP binding protein overexpressed in skeletal muscle(GEM)
21. family with sequence similarity 57 member A(FAM57A)	21. cystathionine gamma-lyase(CTH)	21. nucleolar protein 11(NOL11)	21. heme oxygenase 1(HMOX1)
22. family with sequence similarity 84 member A(FAM84A)	22. 53nkyrin53ed associated activator of morphogenesis 1(DAAM1)	22. palmitoyl-protein thioesterase 2(PPT2)	22. HPS5, biogenesis of lysosomal organelles complex 2 subunit 2(HPS5)
23. fucosidase, alpha-L-1, tissue(FUCA1)	23. ELOVL fatty acid elongase 7(ELOVL7)	23. PH domain and leucine rich repeat protein phosphatase 2(PHLP2)	23. integrin subunit beta 3(ITGB3)
24. gap junction protein beta 2(GJB2)	24. erythrocyte membrane protein band 4.1 like 4B(EPB41L4B)	24. potassium channel tetramerization domain containing 20(KCTD20)	24. KDEL motif containing 1(KDEL1)
25. glycogen synthase 1(GYS1)	25. exophilin 5(EXPH5)	25. pyruvate dehydrogenase (lipoamide) alpha 1(PDHA1)	25. KIAA1462(KIAA1462)
26. hook microtubule tethering protein 2(HOOK2)	26. F11 receptor(F11R)	26. repulsive guidance molecule family member b(RGMB)	26. kinase insert domain receptor(KDR)
27. hypoxia inducible lipid droplet associated(HILPDA)	27. family with sequence similarity 160 member A1(FAM160A1)	27. ring finger protein 13(RNF13)	27. Kruppel like factor 2(KLF2)
28. KIAA1161(KIAA1161)	28. family with sequence similarity 84 member B(FAM84B)	28. RWD domain containing 4(RWDD4)	28. KTI12 chromatin associated homolog(KTI12)
29. mannose phosphate isomerase(MPI)	29. Fc fragment of IgM receptor(FCMR)	29. signal transducer and activator of transcription 5B(STAT5B)	29. LDL receptor related protein 4(LRP4)
30. MAX interactor 1, dimerization protein(MX1)	30. glutamate-cysteine ligase catalytic subunit(GCLC)	30. small integral membrane protein 13(SMIM13)	30. lipoma HMGC fusion partner(LHFP)
31. metallothionein 1X(MTX1)	31. HLA complex P5 (non-protein coding)(HCP5)	31. small nuclear ribonucleoprotein polypeptide B2(SNRPB2)	31. MAPK regulated corepressor interacting protein 1(MCRIP1)
32. methyltransferase like 21B(METTL21B)	32. hook microtubule tethering protein 2(HOOK2)	32. solute carrier family 19 member 2(SLC19A2)	32. mitogen-activated protein kinase kinase kinase 5(MAP4K5)
33. microRNA 6510(MIR6510)	33. inhibin beta E subunit(INHBE)	33. solute carrier family 35 member D1(SLC35D1)	33. monocyte to macrophage differentiation associated(MMD)
34. microRNA 936(MIR936)	34. Kazal type serine peptidase inhibitor domain 1(KAZALD1)	34. spermidine synthase(SRM)	34. multiple coagulation factor deficiency 2(MCFD2)
35. mixed lineage kinase 4(MLK4)	35. keratin 16(KRT16)	35. spindle apparatus coiled-coil protein 1(SPDL1)	35. neuron navigator 3(NAV3)
36. myosin VC(MYO5C)	36. keratin 8(KRT8)	36. tetraspanin 4(TSPAN4)	36. nexilin F-actin binding protein(NEXN)
37. neuritin 1(NRN1)	37. KIAA1161(KIAA1161)	37. transferrin receptor(TFRC)	37. osteopetrosis associated transmembrane protein 1(OSTM1)
38. N-myc downstream regulated 1(NDRG1)	38. Kruppel like factor 5(KLF5)	38. transmembrane protein 209(TMEM209)	38. phorbo1-12-myristate-13-acetate-induced protein 1(PMAIP1)
39. PATJ, crumbs cell polarity complex component(PATJ)	39. long intergenic non-protein coding RNA 601(LINC00601)	39. tRNA methyltransferase 11-2 homolog (S. cerevisiae)(TRMT112)	39. phospholipase C gamma 1(PLCG1)
40. phosphodiesterase 5A(PDE5A)	40. major facilitator superfamily domain containing 6(MFSD6)	40. Wnt family member 5B(WNT5B)	40. prostate transmembrane protein, androgen induced 1(PMEPA1)
41. phosphoglucomutase 1(PGM1)	41. melanoregulin(MREG)		41. protein phosphatase 2 regulatory subunit B'gamma(PPP2R3C)
42. pleckstrin homology domain containing A1(PLEKHA1)	42. microRNA 4724(MIR4724)	** 2 unidentified genes	42. protein phosphatase, Mg2+/Mn2+ dependent 1F(PPM1F)
43. potassium voltage-gated channel subfamily E regulatory subunit 4(KCNE4)	43. microRNA 6510(MIR6510)		43. RAB11 family interacting protein 2(RAB11FIP2)
44. protein phosphatase 1 regulatory subunit 3B(PPP1R3B)	44. microRNA 936(MIR936)		44. radixin(RDX)
45. protein phosphatase 1 regulatory subunit 3E(PPP1R3E)	45. microtubule associated protein 7(MAP7)		45. raftlin, lipid raft linker 1(RFTN1)
46. PTPRF interacting protein alpha 4(PPIA4)	46. mixed lineage kinase 4(MLK4)		46. retinol dehydrogenase 10 (all-
47. Ras association domain family member 4(RASSF4)	47. multiple EGF like domains 10(MEGF10)		
48. rhomboid 5 homolog 2(RHBDF2)	48. myelin protein zero like 3(MPZL3)		
49. SLIT and NTRK like family member 6(SLITRK6)	49. myosin VC(MYO5C)		

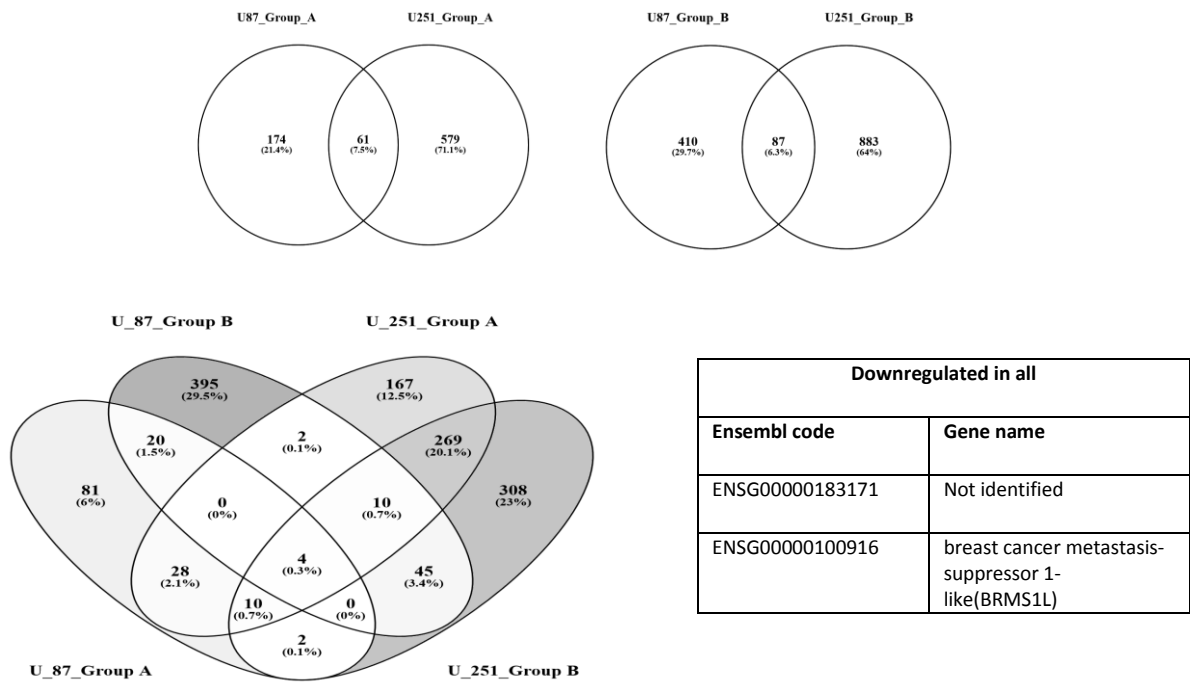
50. SMAD family member 9(SMAD9)	50. PATJ, crumbs cell polarity complex component(PATJ)		trans)(RDH10)
51. solute carrier family 2 member 3(SLC2A3)	51. phosphodiesterase 5A(PDE5A)		47. Rho GTPase activating protein 19(ARHGAP19)
52. solute carrier family 27 member 3(SLC27A3)	52. phospholipid scramblase 4(PLSCR4)		48. RUN and SH3 domain containing 2(RUSC2)
53. solute carrier family 6 member 8(SLC6A8)	53. proline rich and Gla domain 2(PRRG2)		49. Sec23 homolog A, coat complex II component(SEC23A)
54. stratifin(SFN)	54. protein kinase C delta(PRKCD)		50. solute carrier family 35 member B4(SLC35B4)
55. synaptotagmin like 1(SYTL1)	55. RAB17, member RAS oncogene family(RAB17)		51. solute carrier family 45 member 3(SLC45A3)
56. transforming growth factor betainduced(TGFBI)	56. regulator of cell cycle(RGCC)		52. SPOC domain containing 1(SPOCD1)
57. TRPM8 channel associated factor 2(TCAF2)	57. rhomboid 5 homolog 2(RHBDP2)		53. synapse defective Rho GTPase homolog 1(SYDE1)
58. tsukushi, small leucine rich proteoglycan(TSKU)	58. rhophilin Rho GTPase binding protein 2(RHPN2)		54. TMCC1 antisense RNA 1 (head to head)(TMCC1-AS1)
59. vascular endothelial growth factor A(VEGFA)	59. RNA binding motif protein 47(RBM47)		55. WAS protein family member 3(WASF3)
60. zinc finger protein 395(ZNF395)	60. RPARP antisense RNA 1(RPARP-AS1)		56. zinc finger E-box binding homeobox 1(ZEB1)
61. zinc finger SWIM-type containing 5(ZSWIM5)	61. SBF2 antisense RNA 1(SBF2-AS1)		57. zinc finger protein 333(ZNF333)
	62. sodium voltage-gated channel alpha subunit 9(SCN9A)		58. zinc finger protein 697(ZNF697)
	63. solute carrier family 25 member 18(SLC25A18)		** 1 unidentified gene
	64. solute carrier family 29 member 2(SLC29A2)		
	65. solute carrier family 6 member 9(SLC6A9)		
	66. sperm associated antigen 1(SPAG1)		
	67. sphingomyelin phosphodiesterase acid like 3B(SMPDL3B)		
	68. stratifin(SFN)		
	69. synaptotagmin 12(SYT12)		
	70. synaptotagmin like 1(SYTL1)		
	71. syntrophin beta 1(SNTB1)		
	72. tachykinin receptor 1(TACR1)		
	73. tetraspanin 1(TSPAN1)		
	74. tetratricopeptide repeat domain 39A(TTC39A)		
	75. transmembrane protein 184A(TMEM184A)		
	76. transmembrane protein 56(TMEM56)		
	77. tribbles pseudokinase 3(TRIB3)		
	78. uncharacterized LOC102723566(LOC102723566)		
	79. uncharacterized LOC400221(FIJ22447)		
	80. uncharacterized LOC440028(LOC440028)		
	81. vesicle associated membrane protein 8(VAMP8)		
	82. Williams Beuren syndrome chromosome region 27(WBSCR27)		
	83. zinc finger DHHC-type containing 23(ZDHC23)		
	84. zinc finger protein 652(ZNF652)		
	** 3 unidentified genes		

Among the list of deregulated genes found in both cell lines, members of the cyclin dependent kinase family (CDKs), which control the cell cycle and have been described to be direct targets of the miRNA 200 family<sup>2</sup>, appeared to be both down- and upregulated in both groups. Various members of the solute carrier group of membrane transport family (SLCs) also showed to be downregulated. In group B cadherin 3 was downregulated, while the fibroblast growth factor 1 (FGF) was shown to be upregulated. Curiously, ZEB1 also showed to be commonly upregulated in group B (cells overexpressing miR200b 3p, miR200c 3p and miR429).

To further narrow our findings to down- or upregulated genes indifferently of functional group (group A vs. group B) Venn diagrams were performed as seen below.



A)



B)

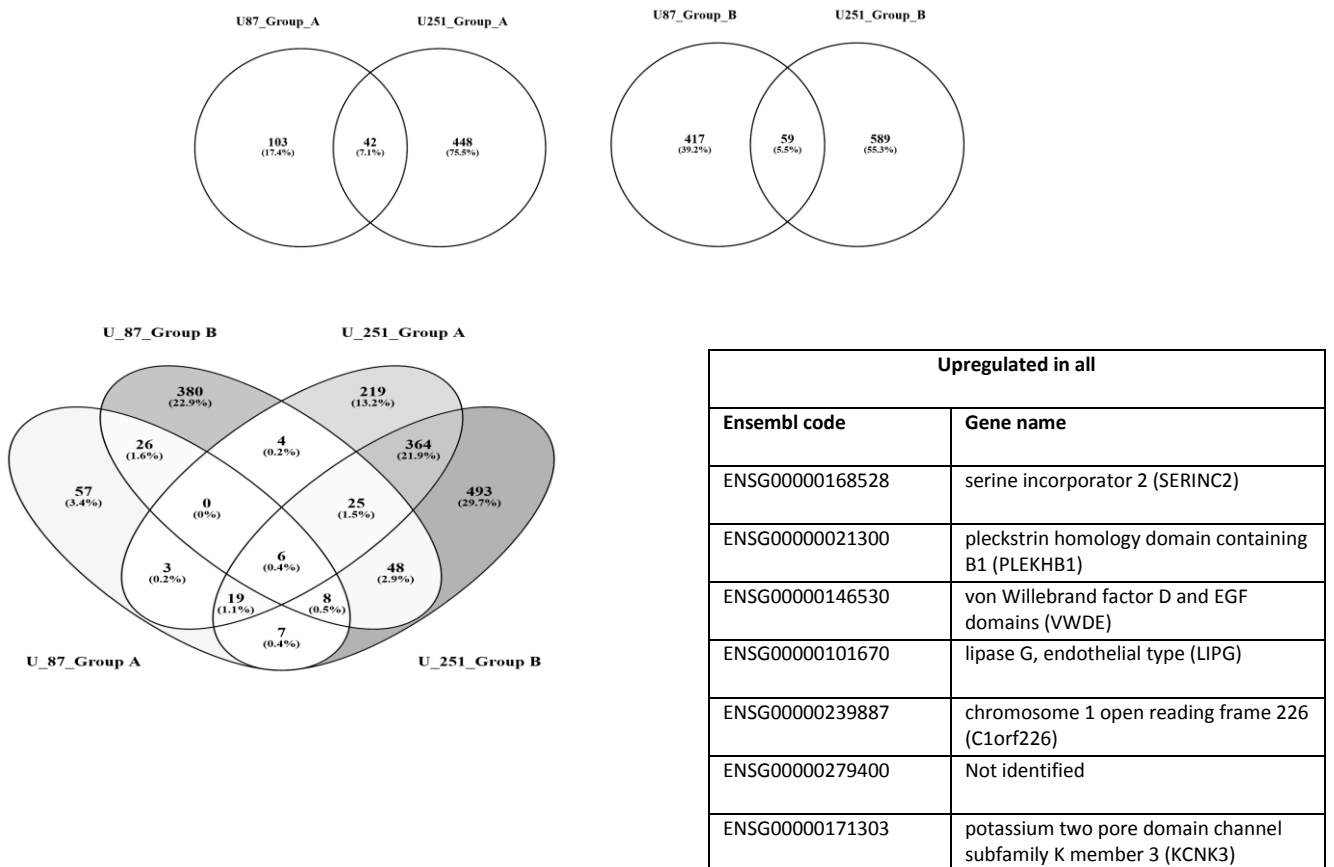


Figure 19. Venn analyses among clustering groups A and B. In figure A are depicted downregulated genes overlapping in both clustering groups for both cell lines. Figure B shows Venn diagrams for upregulated genes common to both clustering groups.

Just a few genes were shown to be commonly deregulated in both functional groups (group A vs. group B) after performing Venn analyses. While the breast cancer metastasis-suppressor 1-like (BRMS1L) gene showed to be downregulated in both groups (a second deregulated gene couldn't be identified), 7 genes were commonly upregulated in both groups (see table above).

To further search for significant enriched GO terms (in biological processes, cellular components or molecular functions) common to each group and to both cell lines, up- and downregulated genes listed above were used to create functional analysis charts using the DAVID bioinformatics software. As cut off points a Benjamini adjusted p-value of < 0.05 was set. No significant enrichment was seen in either set of regulated genes in either group.

To further analyze the NGS data, gene set enrichment analysis (GSEA) was performed using the rlog counts to search for enrichment groups of genes sharing a common biological function, chromosomal location or regulation (gene set). The cut off values were a false discovery rate (fdr) < 0.25 and a normalized p-value of < 0.05.

Table 12. Average expression of the miR200 family in glioblastoma samples.

Group A (miR200a 3p, miR141 3p)	Group B (miR200b 3p, miR200c 3p and miR429)
<p><b>Hallmarks</b></p> <p><u>Upregulated in Group A</u></p> <p>gene_sets.gmt#HALLMARK_UV_RESPONSE_UP  gene_sets.gmt#HALLMARK_DNA_REPAIR  gene_sets.gmt#HALLMARK_E2F_TARGETS  gene_sets.gmt#HALLMARK_UNFOLDED_PROTEIN_RESPONSE  gene_sets.gmt#HALLMARK_MYC_TARGETS_V2  gene_sets.gmt#HALLMARK_G2M_CHECKPOINT  gene_sets.gmt#HALLMARK_OXIDATIVE_PHOSPHORYLATION  gene_sets.gmt#HALLMARK_TNFA_SIGNALING_VIA_NFKB  gene_sets.gmt#HALLMARK_MYC_TARGETS_V1</p> <p><u>Downregulated in Group A</u></p> <p>gene_sets.gmt#HALLMARK_HYPOXIA  gene_sets.gmt#HALLMARK_GLYCOLYSIS  gene_sets.gmt#HALLMARK_ESTROGEN_RESPONSE_EARLY  gene_sets.gmt#HALLMARK_KRAS_SIGNALING_DN</p> <p><b>C2 (metabolism, literature)</b></p> <p><u>Upregulated in Group A</u></p> <p>gene_sets.gmt#REACTOME_METABOLISM_OF_NON_CODING_RNA  gene_sets.gmt#MANALO_HYPOXIA_DN</p> <p><u>Downregulated in Group A</u></p> <p>gene_sets.gmt#ELVIDGE_HIF1A_TARGETS_DN  gene_sets.gmt#ELVIDGE_HYPOXIA_BY_DMOG_UP  gene_sets.gmt#ELVIDGE_HIF1A_AND_HIF2A_TARGETS_DN</p>	<p><b>Hallmarks</b></p> <p><u>Upregulated in Group B</u></p> <p>0</p> <p><u>Downregulated in Group B</u></p> <p>gene_sets.gmt#HALLMARK_INTERFERON_ALPHA_RESPONSE  gene_sets.gmt#HALLMARK_ESTROGEN_RESPONSE_LATE  gene_sets.gmt#HALLMARK_INTERFERON_GAMMA_RESPONSE  gene_sets.gmt#HALLMARK_ESTROGEN_RESPONSE_EARLY  gene_sets.gmt#HALLMARK_GLYCOLYSIS</p> <p><b>C2 (metabolism, literature)</b></p> <p><u>Upregulated in Group B</u></p> <p>0</p> <p><u>Downregulated in Group B</u></p> <p>gene_sets.gmt#COLDREN_GEFITINIB_RESISTANCE_DN  gene_sets.gmt#REACTOME_DEFENSINS  gene_sets.gmt#CHARAFE_BREAST_CANCER_BASAL_VS_MESENCHYMAL_UP  gene_sets.gmt#CHARAFE_BREAST_CANCER_LUMINAL_VS_MESENCHYMAL_UP  gene_sets.gmt#ONDER_CDH1_TARGETS_2_DN  gene_sets.gmt#REACTOME_BETA_DEFENSINS  gene_sets.gmt#HANN_RESISTANCE_TO_BCL2_INHIBITOR_DN  gene_sets.gmt#ROY_WOUND_BLOOD_VESSEL_DN  gene_sets.gmt#JAEGER_METASTASIS_DN</p>

<p>gene_sets.gmt#COLDREN_GEFITINIB_RESISTANCE_DN  gene_sets.gmt#ELVIDGE_HYPOXIA_UP  gene_sets.gmt#FARDIN_HYPOXIA_11  gene_sets.gmt#ONDER_CDH1_TARGETS_2_DN  gene_sets.gmt#CHARAFE_BREAST_CANCER_BASAL_VS_MESENCHYMAL_UP  gene_sets.gmt#MENSE_HYPOXIA_UP  gene_sets.gmt#CHARAFE_BREAST_CANCER_LUMINAL_VS_MESENCHYMAL_UP  gene_sets.gmt#JAEGER_METASTASIS_DN  gene_sets.gmt#LEONARD_HYPOXIA  gene_sets.gmt#QI_HYPOXIA  gene_sets.gmt#MANALO_HYPOXIA_UP</p> <p><b>C3 (Transcription factors, miRNAs)</b></p> <p><u>Upregulated in Group A</u></p> <p>1 common element in "U87_c3_A" and "U251_c3_A":  gene_sets.gmt#CAGTGTT,MIR-141,MIR-200A</p> <p><u>Downregulated in Group A</u></p> <p>0</p>	<p><b>C3 (Transcription factors, miRNAs)</b></p> <p><u>Upregulated in Group B</u></p> <p>1 common element in "U87_c3_B" and "U251_c3_B":  gene_sets.gmt#CAGTATT,MIR-200B,MIR-200C,MIR-429</p> <p><u>Downregulated in Group B</u></p> <p>1 common element in "U87_c3_B" and "U251_c3_B":  gene_sets.gmt#V\$AREB6_01</p>
---	--

Enriched or depleted gene sets (affecting proteins, transcription factors and signaling pathways) as a consequence of overexpressing the 3p strand of the miR200 family are listed in the table above. Here it could be noted that deregulation of signaling pathways/ proteins mainly involved in hypoxia, DNA repair and cell cycle are affected by an increased expression of the miRNA 200 family members.

In group A, G2-M DNA damage checkpoint, an important cell cycle checkpoint in eukaryotic cells which controls DNA damage repair after replication known to be a target of the miR200 family<sup>12</sup>, was upregulated. Another upregulated gene observed in this group was the E2F gene, which codifies a family of transcription factors involved in cell cycle regulation and DNA synthesis<sup>13</sup>. Targets for c-myc as well as TNF $\alpha$  signaling via NF $\kappa$ B, who are also involved in cell growth, cell-cycle, cell adhesion molecules and anti-apoptotic proteins<sup>17, 21</sup> were also shown to be upregulated in group A.

Interestingly, higher expression levels of miR200a 3p and miR141 3p showed to cause a down regulation of the hypoxia-inducible factor HIF1 $\alpha$  and a deregulation of hypoxia metabolism. Moreover, targets of the CDH1 gene, which encodes E-cadherin, were also found to be downregulated in this group.

As for group B, mainly estrogen response elements were downregulated. Estrogen early response has been described to regulate top canonical pathways involved in cell growth and proliferation, whereas estrogen late response regulates signaling pathways involved in DNA replication and repair, cell cycle and cell death<sup>82</sup>.

## 5. Discussion

The miR200 family has been described to exert tumor suppressing functions in different malignant epithelial tumors, and their down regulation has been associated with aggressiveness, metastatic disease, tumor progression, chemoresistance and worse prognosis<sup>83</sup>. Their expression has been highly associated to an epithelial phenotype and their increased expression has been shown to reverse EMT *in vitro* and *in vivo* in diverse malignant epithelial cancers, whereas their low expression has been associated with poor survival and disease progression<sup>19</sup>.

In glioblastoma, over 200 miRNAs have been reported to be upregulated<sup>84</sup>. However, some members of the miR200 family have been shown to be expressed at very low levels in glioblastomas compared to non-neoplastic brain and glial tumors of WHO-grades I-III<sup>85</sup>, and their low expression has been associated to poor prognosis<sup>86</sup>. Even though a relevant role of the miRNA 200 family in glioblastomas has been suggested, no detailed data has been provided regarding differences in functional effects among their two strands, in other terms, establishing which of the two strands is functional active, and if their isolated deregulation has relevant functional effects.

In this work it is shown that the expression levels of the miR200 family vary not only between 3p and 5p strands, but also between glioblastoma cell lines and glioblastoma tumors. While in cell lines the 3p strands are lower expressed compared to 5p strands and compared to non-neoplastic brain tissue, in glioblastoma tumors the expression patterns are inverse, with an overexpression of the 3p strands compared to 5p strands (with a significant overexpression of miR200a 3p, miR141 3p and miR429). To try to explain the discrepancy of the results between a cohort of immortalized glioblastoma cell lines and tumor material from glioblastoma patients, a short research of the tumor characteristics was done (see Table 5.1.).

Table 5.1. Immunohistochemical and molecular characteristics of glioblastoma tumors.

Tumor Id.	EGFR expression	p53 accumulation	MGMT methylation	IDH Mutations
GB42	n.a.	n.a.	n.a.	n.a.
GB44	n.a.	5%	0%	n.a.
GB45	Generalized, strong	Many	52%	WT
GB46	None	Very few	0%	WT
GB47	Partial, strong	Very few	0%	n.a.
GB49	Extensive	Few	0%	WT
GB50	Extensive	Few	15%	WT

GB52	Partial	Very few	6%	WT
GB53	Extensive	Many	31%	n.a.

Since some tumors were resected before the department of Neuropathology was established at our university hospital, not all molecular examinations and immunohistochemical stainings were available for all cases. From the information extracted from the histological examinations, most tumors showed a high expression of EGF receptor and very few had a nuclear accumulation of p53, meaning a lack of p53 mutations. The epithelial growth factor receptor (EGFR) is known to be pathologically overexpressed in glioblastoma<sup>84, 24</sup>. It has been shown, that EGFR induces EMT by downregulating the miR200 family (specifically miR200c) and subsequently reducing the expression of the E-cadherin codifying gene CDH1<sup>84</sup>. On the other hand, the potential role of p53 mutations in EMT was shown by Kim et al<sup>85</sup> in primary HCC cell lines, in which they observed that overexpressing p53 directly targets the posttranslational regulation of the miR200 family (miR200b, miR200c and miR141) causing a consequent repression of ZEB1 and ZEB2 expression and a transformation from a mesenchymal to an epithelial phenotype<sup>85</sup>. Based on data extracted from these previous publications, it would be expected that in our glioblastoma tumor cohort, especially since they show immunohistochemically an overexpression of EGFR and a lack of p53 mutations, the miR200 family would be downregulated. However, regional differences in the tumor microstructure may apply. The miR200 family has been shown to be downregulated in metastasis and metastatic-like primary tumors<sup>19</sup>, which could explain an overexpression of miR200 family in tumor cells located in the tumor center, where they would need an “epithelial” phenotype to adhere, compared to cells in the periphery invasion zone. Of note, our miRNA fraction was extracted from the tumor core and it has been shown by Siebzehrnühl et al. that ZEB1 expression is lower in this region (potentially due to higher miRNA 200 levels)<sup>39</sup>.

To gain further insights into the expression levels of the miR200 family in glioblastoma tumors, TCGA data were extracted for glioblastoma samples. Here, except for miR200b 3p, which showed a significant downregulation ( $p < 0.05$ ), no difference was seen on expression levels between the miR200 family and matched non-neoplastic brain tissue samples. Furthermore, no data regarding 5p strands was available. The conduction of Kaplan-Meier survival curves nevertheless showed a significantly worse outcome in patients harboring tumors with elevated expression of miR200a 3p and miR200b 3p. Contrarily to these findings, in 2014 two publications showed a decreased expression of miR200b in glioblastoma compared normal brain tissue, which correlated with worse overall survival when compared to higher levels of this miRNA<sup>85, 86</sup>. Peng et al. even showed

decreased proliferative capacities in glioblastoma cell lines overexpressing miR200b, and these effects could be extrapolated to cells in xenograft models in which the overexpression of miR200b suppressed glioma cell tumorigenicity<sup>34</sup>.

These findings correlate to our functional *in vitro* results. U-87 MG and U-251 MG cells overexpressing the 3p strands of the miR200 family members showed both a decrease in proliferation and increase in apoptosis compared to those harboring higher expression levels of 5p strands. NGS analyses furthermore showed clustering of 5p strands together with cells transfected with a negative control miRNA, confirming a functional inactivity of 5p strands of the miR200 family members.

The miRNA 200 family has been shown to have an effect on cell proliferation, cell cycle, and tumor growth in gliomas and in brain tumor initiating cells, as well as in chemoresistance<sup>33</sup>. NGS data of U-87MG and U-251 MG cells overexpressing the miR200 family showed upregulation of gene sets implicated in DNA damage/repair, as well as in proteins implicated in cell cycle and cell viability. These effects were mainly seen in cells overexpressing miR200a 3p and miR141 3p (functional cluster A), in which upregulation of the G2/M DNA damage checkpoint, an important cell cycle checkpoint in eukaryotic cells which controls DNA damage repair after replication and before cells enter into Mitosis<sup>87</sup>, as well as targets of the E2F gene which codifies a family of transcription factors involved in cell cycle regulation and DNA synthesis<sup>88</sup>, were observed. These results correlate to findings in previous publications reporting abnormalities of the p16-Rb-E2F1 pathway in gliomas influencing apoptosis, like observed in our cells, and suppressing tumor progress *in vivo*<sup>89, 90</sup>. Moreover, overexpression of the G2/M DNA damage checkpoint has been identified as a major character in the mediation of glioblastoma chemo- and radiotherapy resistance, and histone deacetylase inhibitors produce cell death mainly by targeting the G2 damage checkpoint<sup>91</sup>.

Other gene targets found to be deregulated in functional cluster A where targets of c-myc and TNF $\alpha$  signaling via the nuclear factor (NF)- $\kappa$ B (NF $\kappa$ B), both of which are known to belong to signaling pathways involved in cell growth and cell-cycle progression<sup>92</sup>. c-myc expression is known to be higher in high grade gliomas<sup>93</sup>. It has also been shown that higher levels of c-myc are able to downregulate the expression of the miR200 family through regulation of ZEB1 and ZEB2 in endometrial carcinoma cells<sup>94</sup>. On the other hand NF $\kappa$ B is known to control expression of anti-apoptotic proteins<sup>95</sup>, and has been shown to directly repress E-cadherin through regulation of ZEB1 in epithelial cancer cells<sup>96, 97</sup>. In our cohort, high levels of miR200a3p and miR141 3p reduced

proliferation, induced apoptosis and decreased ZEB1 expression while inducing on RNA level an upregulation of targets of c-myc and NFκB, probably through induction of c-myc inhibitors and promoting activation of NFκB.

High levels of functional cluster A also produced a downregulation of the hypoxia-inducible factor HIF1α and a deregulation of hypoxia response. Hypoxia is a well-known inducer of the EMT in epithelial cancers as well to induce a mesenchymal phenotype in glioblastoma, mainly due to a hypoxia-induced HIF1α-ZEB1 axis, leading to enhanced invasion capacities in glioblastoma cells<sup>98</sup>. Perivascular niches present in glioblastoma have proven to be areas of hypoxia, and surviving tumor cells strongly express HIF-1α<sup>99, 100</sup>. HIF1α is well known to be a master regulator of the hypoxia response and hypoxia itself has been associated to poor prognosis and therapy resistance<sup>101</sup>, as well as a regulator of stem cell markers in brain tumor initiating cells<sup>102</sup>.

In general, our findings suggest that overexpression of functional cluster A (mir200a 3p and miR141 3p) plays an important role in the regulation of targets of signaling pathways involved in cell cycle processes, proliferation, apoptosis and chemotherapy resistance in glioblastoma cells.

On the other hand, overexpression of functional cluster B (miR200b 3p, miR200c 3p and miR429) mainly caused downregulation of estrogen response elements, which have been described to regulate top canonical pathways involved in cell growth and proliferation as well as signaling pathways involved in DNA replication and repair, cell cycle and cell death<sup>103</sup>. This correlates to the results found in our functional assays, where cells overexpressing this miR200 family members also showed decreased proliferative activity and an increase in programmed cell death.

Interestingly, our results show that higher expression levels of 3p strands of all members of the miRNA 200 family induce also downregulation of targets of the CDH1 gene, which encodes E-cadherin, therefore suggesting a further role of this family of miRNAs in cell adhesion and motility.

Even though our results indicate a major regulatory effect of the miRNA 200 family in proliferation and cell viability, further analyses to identify specific targets in the dysregulated pathways must be performed.

Regarding ZEB1/ ZEB2 expression, which has been shown to be regulated by the miR200 family through a double-negative feedback loop, we found that 3p strands of all miRNAs of the miR200

family lead to a decrease in the expression of ZEB1, especially miR200b 3p and miR200c 3p (functional cluster B), as well as in the expression of ZEB2. These findings correlate to results published by Siebzehnrübl et al. (2013), who showed compelling evidence stating the role of ZEB1 in EMT-similar processes in glioblastoma, attributing this effect to the expression of miR200c<sup>39</sup>.



## 6. Conclusion

Altogether, this data shows that glioblastoma cell lines express lower levels of the miR200 family, especially the 3p strand, when compared to non-neoplastic brain tissue. There is a discrepancy to the miRNA expression levels in glioma biopsy samples that needs further clarification. The transfection with miRNA mimics does have clear functional effects. Among both strands of the miR200 family only the 3p strand showed a convincing reduction in proliferation and increase in apoptosis. Furthermore, high levels of the 3p strands of the miR200 family induce an effect on ZEB1 and ZEB2 expression in U-87 MG and U-251 MG cells. Finally, NGS analyses showed on RNA level that these effects are mainly carried out through deregulation of signaling pathways involved in cell cycle regulation and chemoresistance (G2-M DNA damage checkpoint, E2F gene, Nf-k $\beta$  and c-myc), cell motility and adhesion (CDH1 gene) and hypoxia response (HIF1 $\alpha$ ), all known to be major components of EMT. Thus, the miR200 family is likely to carry out tumor suppressive functions in gliomas by interacting with major pathologic pathways, the exact targets of which must be clarified.

## Bibliography

1. Senfter, D; Madlener, S; Krupitza, G; Mader, R. M. (2016): The microRNA-200 family: still much to discover. In: *Biomolecular concepts* 7 (5-6), S. 311–319. DOI: 10.1515/bmc-2016-0020.
2. Humphries, B; Yang, C (2015): The microRNA-200 family: small molecules with novel roles in cancer development, progression and therapy. In: *Oncotarget* 6 (9), S. 6472–6498. DOI: 10.18632/oncotarget.3052.
3. Iorio, M. V.; Croce, C. M. (2012): MicroRNA dysregulation in cancer: diagnostics, monitoring and therapeutics. A comprehensive review. In: *EMBO molecular medicine* 4 (3), S. 143–159. DOI: 10.1002/emmm.201100209.
4. Takahashi, R-U; Miyazaki, H; Ochiya, T (2014): The role of microRNAs in the regulation of cancer stem cells. In: *Frontiers in genetics* 4, S. 295. DOI: 10.3389/fgene.2013.00295.
5. Thiery, J. P.; Acloque, H; Huang, R. Y. J.; Nieto, M. A. (2009): Epithelial-mesenchymal transitions in development and disease. In: *Cell* 139 (5), S. 871–890. DOI: 10.1016/j.cell.2009.11.007.
6. Prat, A; Parker, J. S.; Karginova, O; Fan, C; Livasy, C; Herschkowitz, J. I. et al. (2010): Phenotypic and molecular characterization of the claudin-low intrinsic subtype of breast cancer. In: *Breast cancer research : BCR* 12 (5), R68. DOI: 10.1186/bcr2635.
7. Polyak, K; Weinberg, R. A. (2009): Transitions between epithelial and mesenchymal states: acquisition of malignant and stem cell traits. In: *Nature reviews. Cancer* 9 (4), S. 265–273. DOI: 10.1038/nrc2620.
8. Mani, S. A.; Guo, W; Liao, M-J; Eaton, E. Ng; Ayyanan, A; Zhou, A. Y. et al. (2008): The epithelial-mesenchymal transition generates cells with properties of stem cells. In: *Cell* 133 (4), S. 704–715. DOI: 10.1016/j.cell.2008.03.027.

9. Morel, A-P; Lievre, M; Thomas, C; Hinkal, G; Ansieau, S; Puisieux, A (2008): Generation of breast cancer stem cells through epithelial-mesenchymal transition. In: *PLoS one* 3 (8), e2888. DOI: 10.1371/journal.pone.0002888.
10. May, C. D.; Sphyris, N; Evans, K. W.; Werden, S. J.; Guo, W; Mani, S. A. (2011): Epithelial-mesenchymal transition and cancer stem cells: a dangerously dynamic duo in breast cancer progression. In: *Breast cancer research: BCR* 13 (1), S. 202. DOI: 10.1186/bcr2789.
11. Zaravinos, A (2015): The Regulatory Role of MicroRNAs in EMT and Cancer. In: *Journal of Oncology* 2015, S. 865816. DOI: 10.1155/2015/865816.
12. Bracken, C. P.; Khew-Goodall, Y; Goodall, G. J. (2015): Network-Based Approaches to Understand the Roles of miR-200 and other microRNAs in Cancer. In: *Cancer research* 75 (13), S. 2594–2599. DOI: 10.1158/0008-5472.CAN-15-0287.
13. Diaz-Lopez, A; Moreno-Bueno, G; Cano, A (2014): Role of microRNA in epithelial to mesenchymal transition and metastasis and clinical perspectives. In: *Cancer management and research* 6, S. 205–216. DOI: 10.2147/CMAR.S38156.
14. Cano, A; Nieto, M. A. (2008): Non-coding RNAs take centre stage in epithelial-to-mesenchymal transition. In: *Trends in cell biology* 18 (8), S. 357–359. DOI: 10.1016/j.tcb.2008.05.005.
15. Christoffersen, N. R; Silahtaroglu, A; Orom, U. A.; Kauppinen, S; Lund, A. H. (2007): miR-200b mediates post-transcriptional repression of ZFH1B. In: *RNA (New York, N.Y.)* 13 (8), S. 1172–1178. DOI: 10.1261/rna.586807.
16. Park, S-M; Gaur, A. B.; Lengyel, E; Peter, M. E. (2008): The miR-200 family determines the epithelial phenotype of cancer cells by targeting the E-cadherin repressors ZEB1 and ZEB2. In: *Genes & development* 22 (7), S. 894–907. DOI: 10.1101/gad.1640608.
17. Burk, U; Schubert, J; Wellner, U; Schmalhofer, O; Vincan, E; Spaderna, S; Brabletz, T (2008): A reciprocal repression between ZEB1 and members of the miR-200 family promotes EMT and

- invasion in cancer cells. In: *EMBO reports* 9 (6), S. 582–589. DOI: 10.1038/embor.2008.74.
18. Sundararajan, V; Gengenbacher, N; Stemmler, M. P.; Kleemann, J. A.; Brabletz, T; Brabletz, S (2015): The ZEB1/miR-200c feedback loop regulates invasion via actin interacting proteins MYLK and TKS5. In: *Oncotarget* 6 (29), S. 27083–27096. DOI: 10.18632/oncotarget.4807.
  19. Feng, X; Wang, Z; Fillmore, R; Xi, Y (2014): MiR-200, a new star miRNA in human cancer. In: *Cancer letters* 344 (2), S. 166–173. DOI: 10.1016/j.canlet.2013.11.004.
  20. Gladson, C. L.; Prayson, R. A.; Liu, W. M. (2010): The pathobiology of glioma tumors. In: *Annual review of pathology* 5, S. 33–50. DOI: 10.1146/annurev-pathol-121808-102109.
  21. Holland, E. C. (2000): Glioblastoma multiforme: The terminator. In: *Proceedings of the National Academy of Sciences of the United States of America* 97(12).
  22. Rao, R. D.; Uhm, J. H.; Krishnan, S; James, C. D. (2003): Genetic and signaling pathway alterations in glioblastoma: relevance to novel targeted therapies. In: *Front. Biosci.* 8: e270-280.
  23. Soni, D; King, J. A. J.; Kaye, A. H.; Hovens, C. M. (2005): Genetics of glioblastoma multiforme: mitogenic signaling and cell cycle pathways converge. In: *Journal of clinical neuroscience : official journal of the Neurosurgical Society of Australasia* 12 (1), S. 1–5. DOI: 10.1016/j.jocn.2004.04.001.
  24. Louis, D. N. (2006): Molecular pathology of malignant gliomas. In: *Annual review of pathology* 1, S. 97–117. DOI: 10.1146/annurev.pathol.1.110304.100043.
  25. Mason W. P.; Cairncross, J. G. (2008): The expanding impact of molecular biology on the diagnosis and treatment of gliomas. In: *Neurology* 71: 365-373.
  26. Sathornsumetee, S; Rich, J. N. (2008): Designer therapies for glioblastoma multiforme. In: *Annals of the New York Academy of Sciences* 1142, S. 108–132. DOI: 10.1196/annals.1444.009.

27. Ohgaki, H; Kleihues, P (2007): Genetic pathways to primary and secondary glioblastoma. In: *The American journal of pathology* 170 (5), S. 1445–1453. DOI: 10.2353/ajpath.2007.070011.
28. Mrugala, M. M.; Chamberlain, M. C. (2008): Mechanisms of disease: temozolomide and glioblastoma--look to the future. In: *Nature clinical practice. Oncology* 5 (8), S. 476–486. DOI: 10.1038/ncponc1155.
29. Hegi, M. E.; Diserens, A-C; Gorlia, T; Hamou, M-F; de Tribolet, N; Weller, M et al. (2005): MGMT Gene Silencing and Benefit from Temozolomide in Glioblastoma. In: *The New England journal of medicine* 10; 352 (10), S. 997-1003. DOI:10.1056/NEJMoa043331
30. Meyer, M. A. (2008): Malignant gliomas in adults. In: *The New England journal of medicine* 359 (17), 1850; author reply 1850. DOI: 10.1056/NEJMc086380.
31. Stupp, R; Mason, W. P.; van den Bent, M. J.; Weller, M; Fisher, B; Taphoorn, M. J.B. et al. (2005): Radiotherapy plus concomitant and adjuvant temozolomide for glioblastoma. In: *Cancer/Radiothérapie* 9 (3), S. 196–197. DOI: 10.1016/j.canrad.2005.05.001.
32. Carro, M. S.; Lim, W. K.; Alvarez, M. J.; Bollo, R. J.; Zhao, X.; Snyder, E. Y. et al. (2010): The transcriptional network for mesenchymal transformation of brain tumours. In: *Nature* 463 (7279), S. 318–325. DOI: 10.1038/nature08712.
33. Garg, N; Vijayakumar, T; Bakhshinyan, D; Venugopal, C; Singh, S. K. (2015): MicroRNA Regulation of Brain Tumour Initiating Cells in Central Nervous System Tumours. In: *Stem cells international* 2015, S. 141793. DOI: 10.1155/2015/141793.
34. Peng, B; Hu, S; Jun, Q; Luo, D; Zhang, X; Zhao, H; Li, D (2013): MicroRNA-200b targets CREB1 and suppresses cell growth in human malignant glioma. In: *Molecular and cellular biochemistry* 379 (1-2), S. 51–58. DOI: 10.1007/s11010-013-1626-6.
35. Y. Su; Q. He; L. Deng et al. (2014): "MiR-200a impairs glioma cell growth, migration, and invasion by targeting SIM2-s," In: *NeuroRe- port*, vol. 25, no. 1, pp. 12–17. doi: 10.1097/WNR.0000000000000032

36. Men, D; Liang, Y; Chen, L (2014): Decreased expression of microRNA-200b is an independent unfavorable prognostic factor for glioma patients. In: *Cancer Epidemiol.* 38 (2): 152-6. doi: 10.1016/j.canep.2014.01.003.
37. Ning, X; Shi, Z; Liu, X; Zhang, A; Han, L; Jiang, K; Kang, C; Zhang, Q (2015): DNMT1 and EZH2 mediated methylation silences the microRNA-200b/a/429 gene and promotes tumor progression. In: *Cancer Lett.* 10; 359(2):198-205. doi: 10.1016/j.canlet.2015.01.005.
38. Fu, J; Rodova, M; Nanta, R; Meeker, D; van Veldhuizen, P. J.; Srivastava, R. K.; Shankar, S (2013): NPV-LDE-225 (Erismodegib) inhibits epithelial mesenchymal transition and self-renewal of glioblastoma initiating cells by regulating miR-21, miR-128, and miR-200. In: *Neuro-oncology* 15 (6), S. 691–706. DOI: 10.1093/neuonc/not011.
39. Siebzehnruhl, F. A.; Silver, D. J.; Tugertimur, B; Deleyrolle, L. P.; Siebzehnruhl, D; Sarkisian, M. R. et al. (2013): The ZEB1 pathway links glioblastoma initiation, invasion and chemoresistance. In: *EMBO molecular medicine* 5 (8), S. 1196–1212. DOI: 10.1002/emmm.201302827.
40. Hirn-Tumorzellen - CLS Online Shop. Online available under [http://clsgmbh.de/c385\\_Humane\\_Zelllinien\\_Hirn-Tumorzellen.html](http://clsgmbh.de/c385_Humane_Zelllinien_Hirn-Tumorzellen.html)
41. Campos, B; Gal, Z; Baader, A; Schneider, T; Sliwinski, C; Gassel, K et al. (2014): Aberrant self-renewal and quiescence contribute to the aggressiveness of glioblastoma. In: *The Journal of pathology* 234 (1), S. 23–33. DOI: 10.1002/path.4366.
42. Bady, P; Diserens, A-C; Castella, V; Kalt, S; Heinimann, K; Hamou, M-F et al. (2012): DNA fingerprinting of glioma cell lines and considerations on similarity measurements. In: *Neuro-oncology* 14 (6), S. 701–711. DOI: 10.1093/neuonc/nos072.
43. Details: ACC-74. Availbe online under: <https://www.dsmz.de/catalogues/details/culture/ACC-74.html>
44. Johnson, J. P.; Demmer-Dieckmann, M; Meo, T; Hadam, M. R.; Riethmuller, G (1981): Surface antigens of human melanoma cells defined by monoclonal antibodies. I. Biochemical

- characterization of two antigens found on cell lines and fresh tumors of diverse tissue origin. In: *European journal of immunology* 11 (10), S. 825–831. DOI: 10.1002/eji.1830111015.
45. Pontén, J; Macintyre, E. H. (1968): Long term culture of normal and neoplastic human glia. In: *Acta Pathol. Microbiol. Scand.* 74: 465-485.
46. Huang, H-L; Hsing, H-W; Lai, T-C; Chen, Y-W; Lee, T-R; Chan, H-T et al. (2010): Trypsin-induced proteome alteration during cell subculture in mammalian cells. In: *Journal of biomedical science* 17, S. 36. DOI: 10.1186/1423-0127-17-36.
47. Oscar B. Cell Counting with Neubauer Chamber. Online available under <http://www.celeromics.com/en/resources/Technical%20Notes/cells-chamber-counting.php>
48. Groskreutz, D; Schenborn, E. T. (1997): Reporter systems. In: *Methods in Molecular Biology* 63, 11ed. R. Tuan, Humana Press, NJ.
49. Technologies, Life: Lipofectamine® 2000 Reagent. Online available under [https://tools.thermofisher.com/content/sfs/manuals/Lipofectamine\\_2000\\_Reag\\_protocol.pdf](https://tools.thermofisher.com/content/sfs/manuals/Lipofectamine_2000_Reag_protocol.pdf)
50. RNA Interference (RNAi). Online verfügbar unter <https://www.ncbi.nlm.nih.gov/probe/docs/technai/>, zuletzt geprüft am 15.03.2017.
51. Jin, H. Y.; Gonzalez-Martin, A; Miletic, A. V.; Lai, M; Knight, S; Sabouri-Ghomi, M et al. (2015): Transfection of microRNA Mimics Should Be Used with Caution. In: *Frontiers in genetics* 6, S. 340. DOI: 10.3389/fgene.2015.00340.
52. Elbashir, S. M.; Harborth, J; Lendeckel, W; Yalcin, A; Weber, K; Tuschl, T (2001): Duplexes of 21-nucleotide RNAs mediate RNA interference in cultured mammalian cells. In: *Nature* 411 (6836), S. 494–498. DOI: 10.1038/35078107.
53. Thomson, D. W.; Bracken, C. P.; Szubert, J. M.; Goodall, G. J. (2013): On measuring miRNAs after transient transfection of mimics or antisense inhibitors. In: *PloS one* 8 (1), e55214. DOI: 10.1371/journal.pone.0055214.

54. Technologies, Life: mirVana™ miRNA Mimics. Online available under [http://tools.thermofisher.com/content/sfs/manuals/OOBE\\_mirVana\\_miRNA\\_Mimics\\_man.pdf](http://tools.thermofisher.com/content/sfs/manuals/OOBE_mirVana_miRNA_Mimics_man.pdf)
55. Manjunath, N; Dykxhoorn, DM (2010): Advances in synthetic siRNA delivery. In: *Discov Med.* 9(48):418–430.
56. Ramon, A; Bertrand, J; Malvy, C (2008): Delivery of small interfering RNA. A review and an example of application to a junction oncogene. In: *Tumori* 94 (2): 254 - 263.
57. miRNeasy micro Handbook. Online available at: <https://www.qiagen.com/us/shop/sample-technologies/rna/mirneasy-micro-kit/#resources>
58. miRNA Reverse Transcription Kit: miScript II RT Kit - QIAGEN Online Shop. Online verfügbar unter <https://www.qiagen.com/de/shop/pcr/real-time-pcr-enzymes-and-kits/two-step-qrt-pcr/miscript-ii-rt-kit/#productdetails>.
59. Real-time PCR: A review of approaches to data analysis. Available online under <http://www.gene-quantification.de/rebrikov-trofimov-real-time-pcr-review-2005.pdf>
60. miScript PCR System Handbook. Online available at: <https://www.qiagen.com/us/shop/pcr/real-time-pcr-enzymes-and-kits/two-step-qrt-pcr/miscript-ii-rt-kit/#orderinginformation>.
61. SNORD68 small nucleolar RNA, C/D box 68 [Homo sapiens (human)] - Gene - NCBI. Online available under <https://www.ncbi.nlm.nih.gov/gene/606500>
62. Hyde, D (2011): PrimerBank. Online available under <https://pga.mgh.harvard.edu/primerbank/>
63. Cell Proliferation ELISA, BrdU (chemiluminescent) 11669915001. Online verfügbar unter <http://www.sigmaaldrich.com/catalog/product/roche/11669915001?lang=de&region=DE>.



64. Earnshaw, W. C.; Martins, L. M.; Kaufmann, S. H. (1999): Mammalian caspases: structure, activation, substrates, and functions during apoptosis. In: *Annual review of biochemistry* 68, S. 383–424. DOI: 10.1146/annurev.biochem.68.1.383.
65. Corporation, Promega: Apo-ONE(R) Homogeneous Caspase-3/7 Assay Technical Bulletin, TB295. Available online under <https://www.promega.de/-/media/files/resources/protocols/technical-bulletins/0/apoone-homogeneous-caspase-3-7-assay-protocol.pdf>
66. Corporation, Promega: Measuring Fluorescence Using the Apo-ONE® Homogeneous Caspase-3/7 Assay with the GloMax® Discover System.
67. Brennan, C. W.; Verhaak, R. G. W.; McKenna, A; Campos, B; Noushmehr, H; Salama, S. R. et al. (2013): The somatic genomic landscape of glioblastoma. In: *Cell* 155 (2), S. 462–477. DOI: 10.1016/j.cell.2013.09.034.
68. Ritchie, M. E.; Phipson, B; Di W; Hu, Y; Law, C. W.; Shi, W; Smyth, G. K. (2015): limma powers differential expression analyses for RNA-sequencing and microarray studies. In: *Nucleic acids research* 43 (7), e47. DOI: 10.1093/nar/gkv007.
69. Silver, J. D.; Ritchie, M. E.; Smyth, G. K. (2009): Microarray background correction: maximum likelihood estimation for the normal-exponential convolution. In: *Biostatistics (Oxford, England)* 10 (2), S. 352–363. DOI: 10.1093/biostatistics/kxn042.
70. Bolstad, B. M.; Irizarry, R. A.; Astrand, M; Speed, T. P. (2003): A comparison of normalization methods for high density oligonucleotide array data based on bias and variance. In: *Bioinformatics* 19, 185-193.
71. Benjamini, Y; Hochberg, Y (1995): Controlling the false discovery rate: a practical and powerful approach to multiple testing. In: *Journal of the Royal Statistical Society Series B* 57, 289–300.
72. Andrews S. (2010): FastQC: a quality control tool for high throughput sequence data. Available online at: <http://www.bioinformatics.babraham.ac.uk/projects/fastqc>

73. Huber, W; Carey, V. J.; Gentleman, R; Anders, S; Carlson, M; Carvalho, B. S. et al. (2015): Orchestrating high-throughput genomic analysis with Bioconductor. In: *Nature methods* 12 (2), S. 115–121. DOI: 10.1038/nmeth.3252.
74. Borg, I.; Groenen, P. (2005): In: *Modern Multidimensional Scaling: theory and applications* (2nd ed.). New York: Springer-Verlag. pp. 207–212. ISBN 0-387-94845-7.
75. Jolliffe, I. T.; Cadima, J (2016): Principal component analysis: a review and recent developments. In: *Philosophical transactions. Series A, Mathematical, physical, and engineering sciences* 374 (2065), S. 20150202. DOI: 10.1098/rsta.2015.0202.
76. Collazos, J. C. O. (2016): Venny 2.1.0. Available online under <http://bioinfogp.cnb.csic.es/tools/venny/>
77. Huang, D. W.; Sherman, B. T.; Lempicki, Richard A (2009): Bioinformatics enrichment tools: paths toward the comprehensive functional analysis of large gene lists. In: *Nucleic acids research* 37 (1), S. 1–13. DOI: 10.1093/nar/gkn923.
78. Huang, D. W.; Sherman, B. T.; Lempicki, R. A. (2009): Systematic and integrative analysis of large gene lists using DAVID bioinformatics resources. In: *Nature protocols* 4 (1), S. 44–57. DOI: 10.1038/nprot.2008.211.
79. Subramanian, A; Tamayo, P; Mootha, V. K.; Mukherjee, S; Ebert, B. L.; Gillette, M. A. et al. (2005): Gene set enrichment analysis: a knowledge-based approach for interpreting genome-wide expression profiles. In: *Proceedings of the National Academy of Sciences of the United States of America* 102 (43), S. 15545–15550. DOI: 10.1073/pnas.0506580102.
80. Reich, M; Liefeld, T; Gould, J; Lerner, J; Tamayo, P; Mesirov, J. P. (2006): GenePattern 2.0. In: *Nature genetics* 38 (5), S. 500–501. DOI: 10.1038/ng0506-500.
81. Livak K. J.; Schmittgen, T. D. (2001): Analysis of relative gene expression data using real-time quantitative PCR and the 2- $\Delta\Delta$ CT method. *Methods* 25(4):402–408.

82. Jagannathan, V; Robinson-Rechavi, M (2011): Meta-analysis of estrogen response in MCF-7 distinguishes early target genes involved in signaling and cell proliferation from later target genes involved in cell cycle and DNA repair. In: *BMC systems biology* 5, S. 138. DOI: 10.1186/1752-0509-5-138.
83. Zhang, Z; Liu, Z-B; Ren, W-M; Ye, X-G; Zhang, Y-Y (2012): The miR-200 family regulates the epithelial-mesenchymal transition induced by EGF/EGFR in anaplastic thyroid cancer cells. In: *International journal of molecular medicine* 30 (4), S. 856–862. DOI: 10.3892/ijmm.2012.1059.
84. Serna, E; Lopez-Gines, C; Monleon, D; Muñoz-Hidalgo, L; Callaghan, R. C.; Gil-Benso, R et al. (2014): Correlation between EGFR Amplification and the Expression of MicroRNA-200c in Primary Glioblastoma Multiforme. In: *PLoS ONE* 9 (7), e102927. DOI: 10.1371/journal.pone.0102927.
85. Liu, Q; Tang, H; Liu, X; Liao, Y; Li, H; Zhao, Z et al. (2014): miR-200b as a prognostic factor targets multiple members of RAB family in glioma. In: *Medical oncology* 31 (3), S. 859. DOI: 10.1007/s12032-014-0859-x
86. Men, D; Liang, Y; Chen, L (2014): Decreased expression of microRNA-200b is an independent unfavorable prognostic factor for glioma patients. In: *Cancer Epidemiology* 2 (38), S. 152 - 156. DOI:10.1016/j.canep.2014.01.003
87. Cuddihy, A. R.; O'Connell, M. J. (2003): "Cell-cycle responses to DNA damage in G2". In: *International review of cytology* 222: 99–140.
88. Zheng, N; Fraenkel, E; Pabo, C. O.; Pavletich, N. P. (1999): "Structural basis of DNA recognition by the heterodimeric cell cycle transcription factor E2F-DP". In: *Genes Dev.* 13 (6): 666–74. doi:10.1101/gad.13.6.666. PMC 316551. PMID 10090723
89. Gomez-Manzano, C; Fueyo, J; Alameda, F; Kyritsis, A. P.; Yung, A. W.K. (1999): Gene therapy for gliomas: p53 and E2F-1 proteins and the target of apoptosis (Review). In: *INTERNATIONAL JOURNAL OF MOLECULAR MEDICINE* 3, S. 81–85.

90. Fueyo, J; Gomez-Manzano, C; Yung, A. W.K.; Liu, T. J.; Arleman, R; McDonell, T. J.; Shi, X et al (1998): Overexpression of E2F-1 in glioma triggers apoptosis and suppresses tumor growth in vitro and in vivo. In: *Nature Medicine* 4 (6), S. 685–690.
91. Cornago, M; Garcia-Alberich, C; Blasco-Angulo, N; Vall-Llaura, N; Nager, M; Herreros, J et al. (2014): Histone deacetylase inhibitors promote glioma cell death by G2 checkpoint abrogation leading to mitotic catastrophe. In: *Cell death & disease* 5, e1435. DOI: 10.1038/cddis.2014.412.
92. Lin, C-H; Jackson, A. L.; Guo, J; Linsley, P. S.; Eisenman, R. N. (2009): Myc-regulated microRNAs attenuate embryonic stem cell differentiation. In: *The EMBO journal* 28 (20), S. 3157–3170. DOI: 10.1038/emboj.2009.254.
93. Herms, J. W.; Loewenich, F. D. von; Behnke, J; Markakis, E; Kretzschmar, H. A. (1999): c-myc oncogene family expression in glioblastoma and survival. In: *Surgical Neurology* 51 (5), S. 536–542. DOI: 10.1016/S0090-3019(98)00028-7.
94. Bai, J-X; Yan, B; Zhao, Z-N; Xiao, X; Qin, W-W; Zhang, R et al. (2013): Tamoxifen represses miR-200 microRNAs and promotes epithelial-to-mesenchymal transition by up-regulating c-Myc in endometrial carcinoma cell lines. In: *Endocrinology* 154 (2), S. 635–645. DOI: 10.1210/en.2012-1607.
95. Brasier, A. R. (2006): The NF- $\kappa$ B Regulatory Network. In: *Cardiovascular Toxicology* (06), S. 111–130.
96. Maier, H. J.; Schmidt-Strassburger, U; Huber, M. A.; Wiedemann, E. M.; Beug, H; Wirth, T (2010): NF-kappaB promotes epithelial-mesenchymal transition, migration and invasion of pancreatic carcinoma cells. In: *Cancer letters* 295 (2), S. 214–228. DOI: 10.1016/j.canlet.2010.03.003.
97. Chua, H. L.; Bhat-Nakshatri, P; Clare, S. E.; Morimiya, A; Badve, S; Nakshatri, H (2007): NF-kB represses E-cadherin expression and enhances epithelial to mesenchymal transition of mammary epithelial cells: potential involvement of ZEB-1 and ZEB-2. In: *Oncogene* (26), S. 711–724. DOI: 10.1038/sj.onc.1209808

98. Joseph, J. V.; Conroy, S.; Pavlov, K.; Sontakke, P; Tomar, T; Eggens-Meijer, E et al. (2015): Hypoxia enhances migration and invasion in glioblastoma by promoting a mesenchymal shift mediated by the HIF1 $\alpha$ –ZEB1 axis. In: *Cancer letters* 359 (1), S. 107–116. DOI: 10.1016/j.canlet.2015.01.010.
99. Zhong, H; De Marzo, A. M.; Laughner, E; Lim, M; Hilton, D. A.; Zagzag, D; Buechler, P; Isaacs, W. B.; Semenza, G. L.; Simons, J. W. (1999): Overexpression of hypoxia-inducible factor 1 $\alpha$  in common human cancers and their metastases. In: *Cancer Res.*59(22): 5830-5835.
100. Tuettenberg, J; Friedel C; Vajkoczy, P (2006): Angiogenesis in malignant glioma -- a target for antitumor therapy? In: *Critical reviews in oncology/hematology* 59(3): 181-1 93
101. Li, Z; Bao, S; Wu, Q; Wang, H; Eyler, C; Sathornsumetee, S et al. (2009): Hypoxia-inducible factors regulate tumorigenic capacity of glioma stem cells. In: *Cancer cell* 15 (6), S. 501–513. DOI: 10.1016/j.ccr.2009.03.018.
102. Bar, E. E. (2011): Glioblastoma, cancer stem cells and hypoxia. In: *Brain pathology (Zurich, Switzerland)* 21 (2), S. 119–129. DOI: 10.1111/j.1750-3639.2010.00460.x.
103. Jagannathan, V; Robinson-Rechavi, M (2011): Meta-analysis of estrogen response in MCF-7 distinguishes early target genes involved in signaling and cell proliferation from later target genes involved in cell cycle and DNA repair. In: *BMC systems biology* 5, S. 138. DOI: 10.1186/1752-0509-5-138.

## Natalia Vélez Char, M.D., M.Sc.

Geburtsdatum / -ort: 20.08.1983 / Cartagena, Kolumbien

Familienstand: ledig

Staatsangehörigkeit: Kolumbianisch

### BERUFLICHER WERDEGANG

08/2012 – heute **Assistenzärztin**  
Abteilung für Neuropathologie  
Universitätsklinikum Regensburg, 93053 Regensburg

10/2011 – 07/2012 **Assistenzärztin**  
Institut für Neuropathologie  
Universitätsklinikum Bonn, 53127 Bonn

08/2011 – 09/2011 **Wissenschaftliche Mitarbeiterin**  
Institut für Neuropathologie  
Universitätsklinikum Bonn, 53127 Bonn

### AUSBILDUNG

10/2013 Approbation als Ärztin in der Bundesrepublik Deutschland

09/2009 – 10/2011 **Experimental and Clinical Neuroscience**  
Universität Regensburg, 93053  
Studienschwerpunkte: Neurowissenschaft  
Thesis-Thema: Transition of neural stem cells (NSC) to brain tumor initiating cells (BTIC): Comparative analysis of transformed NSCs and BTICs with regard to epithelial-mesenchymal transition (EMT)-associated gene expression patterns.  
Abschluss: **Master of Science (M.Sc.)**

11/2008 Approbation als Ärztin im Königreich Spanien

04/2008 Approbation als Ärztin in der Republik Kolumbien

08/2001 – 12/2007 **Studium der Human Medizin**  
Universidad del Norte, Barranquilla (Kolumbien)

Thesis-Thema: Risk factors related to flares in patients with Rheumatoid Arthritis  
visiting our Rheumatology Outpatient Clinic at the Universidad del Norte in  
Barranquilla, Colombia from June 2005 to May 2006. (Undergraduate Thesis).

Abschluss: **Medica cirujana**

08/1997 – 06/2001

**High School/ Bachillerato** (doppelte Diplome US- amerikanisch und kolumbianisch)

Colegio Jorge Washington, Cartagena (Kolumbien)

National Honor Society Member (USA)

Abschluss: **Graduate/ Bachiller**

## **BESONDERE KENNTNISSE**

Sprachkenntnisse	Spanisch (Muttersprache)
	Englisch (fließend)
	Deutsch (Verhandlungssicher)
	Italienisch (Grundkenntnisse)

Regensburg, 02.08.2017

Natalia Vélez Char

## Aknowledgements

First, I would like to express my sincere gratitude to my advisor Prof. Dr. Markus J. Riemenschneider for the continuous support of my PhD research, motivation and immense knowledge. His guidance helped me every single way during the time of this research and also during the writing of this thesis. I could not have imagined having a better advisor and mentor.

Besides my advisor, I would like to thank the rest of our department, especially Dr. Markus Schulze, Susanne Bruggemann and Maria Hirblinger for their unconditional support in all the methodological contents of this project, but also Gabrielle Sommer and Gerlinde Hiltl for their support, patience and motivation.

My sincere thanks also goes to Prof. Dr. Peter Hau, who not long ago provided me the opportunity to join his team as a master student, giving me my first insights into research and introducing me to Neuropathology.

Regensburg, 02.08.2017